
**Pacific Northwest
National Laboratory**

Operated by Battelle for the
U.S. Department of Energy

**Validation Testing of the Nitric Acid
Dissolution Step Within the K Basin
Sludge Pretreatment Process**

A. J. Schmidt	E. W. Hoppe
C. H. Delegard	J. C. Hayes
K. L. Silvers	D. E. Rinehart
P. R. Bredt	S. R. Gano
C. D. Carlson	B. M. Thornton

February 1999

RECEIVED
APR 05 1999
OSTI



Prepared for the U.S. Department of Energy
under Contract DE-AC06-76RLO 1830

DISCLAIMER

This report was prepared as an account of work sponsored by an agency of the United States Government. Neither the United States Government nor any agency thereof, nor Battelle Memorial Institute, nor any of their employees, makes any warranty, express or implied, or assumes any legal liability or responsibility for the accuracy, completeness, or usefulness of any information, apparatus, product, or process disclosed, or represents that its use would not infringe privately owned rights. Reference herein to any specific commercial product, process, or service by trade name, trademark, manufacturer, or otherwise does not necessarily constitute or imply its endorsement, recommendation, or favoring by the United States Government or any agency thereof, or Battelle Memorial Institute. The views and opinions of authors expressed herein do not necessarily state or reflect those of the United States Government or any agency thereof.

PACIFIC NORTHWEST NATIONAL LABORATORY

operated by

BATTELLE

for the

UNITED STATES DEPARTMENT OF ENERGY

under Contract DE-AC06-76RLO 1830

Printed in the United States of America

Available to DOE and DOE contractors from the
Office of Scientific and Technical Information, P.O. Box 62, Oak Ridge, TN 37831;
prices available from (615) 576-8401.

Available to the public from the National Technical Information Service,
U.S. Department of Commerce, 5285 Port Royal Rd., Springfield, VA 22161



This document was printed on recycled paper.

(9/97)

DISCLAIMER

Portions of this document may be illegible in electronic image products. Images are produced from the best available original document.

Validation Testing of the Nitric Acid Dissolution Step Within the K Basin Sludge Pretreatment Process

A. J. Schmidt
C. H. Delegard
K. L. Silvers
P. R. Bredt
C. D. Carlson
E. W. Hoppe
J. C. Hayes
D. E. Rinehart
S. R. Gano
B. M. Thornton

February 1999

Prepared for
the U.S. Department of Energy EM-67 in support of
Numatec Hanford Corporation

Work supported by
the U.S. Department of Energy
under Contract DE-AC06-76RLO 1830

Pacific Northwest National Laboratory
Richland, Washington 99352

Summary and Conclusions

The work described in this report involved comprehensive bench-scale testing of nitric acid (HNO_3) dissolution of actual sludge materials from the Hanford K East (KE) Basin to confirm the baseline chemical pretreatment process. In addition, process monitoring and material balance information was collected to support the development and refinement of process flow diagrams. The testing was performed by Pacific Northwest National Laboratory (PNNL) for the U.S. Department of Energy's Office of Spent Fuel Stabilization (EM-67) and Numatec Hanford Corporation (NHC) to assist in the development of the K Basin Sludge Pretreatment Process.

The baseline chemical pretreatment process for K Basin sludge is nitric acid dissolution of all particulate material passing a ¼-in. screen. The acid-insoluble fraction (residual solids) will be stabilized (possibly by chemical leaching/rinsing and grouting), packaged, and transferred to the Hanford Environmental Restoration Disposal Facility (ERDF). The liquid fraction is to be diluted with depleted uranium for uranium criticality safety and iron nitrate for plutonium criticality safety, and neutralized with sodium hydroxide. The liquid fraction and associated precipitates are to be stored in the Hanford Tank Waste Remediation Systems (TWRS) pending vitrification. It is expected that most of the polychlorinated biphenyls (PCBs), associated with some K Basin sludges, will remain with the residual solids for ultimate disposal to ERDF. Filtration and precipitation during the neutralization step will further remove trace quantities of PCBs within the liquid fraction.

The purpose of the work discussed in this report was to examine the dissolution behavior of actual KE Basin sludge materials at baseline flowsheet conditions and validate the dissolution process step through bench-scale testing. The progress of the dissolution was evaluated by measuring the solution electrical conductivity and concentrations of key species in the dissolver solutions as a function of reaction (dissolution) time, by analyzing offgas generation rate and composition, and by analyzing intermittent and final acid-insoluble solids at the end of the dissolution. The testing was conducted in a system designed to assess parameters that can influence sludge dissolution and provide information that can be used to determine operating conditions for the actual system.

Test Matrix for Dissolution of Actual KE Basin Materials

Before the dissolution tests with radioactive materials were initiated, extensive cold shakedown testing was conducted to develop testing protocols, validate the test configurations, and confirm the process monitoring techniques (i.e., electrical conductivity and offgas analysis). Once cold shakedown tests were completed, three dissolution validation tests were performed in a 1-L dissolver vessel with ~60 g of sludge material in each test. The test materials were sludge composites that approximated the composition of the KE Stream 1 (KE Basin floor and Weasel Pit sludge) and the KE Stream 2 (KE canister sludge and fuel fragments). The sludge composites were built by combining portions of individual sludge samples that were originally collected for characterization purposes. The two composites used for this testing were KE Canister Sludge Composite (Test 1) and KE Areas Sludge Composite (built from individual KE floor and KE Weasel Pit sludge samples) (Test 3). For the testing with the sludge material representative of Stream 2 (Test 2), irradiated uranium fuel fragments were dissolved, as well as KE Canister Sludge Composite. The following table summarizes the parameters and conditions used for these tests. The results and conclusions from these tests are discussed below.

Parameters and Conditions for Dissolution Validation Testing

Parameter/Condition	Test 1	Test 2	Test 3
Test Start Date	7/24/98	8/5/98	8/19/98
Feed Material and Mass (dry basis)	KE Canister Sludge, 71.3 g	Fuel fragments, 30.7 g; KE Canister Sludge, 40.0 g	KE Areas Sludge Composite, 52.7 g; ion exch. material, 1.98 g (air dry)
HNO ₃ Concentration	6 M	6 M	6 M
HNO ₃ Volume, ml	498 ml	500 ml 6 M (start) + 80 ml 16 M (during run) 580 ml - total	550 ml 6 M (start) + 150 ml 16 M (during run) 700 ml - total
Solids Content (mass of initial solids divided by total acid volume)	146 g/L	122 g/L	75 g/L
Dissolution Temp.	95°C	95°C	95°C
Dissolution Time, starting after final sludge addition	20 hr	21 hr – Fuel fragments 6 hr – Canister sludge	7 hr
Conductivity Monitored	yes	yes	yes
Offgas Analysis	no	yes	yes

For each test, the system was completely assembled; approximately 500 ml of 6 M HNO₃ were added to the dissolver vessel; and the acid solution was heated to 95°C. Solution electrical conductivity data and temperature data were collected once every 5 seconds for the duration of each test. Dissolver offgas was sampled and analyzed continuously during Tests 2 and 3 for O₂, NO, NO₂, N₂O, N₂, H₂, CO, CO₂, Xe, and Kr. After the acid solution temperature stabilized at ~95°C, the sludge was added. Frozen sludge feed pellets (and fuel fragments) were then fed to the dissolver vessel at 10- to 15-min intervals. By using frozen sludge pellets, the entire desired quantity of sludge could be introduced as an intact plug to the dissolver solution without unwanted holdup on the sludge addition valve.

Liquid samples (~10 per test) were collected in syringes through the liquid sampling port at specified times during the dissolution tests. These samples were then analyzed for key species to evaluate the effectiveness of the sludge dissolution as a function of dissolution time. Approximately midway through each test, a slurry sample (i.e., dissolver solution and solids) was collected to evaluate the level of decontamination that was achieved for the residual solids at an intermediate time during dissolution. When the specified dissolution period for each test was completed, heating and agitation to the dissolver was stopped and the dissolver solution allowed to settle. After settling, the supernatant was decanted and filtered. A series of washes were performed on the insoluble residual solids: two washes with 2% HNO₃, and a final wash with deionized water.

Results from Dissolution Validation Testing

Overall Conclusions

Bench-scale testing of the nitric acid dissolution step confirmed the efficacy of the process. For the KE Canister Sludge Composite and fuel fragments, greater than 99.9% of the uranium and radionuclides dissolved. For the KE Areas Sludge Composite, ~99.99% of the uranium, greater than 99% of the transuranics (TRU), and ~98.9% of the ^{137}Cs dissolved. The KE Canister Sludge Composite dissolved almost instantaneously. The KE Areas Sludge Composite achieved essentially complete dissolution within about 40 min. Large fragments of irradiated fuel (i.e., ~ ¼-in. diameter) may require 12 to 16 hr to achieve complete dissolution in 6 M HNO_3 at 95° C. The K Basin sludge materials subjected to the dissolution testing reasonably bracketed the composition of sludge materials from the KE Basin that will be dissolved in the actual treatment process (i.e., floor, Weasel Pit, canister, and fuel wash sludge).

Measurements and observations of the dissolution testing showed that introducing the various sludge types and fragments of irradiated metallic uranium fuel, at controlled rates, into heated (95°C) 6 M HNO_3 proceeded in a controllable and predictable manner. There was no evidence of excessive offgas surges, temperature excursions, or significant foaming.

Solution electrical conductivity monitoring and offgas analyses were shown to be effective online techniques for tracking the progress of the sludge dissolution reactions. The gas chromatograms and conductivity plots corresponded with the test events (e.g., sludge addition, acid addition, sample collection) and the results from the analyses of the solution samples (i.e., completion of dissolution reactions).

Results from the chemical and radiochemical analyses of the dissolver solutions and acid-insoluble residual solids were consistent with results from previous, smaller-scale dissolution tests performed on KE Canister Sludge and KE Areas Sludge Composites, which served as input to the baseline process flowsheets (issued in August 1998). Consistent and comparable results were obtained for percent residual solids and concentrations of chemical constituents and radionuclides within the residual solids.

Specific Conclusions and Findings

Electrical Conductivity Behavior

It was demonstrated that solution electrical conductivity could be used to track the progress of sludge dissolution. During sludge additions, the solution conductivity decreased almost instantaneously. With the KE Canister Sludge Composite (Tests 1 and 2), the solution conductivity leveled out within minutes of the sludge additions, indicating that the dissolution reactions go to completion very rapidly. With the KE Areas Sludge Composite (Test 3), conductivity continued to decrease for about 40 min following the sludge additions. In Test 2, during uranium fuel dissolution, the conductivity continued to decrease with time as the fuel fragments slowly dissolved.

Conductivity decreases with sludge and fuel fragment dissolution, since the dissolution reactions consume the hydrogen ion and place metal nitrate salts (such as uranyl nitrate and ferric nitrate) in solution. Because the hydrogen ion is the primary conductor in the acid solution, consumption of the hydrogen ion directly decreases conductivity. The creation of metal nitrate salts during dissolution decreases the solution conductivity by suppressing nitric acid dissociation by the common ion effect of nitrate.

However, the effect of metal nitrate salts on solution conductivity decreases with decreasing nitric acid concentration. Therefore, as nitric acid is consumed, conductivity becomes a more direct indicator of residual free acid concentration.

In one dissolution test, the protective glass sheath around the conductivity probe broke. While the absolute accuracy of the conductivity measurements from the broken probe was questionable, the data still showed that the reaction progress was reflected by the conductivity measurements. From this and other observations, it is clear that strict control of the conductive environment around the electrodes (no bubbles, fixed conduction path) is required to obtain accurate and reliable data.

Offgas Generation/Composition

Results from offgas monitoring for nitrogen oxides (NO_x , which includes NO , NO_2 , and N_2O) are in good agreement with the sludge and fuel fragment dissolution reactions. The quantity of NO_x measured ranged from 50% to 90% of the quantity predicted. The monitoring of carbon dioxide in the offgas can also be used as an indication of the progress of the dissolution reactions.

The mole ratios of NO_2 : NO generated during dissolution tests were about 1:3 for fuel fragments and KE Canister Sludge Composite and about 1:0.9 for KE Areas Sludge Composite. Based on the maximum measured values, approximately 600 kg each of NO_2 and NO will be generated during acid dissolution of the KE Basin sludge inventory [i.e., 21.5 metric ton (MT) KE floor and pit sludge; 4.3 MT KE canister, coating and internal sludge; and 1.6 MT of fuel fragments – dry sludge basis]. In the actual process, the quantities of NO_2 and NO will most likely be lower than those observed for the dissolution validation tests. Injection of air into the plenum of the dissolver, and a more efficient condenser, will likely reduce the NO_2 and NO concentrations downstream of the condenser. If necessary, further decreases can be achieved with a NO_x scrubber.

Gel Formation Behavior

Significant gel formation was observed during all three dissolution tests. In Test 1, gel was first observed about 5 hr after the last sludge addition. During the next 15 hr of dissolution in Test 1, the gel particles increased in size and volume.

In all tests, during settling, gel material adhered to the vessel walls. Significant gel buildup on the temperature and conductivity probes was noted. The gel was easily rinsed off the vessel walls and probes, and no mass gain was measured for the reactor vessel, indicating no permanent accumulation of gel material.

In Test 3 (KE Areas Sludge Composite), a very significant quantity of gel was formed. The mass of the dewatered, but moist, residual solids (mostly gel, which was readily dewatered on the filter) was about 50% of the mass of the dry feed sludge. After drying, the mass of the residual solids was about 17% of the mass of the dry feed sludge.

Silica is believed to be the primary component of the gel. In Tests 1 and 2, the silicon concentrations in the dissolver solutions were 5 to 10 times above that expected for the solubility of amorphous silica in 95°C HNO_3 . [In Test 3, the silicon level in the dissolver was near the solubility of amorphous silica.] Furthermore, in previous PNNL work, gel was isolated and found to contain amorphous material, as well as quartz and approximately 23 wt% anorthosite [a mixture of albite ($\text{NaAlSi}_3\text{O}_8$) and anorthite ($\text{CaAl}_2\text{Si}_2\text{O}_8$)].

The technical literature indicates that silica gel and high silica glass can sorb plutonium from strong acid solutions. Based on the literature, distribution coefficients, K_{ds} ($[Pu_{solid}]/[Pu_{solution}]$), of 0.2 to 1 ml/g were observed. To determine whether the gel formed during the dissolution tests could be sorbing plutonium, all plutonium solid/solution data available from nitric acid processing tests of K Basin sludges were plotted. It was found that the plutonium concentrations on the K Basin sludge residual solids were roughly proportional to the plutonium solution concentration regardless of the sludge type and could be described by distribution coefficients that are consistent with the literature values for silica gel and high silica glass.

Solid/Liquid Separations

After the dissolution test durations were completed, the contents of the dissolver were allowed to cool and settle for several hours. In general, good separation of the acid-insoluble residuals and gel from the dissolver solution was observed. However, in Tests 1 and 2, when the clarified dissolver solutions (~500 to 600 ml) were decanted onto 0.45- μ m cellulose acetate filters, the filters blinded. In Test 2, only 5 ml of filtrate were obtained prior to filter blinding. For Test 2, the dissolution solution was allowed to settle for an additional 24 hr and refiltered. This filter also blinded, but approximately 500 ml of solution were filtered first. For these tests, it is believed that the presence of suspended gelatinous material caused the filter blinding.

Although the quantity of gel formed in Test 3 was much greater than in Tests 1 and 2, the 0.45- μ m polyvinylidene fluoride filter did not blind when filtering the clarified dissolver solution.

After the dissolver solutions were decanted, acid-insoluble residual solids were rinsed twice with 2% HNO_3 and once with deionized water. Between each contact with the rinse solution, the solids were allowed to settle and the solution was decanted onto a filter. Good settling behavior was exhibited after contacts with the rinse solutions in all tests. The decanted rinse solutions did not cause any filters to blind.

Dissolution of Irradiated Fuel Fragments

As anticipated, the dissolution of fragments of irradiated uranium fuel occurred at a significantly slower rate than the near-instantaneous dissolution rates exhibited by the bulk of the sludge components. The dissolution rates of the fuel fragments will likely determine the batch dissolution time used in the K Basin Sludge Pretreatment Process.

About 30.67 g of fuel fragments (28.92 g after deducting the cladding) were added in the first 2.5 hr of Test 2. Visual observation showed that, after 16 hr, one fuel fragment still was not completely dissolved. That is, at least one piece of metal required more than 13.5 hr to dissolve. The heaviest fragment added was about 6.25 g. A spherical piece of this mass would require the longest dissolution time and would be about 8.6 mm in diameter based on a uranium density of 19.1 g/cm³. The maximum linear corrosion rate thus would be 4.3 mm per 13.5 hr or 0.32 mm/hr. This corrosion rate is compatible with the rates found in the literature.

Fate of Zirconium Cladding

As expected, the zirconium-based cladding (introduced into the dissolver vessel with fuel fragments in Test 2) survived the nitric acid dissolution. Prior studies have shown that interdiffusion of zirconium into uranium and uranium into zirconium occurs in the fuel fabrication process. The uranium trapped in the Zircaloy cladding will undergo fission and activation during irradiation. The activation and fission products, likewise, will remain trapped in the Zircaloy matrix and will not be released unless the Zircaloy itself has dissolved. Analyses of residual cladding in Test 2 showed that the total alpha activity was about 1800 nCi/g. In comparison, nitric acid-treated cladding from irradiated N Reactor fuel (weapons grade) has been found to contain TRU activity at about 200 to 400 nCi/g. The higher TRU/alpha activity content in the cladding from the present testing is likely due to the uranium fuel having undergone significantly more irradiation (i.e., it was fuels grade) than the weapons grade fuel examined in the previous study.

Behavior of Ion Exchange Material During Dissolution

Ion exchange (IX) material in sludge that is subjected to acid dissolution picks up significant concentrations of TRU. The IX material (~65% organic ion exchange resin – NRW-37 and ~35% inorganic ion exchange material – Zeolon 900) from a KE Basin floor sample was suspended in the dissolver solution during Test 3. When the IX material was exposed to the acidic dissolver solution, the plutonium concentration increased by factors of 275 and 9 for the organic and the inorganic IX material fractions, respectively. During acid dissolution, the ^{137}Cs concentration decreased about 7-fold on the organic resin and about 120-fold on the inorganic fraction. Overall, in the combined IX material (organic + inorganic), the alpha activity increased by a factor of 60 (from 447 nCi/g to 27,100 nCi/g), while the ^{137}Cs activity decreased by a factor of 100 (from 186 $\mu\text{Ci/g}$ to 1.93 $\mu\text{Ci/g}$). In general, exposing the IX material to the dissolver solution decreased monovalent cation (Na^+ and Cs^+) concentrations, had little effect on divalent cation (Co^{2+} and UO_2^{2+} but not Ca^{2+}) concentrations, and increased trivalent cation (Fe^{3+} , Eu^{3+} , and Am^{3+} but not Al^{3+}) and tetravalent cation (Pu^{4+}) concentrations.

Composition of Residual Solids

The compositions of the residual solids from the dissolution validation testing were comparable to the compositions of the residual solids from similar sludges obtained during previous, smaller-scale dissolution testing. The dominant constituent in the residual solids is silicon (~30 wt%). If it is assumed that the silicon exists as silica (SiO_2), then ~65% of the mass of the residual solids would be composed of silica. The crystalline phases in the residual solids identified by X-ray diffraction are quartz, anorthite, and muscovite; all are found in Hanford soils. Aside from IX material and cladding, no phases were identified in the residual solids originating from the fuel, K Basin structural materials, or K Basin process or storage activities.

For the tests conducted with the KE Canister Sludge Composite, the residual solids ranged from about 1% to 2% of the initial dry sludge amount. The residual solids also contained about 0.5 to 7 wt% uranium, which is about 4 to 50 times the relevant ERDF criterion. The concentrations of ^{137}Cs found in the residual solids ranged from about 15 to 85 $\mu\text{Ci/g}$ or about 1 to 5 times the ERDF criterion. The concentrations of plutonium found in the residual solids ranged from about 5 to 27 $\mu\text{Ci/g}$ or about 170 to 1000 times the ERDF criterion. Americium concentrations ranged from about 1.6 to 7 $\mu\text{Ci/g}$ or 60 to 270 times the ERDF criterion. The separate TRU criterion, which accounts for both the plutonium and americium, was exceeded by 70- to 400-fold. Thus, the radionuclides of most concern for leaching and ultimate disposal to ERDF for the KE canister sludge residual solids are the transuranium isotopes, $^{239,240}\text{Pu}$ and ^{241}Am .

The residual solids weights from KE Areas Sludge Composite were about 17 wt% of the starting material dry weight. The iron concentrations in the residual solids decreased with increasing leach time, acid concentration, and sludge loading in the dissolution. Iron concentrations ranged from about 1 to 21 wt% of the residual solids. The residual solids from the KE Areas Sludge Composite were much less concentrated in uranium and radionuclides than the KE Canister Sludge Composite residual solids. The uranium concentrations ranged from 0.005 to about 0.5 wt% (0.04 to about 4 times the ERDF criterion). The ^{137}Cs concentrations ranged from about 5 to 64 $\mu\text{Ci/g}$ or 0.3 to 4 times the ERDF criterion. Plutonium was present at about 0.13 to 3 $\mu\text{Ci/g}$ or 6 to 140 times the ERDF criterion; americium was about 0.08 to 0.6 $\mu\text{Ci/g}$ or 3 to 24 times the ERDF criterion. The ERDF criterion for TRU was exceeded from 2.5- to 40-fold. The radionuclides with the most impact on reaching the ERDF criteria for residuals from the KE Areas Sludge Composite again are ^{241}Am and, particularly, $^{239,240}\text{Pu}$.

The TRU content in both of these types of residual solids exceeds the ERDF criterion of 100 nCi/g; however, in the baseline treatment process, the acid-insoluble solids will be subjected to a leaching step prior to disposition to ERDF. While the residual solids from the KE Canister Sludge Composite contain about 10 times the level of radionuclides as the KE Areas Sludge Composite, they comprise only a small fraction (~1% of the total mass, dry weight basis) of the total residual solids that will be generated from processing K Basin sludge in the pretreatment process. Also, in accordance with ERDF rules, compliance with the ERDF criteria will be based on the concentrations of analytes within the final waste form matrix (grout).

Recommendations for Further Testing to Refine the Dissolution Process

The results from the dissolution validation testing have provided additional confidence in the use of nitric acid dissolution to successfully process the K Basin sludge. The testing results have also led to the identification of areas that should be further developed to improve the implementability of the acid dissolution process. Provided below are recommendations for testing to refine the acid dissolution process.

Integrated testing of all steps (dissolution, solid/liquid separations, solids leaching, and alkaline treatment/precipitation) within the K Basin Sludge Pretreatment Process should be performed using actual K Basin sludge materials to comprehensively demonstrate the process and to provide information for the process conceptual design. Testing with actual K Basin sludge materials should also be conducted to confirm the disposition of PCBs within the process.

Attempts to track dissolution reaction progress and consumption of nitric acid by analyzing the dissolver solution for the hydrogen ion (H^+) and nitrate (NO_3^-) were not completely successful. While the data in general followed the predicted trends, inconsistencies limited the usefulness of the data (e.g., after nitric acid additions to the dissolver, expected increases in these analyte concentrations were not consistently observed). Further work is required to determine whether these analytes can be more accurately measured to provide useful information to monitor and control the actual dissolution process. The analytical methods used may require modification.

Gel formation was shown to have an adverse impact on filtration. To better assess the impact of gel formation to the process, additional filtration testing is needed in a system that is more prototypical of the solids/liquid separation technique that will be used in the K Basin Sludge Pretreatment Process (i.e., centrifugation followed by a polishing cartridge filter).

To potentially obtain higher levels of residual solids decontamination and determine if ion exchange is the mechanism for plutonium retention on the siliceous solids (gel), leaching tests with $\text{HNO}_3/\text{H}_2\text{C}_2\text{O}_4$ or $\text{HNO}_3/\text{H}_2\text{C}_2\text{O}_4/\text{HF}$ should be conducted. The results would then be compared with those previously obtained from residual solids leaching tests performed with HNO_3/HF .

It is likely that the dissolution rate of uranium fuel fragments will determine how long each batch of K Basin sludge will be processed in the baseline process. Consequently, more precise data are needed on fuel fragment dissolution. Tests should be conducted in which one or several fuel fragments of known size and geometry are added to the dissolver. The uranium concentration in the dissolver would be tracked over time.

To accelerate the fuel fragment dissolution rates, the use of chemical reagents and increased nitric acid concentrations should be investigated through additional dissolution testing. Chemical reagents that could increase the dissolution rates include phosphoric acid and fluoride [HF or $(\text{NH}_4)_2\text{SiF}_6$].

The target level of decontamination that must be achieved in the acid dissolution process needs to be set. While testing showed that further decontamination of the residual solids was being achieved at longer dissolution periods, it may be more efficient to cut the dissolution time down and perform more aggressive leaching on the small volume of residual solids. Further dissolution testing with more frequent solids sampling may be required to resolve this issue.

Fresh KE Basin sludge material will be acquired in early CY 1999. Dissolution testing, including offgas analyses, should be conducted using this material since it will likely be more representative of the sludge that will be treated in the actual process. The sludge composites used for the validation testing were built from individual samples that had been archived for 2 to 3 years. The fresh sludge may contain higher concentrations of metallic uranium and reduced uranium compounds, and has the potential to be more chemically reactive (e.g., produce more offgas and heat) during acid dissolution.

Acknowledgments

The authors would like to acknowledge Jim Boyd of the EM-67 Fuel Stabilization Program for his financial support and Bob Holt of DOE-RL for his efforts in making this opportunity a successful one.

The technical basis and end-user contributions provided by Thierry Flament, Chris Peterson, and Wally Rutherford of Numatec Hanford Corporation significantly enhanced the value of this research effort.

Programmatic support from Ron Baker, Duke Engineering & Services Hanford Sludge Characterization Project, ensured the availability of characterized K Basin sludge and fuel materials and provided significant technical oversight.

The authors would also like to gratefully acknowledge the support of other project staff at PNNL who contributed to the successful completion of this report: I. E. Burgeson, O. P. Bredt, K. J. Smith, R. T. Steele, F. V Hoopes, J. L. Ryan, C. Z. Soderquist, S. K. Fiskum, L. R. Greenwood, R. T. Ratner, M. W. Urie, J. J. Wagner, D. R. Sanders, T. L. Almeida, K. K. Thomas, L. P. Darnell, T. L. Trang-Le, J. M. Tingey, and R. J. Elovich.

Contents

Summary and Conclusions	iii
Acknowledgments	xi
1.0 Introduction	1.1
2.0 Test Matrix	2.1
2.1 Summary Description of Test 1	2.1
2.2 Summary Description of Test 2	2.1
2.3 Summary Description of Test 3	2.2
3.0 Materials, Equipment, and Approach	3.1
3.1 Test Materials	3.1
3.1.1 KE Canister Sludge Composite	3.1
3.1.2 KE Areas Sludge Composite	3.2
3.1.3 Fuel Fragments	3.5
3.1.4 Ion Exchange Material	3.5
3.2 Equipment Description	3.6
3.2.1 Dissolver Vessel Size	3.6
3.2.2 Heating System	3.9
3.2.3 Agitation System	3.9
3.2.4 Liquid/Slurry Sampling Port	3.9
3.2.5 Sludge/Solid Feed Addition	3.9
3.2.6 Liquid Addition	3.9
3.2.7 Purge/Cover Gas Injection	3.9
3.2.8 Offgas Condenser	3.10
3.2.9 Offgas Sampling Port	3.10
3.2.10 Offgas Analysis System	3.10
3.2.11 Conductivity/Temperature Measurement	3.10
3.3 Test Approach	3.11
3.3.1 Feed Preparation	3.11
3.3.2 System Startup	3.11
3.3.3 Offgas Analysis	3.12
3.3.4 Sludge/Feed Addition	3.12
3.3.5 Acid Addition	3.13
3.3.6 Sample Collection	3.13
3.3.7 Collection of Residual Solids	3.13
3.3.8 Sample Analysis	3.13
4.0 Results and Discussion	4.1
4.1 Shakedown Testing	4.1
4.1.1 Physical/Uranium Sludge Simulant Shakedown Tests	4.1
4.1.2 Chemical Simulant Shakedown Testing	4.2
4.1.3 Shakedown, Demonstration, and Calibration of the Conductivity Probe	4.2

Contents (continued)

4.2	Test 1	4.3
4.2.1	Qualitative Results	4.3
4.2.2	Temperature and Electrical Conductivity.....	4.6
4.2.3	Hydrogen Ion and Metal Concentration Analyses	4.6
4.2.4	Residual Solids Concentrations.....	4.7
4.2.5	Residual Solids Particle Size Distribution.....	4.8
4.2.6	Fractional Dissolution	4.10
4.2.7	Material Balance.....	4.11
4.3	Test 2	4.11
4.3.1	Qualitative Results	4.11
4.3.2	Temperature and Electrical Conductivity.....	4.14
4.3.3	Hydrogen Ion and Metal Concentration Analyses	4.16
4.3.4	Residual Solids Concentrations.....	4.16
4.3.5	Residual Solids Particle Size Distribution.....	4.19
4.3.6	Fractional Dissolution	4.19
4.3.7	Material Balance.....	4.20
4.4	Test 3	4.21
4.4.1	Qualitative Results	4.21
4.4.2	Temperature and Electrical Conductivity.....	4.24
4.4.3	Metal Concentration Analyses	4.25
4.4.4	Residual Solids Concentrations.....	4.26
4.4.5	Residual Solids Particle Size Distribution.....	4.28
4.4.6	Fractional Dissolution	4.29
4.4.7	Material Balance.....	4.29
4.5	Evaluation and Comparison of Residual Solids Compositions	4.31
4.5.1	ERDF Criteria	4.31
4.5.2	KE Canister Sludge Residual Solids	4.32
4.5.3	KE Areas Sludge Composite Residual Solids	4.34
4.5.4	Plutonium Concentrations on Residual Solids	4.35
5.0	Dissolver Offgas Analysis.....	5.1
5.1	Offgas Analysis, Sampling, and Instrumentation	5.1
5.2	Calibration	5.2
5.3	Data Acquisition	5.4
5.4	Quantitation	5.4
5.5	Results and Discussion	5.5
5.5.1	System Response Time Tests	5.5
5.5.2	Test 2 System Performance.....	5.5
5.5.3	Test 3 System Performance.....	5.6
5.5.4	Quantities of Gas Projected in Validation Testing.....	5.6
5.5.5	Comparison of Projected and Measured Offgas Quantities	5.9
6.0	References	6.1

Contents (continued)

Appendix A Photographs from Test 1	A.1
Appendix B Photographs from Test 2	B.1
Appendix C Photographs from Test 3	C.1
Appendix D Mass Spectrometry Offgas Data for Test 2.....	D.1
Appendix E Gas Chromatography Offgas Data for Test 2.....	E.1
Appendix F Mass Spectrometry and Gas Chromatography Offgas Data for Test 3	F.1
Appendix G Electrical Conductivity Measurements of Nitric Acid Solutions.....	G.1

Tables

2.1	Parameters and Conditions for Dissolution Validation Testing	2.1
3.1	KE Sludge and Materials Used for Dissolution Tests	3.1
3.2	Samples Used to Build the KE Canister Sludge Composite	3.1
3.3	Concentrations of Key Radionuclides and Chemical Constituents in KE Canister Sludge Composite (Dry Basis)	3.2
3.4	KE Weasel Pit Sludge Composite	3.3
3.5	KE Floor Sludge Composite.....	3.3
3.6	KE Areas Sludge Composite.....	3.4
3.7	Concentrations of Key Radionuclides and Chemical Constituents in KE Areas Sludge Composite.....	3.4
3.8	Concentrations of Key Radionuclides and Chemical Constituents in IX Material (Sample H-08 Bead G)	3.6
3.9	Functional Requirements for K Basin Sludge Dissolution Test System	3.7
3.10	Analytical Procedures.....	3.14
4.1	Event History for Dissolution Test 1.....	4.4
4.2	Chemical Concentrations in Test 1 Dissolver Solutions	4.8
4.3	Chemical and Radionuclide Concentrations in Test 1 Residual Solids.....	4.9
4.4	Overall Particle Size Distribution for Test 1 Residual Solids	4.9
4.5	Particle Size Distribution Below 6 Microns for Test 1 Residual Solids.....	4.9
4.6	Material Balance for Test 1	4.11
4.7	Event History for Dissolution Test 2.....	4.13
4.8	Chemical and Radionuclide Concentrations in Test 2 Dissolver Solutions	4.16
4.9	Radioelement Concentrations in Zircaloy Cladding Residues from Test 2 and from Previously Reported Tests	4.17
4.10	Chemical and Radionuclide Concentrations in Test 2 Particulate Residual Solids.....	4.18
4.11	Overall Particle Size Distribution for Test 2 Residual Solids	4.19

Tables (continued)

4.12	Particle Size Distribution Below 6 Microns for Test 2 Residual Solids.....	4.19
4.13	Material Balance for Test 2	4.21
4.14	Event History for Dissolution Test 3	4.22
4.15	Chemical and Radionuclide Concentrations in Test 3 Dissolver Solutions	4.26
4.16	Chemical and Radionuclide Concentrations in Test 3 Residual Solids.....	4.27
4.17	Chemical and Radionuclide Concentrations in Test 3 Ion Exchange Materials	4.28
4.18	Overall Particle Size Distribution for Test 3 Residual Solids	4.28
4.19	Particle Size Distribution Below 6 Microns for Test 3 Residual Solids.....	4.29
4.20	Material Balance for Test 3	4.30
4.21	Equivalent Concentrations for the ERDF Criteria.....	4.32
4.22	Chemical and Radionuclide Concentrations in KE Canister Sludge Residual Solids and Comparison to ERDF Criteria	4.33
4.23	Chemical and Radionuclide Concentrations in KE Floor and Weasel Pit Sludge Residual Solids	4.34
5.1	Calibration Gases Used As Standards	5.3
5.2	Gases Used As Cover/Internal Standards During Testing.....	5.4
5.3	Mass Spectrometer Quantitation Ions and Corrections for Gas Components	5.5
5.4	Projected Quantities of Offgas	5.8
5.5	Quantities of Carbon Dioxide in Tests 2 and 3	5.9
5.6	Equivalents of Nitrate Reduction Gases in Tests 2 and 3.....	5.10

Figures

1.1	Conceptual Flowchart for Baseline K Basin Sludge Pretreatment Process.....	1.2
3.1	Schematic of Experimental Dissolver	3.8
4.1	Conductivity and Temperature Measurements of Test 1.....	4.7
4.2	Fractions of Analytes Dissolved in Test 1 as a Function of Time.....	4.10
4.3	Conductivity and Temperature Measurements of Test 2.....	4.15
4.4	Fractions of Analytes Dissolved in Test 2 as a Function of Time.....	4.20
4.5	Conductivity and Temperature Measurements of Test 3.....	4.25
4.6	Fractions of Analytes Dissolved in Test 3 as a Function of Time.....	4.30
4.7	Plutonium Concentrations in Solid Residues as a Function of Plutonium Solution Concentrations from Nitric Acid Treatment and Leaching of K Basin Sludge.....	4.36
4.8	Cesium-137 Concentrations in Solid Residues as a Function of Cesium-137 Solution Concentrations from Nitric Acid Treatment and Leaching of K Basin Sludge.....	4.37
5.1	Schematic of Offgas Flow and Analysis System for K Basin Sludge Dissolution Testing	5.2
5.2	NO ₂ :NO Ratio as a Function of Total (NO ₂ + NO) Pressure	5.11

1.0 Introduction

Two water-filled concrete pools [K East (KE) and K West (KW) Basins] in the 100K Area of the Hanford Site contain over 2100 metric tons of N Reactor fuel elements stored in aluminum or stainless steel canisters. During the time the fuel has been stored, approximately 52 m³ of heterogeneous solid material, sludge, have accumulated in the K Basins. The sludge is located in the fuel canisters, as well as on the floor and in the associated pits. This sludge is a mixture of spent fuel element corrosion products, ion exchange (IX) material (organic and inorganic), graphite-based gasket materials, iron and aluminum metal corrosion products, sand, and debris (Makenas et al. 1996, 1997, 1998). The inventory and compositions of all K Basin sludge materials are described in detail by Pearce et al. (1998). Ultimately, it is planned to transfer the K Basin sludge to the Hanford double shell tanks (DSTs), managed under the Tank Waste Remediation Systems (TWRS). Pretreatment is required to address criticality and pyrophoricity issues and to destroy or remove polychlorinated biphenyls (PCBs), found in some samples, before the K Basin sludge can be transferred to the DSTs.

The baseline K Basin Sludge Pretreatment Process is nitric acid (HNO₃) dissolution of particulate material passing a ¼-in. screen. In this process, the acid-insoluble (residual solids) fraction will be washed and leached as necessary and then transferred to the Environmental Restoration Disposal Facility (ERDF). The dissolver solution will be mixed with depleted uranium and iron nitrate for criticality safety, and neutralized and made alkaline through caustic [sodium hydroxide (NaOH)] adjustment. Pending vitrification, the alkaline liquid fraction and associated precipitates will be stored in the TWRS. The baseline K Basin Sludge Pretreatment Process, shown in Figure 1.1, is described in detail by Westra et al. (1998).

The work described here involved comprehensive testing of nitric acid dissolution to confirm the baseline pretreatment process. In addition, material balance information was collected to support the development and refinement of process flow diagrams. The testing was performed by Pacific Northwest National Laboratory (PNNL) for the U.S. Department of Energy's Office of Spent Fuel Stabilization (EM-67) and Numatec Hanford Corporation (NHC) to assist in the development of the K Basin Sludge Pretreatment Process. The work was performed in accordance the Statement of Work for Task 2 of the K Basin Sludge Process Design and Evaluation Project. The testing was also consistent with the objectives and approach described in the report, "Testing Strategy to Support the Development of K Basin Sludge Treatment Process" (Flament 1998). All testing and analyses were conducted in accordance with the Quality Assurance Project Plan for Project #28004.

In the baseline K Basin sludge retrieval plans, two sludge process streams from KE Basin will require pretreatment (Westra et al. 1998; Pearce et al. 1998). Stream 1 will be composed of sludge less than 6.35 mm (6.35 mm = 6350 µm = ¼ in.) from the Weasel Pit, various other basin pits, the floor area, as well as particles less than 250 µm generated during canister and fuel washing steps. Stream 2, KE dropout drum sludge, will be composed of particles between 250 µm and 6350 µm generated during canister and fuel washing steps.

Under separate projects, initial testing with K Basin simulant material and actual K Basin sludge has been performed to examine K Basin sludge pretreatment (Makenas 1999; Carlson et al. 1998a, b). Results from this testing and from engineering evaluations have provided information to establish the initial baseline process conditions (Westra et al. 1998).

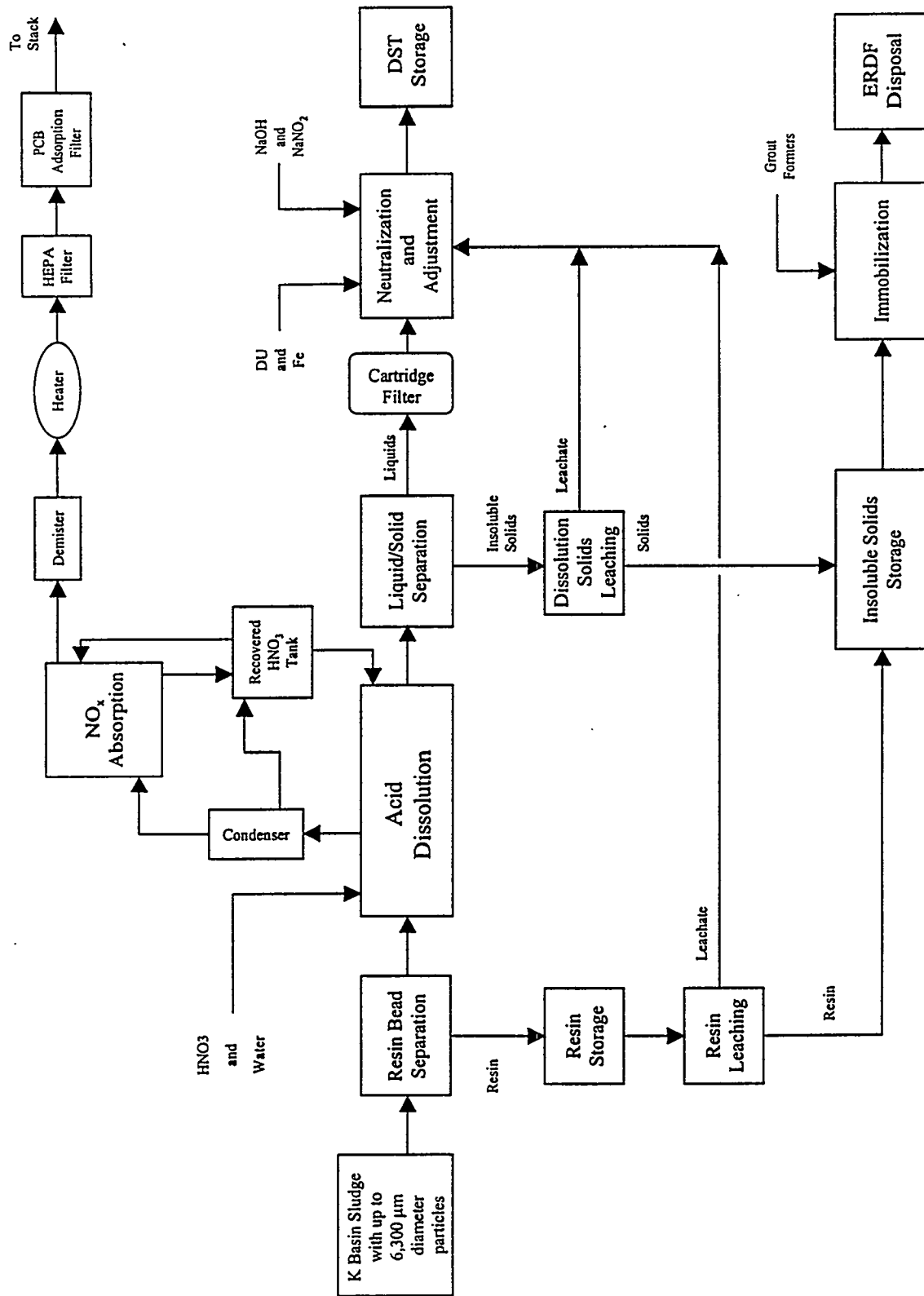


Figure 1.1. Conceptual Flowchart for Baseline K Basin Sludge Pretreatment Process

The objectives of the work discussed in this report were to examine the dissolution behavior of actual KE Basin sludge materials at baseline flowsheet conditions, validate the dissolution process step through bench-scale testing, and evaluate online methods to monitor the process (i.e., temperature, solution electrical conductivity, and offgas composition and generation rates). The effectiveness of the dissolution was evaluated by measuring the concentrations of key species in the dissolver solutions as a function of reaction (dissolution) time, and by analyzing intermittent and final acid-insoluble solids. The test system and strategies for feed addition and sample collection were designed to assess parameters that can influence sludge dissolution and to provide information for determining the operating conditions for the actual system.

Three tests were performed in a 1-L dissolver vessel with ~60 g of material in each test. The test materials were sludge composites representative of the KE Stream 1 (KE Basin floor and Weasel Pit sludge) and the KE Stream 2 (KE canister sludge and fuel fragments). The sludge composites were built by combining portions of individual sludge samples that were originally collected for characterization purposes. The two composites used for this testing were KE Canister Sludge Composite and KE Areas Sludge Composite (built from KE floor and KE Weasel Pit sludge samples). For the testing with the stream representative of Stream 2, a series of irradiated uranium fuel fragments and a series of KE Canister Sludge Composite samples were sequentially added to the dissolver.

A Research and Development (R&D) permit (EPA 1997) under the Toxic Substance Control Act (TSCA) was pursued and obtained on December 17, 1997, under this project. The R&D permit was required because the PCB in the actual K Basin sludge was subjected to treatment. PNNL was able to expiate the permitting process by amending an existing TSCA R&D permit issued by the U.S. Environmental Protection Agency's Office of Pollution Prevention and Toxics.

This report presents the results of the nitric acid dissolution testing with the actual KE Basin materials. Section 2.0 provides the test matrix and summarizes the three tests. Section 3.0 describes the materials, equipment, and approach used for the experiments. The materials included the KE Canister Sludge Composite; KE Areas Sludge Composite (floor and Weasel Pit); the fuel fragments; and ion exchange material [organic ion exchange resin (OIER) and inorganic ion exchange material (Zeolon-900)], which has been found in some KE sludge samples (Makenas et al. 1996). The equipment was selected based on functional requirements and key parameters affecting nitric acid dissolution. Before the tests on actual samples were conducted, shakedown testing was performed to verify system performance. For the three validation tests, the process steps consisted of feed preparation, system startup, startup of offgas analysis equipment, sludge/feed addition, acid addition, sample collection, residual solids collection, and sample analysis. Section 4.0 discusses both qualitative and quantitative results and how these results further validate the baseline K Basin Sludge Pretreatment Process. Results of offgas analyses, performed for Tests 2 and 3, are provided in Section 5.0. Appendices A through C include photographs from videotapes used for the qualitative analysis (Tests 1 through 3, respectively). Plots from the offgas analyses are provided in Appendices D through F. Appendix G provides results on the influence of iron, aluminum, uranium, nitric acid, and temperature on solution electrical conductivity measurements (to assist in interpretation of conductivity data acquired from the dissolution testing).

2.0 Test Matrix

Following a series of cold shakedown tests (described in Section 4.1), three dissolution validation tests were conducted using actual K Basin sludge materials (described in Section 3.1). Table 2.1 summarizes the parameters and conditions used for the tests. An overview of each test is given here, with detailed descriptions and results presented in Sections 4.2 through 4.5.

Table 2.1. Parameters and Conditions for Dissolution Validation Testing

Parameter/Condition	Test 1	Test 2	Test 3
Test Start Date	7/23/98	8/5/98	8/19/98
Feed Material and Mass (dry basis)	KE Canister Sludge, 71.3 g	Fuel fragments, 30.7 g; KE Canister Sludge, 40.0 g	KE Areas Sludge Composite, 52.7 g; IX material, 1.98 g (air dry)
HNO ₃ Concentration	6 <u>M</u>	6 <u>M</u>	6 <u>M</u>
HNO ₃ Volume, ml	498 ml	500 ml 6 <u>M</u> (start) + 80 ml 16 <u>M</u> (during run) 580 ml – total	550 ml 6 <u>M</u> (start) + 150 ml 16 <u>M</u> (during run) 700 ml – total
Solids Content (mass of initial solids divided by total acid volume)	146 g/L	122 g/L	75 g/L
Dissolution Temp.	95°C	95°C	95°C
Dissolution Time, starting after final sludge addition	20 hr	21 hr – Fuel fragments 6 hr – Canister sludge	7 hr
Conductivity monitoring	yes	yes	yes
Offgas Analysis	no	yes	yes

2.1 Summary Description of Test 1

Test 1 was conducted to examine the dissolution behavior of KE Canister Sludge Composite at a significantly larger scale than in previous testing (Carlson et al. 1998a). In Test 1, ~71 g (dry basis) of sludge were added to the dissolver in 15 separate additions over a 4-hr period. The additions ranged from 0.28 g to 9.1 g (settled sludge basis). The dissolver contained about 500 ml 6 M HNO₃, which had been preheated to 95°C. After the last sludge addition, the material in the dissolver test vessel was dissolved for an additional 20 hr at 95°C.

2.2 Summary Description of Test 2

Test 2 was conducted using two types of sludge material: 1) fuel fragments (less than ¼-in. diameter) and 2) KE Canister Sludge Composite. First, ~31 g of fuel fragments (collected during examination and characterization of KE fuel elements) were added to the dissolver in 11 separate additions (each addition consisted of a fuel fragment from to ~0.25 to ~6 g). Next, after the fuel fragments had been subjected to

dissolution at 95°C for ~14 hr, ~40 g (dry basis) of KE Canister Sludge Composite were added in six separate additions (5.7 to 7.9 g for each addition – dry basis). After the last sludge addition, the material in the dissolver test vessel was dissolved for an additional 6 hr at 95°C. During the dissolution, several additions of 16 M HNO₃ were made to replenish the solution with acid consumed during the dissolution reactions (i.e., maintain the HNO₃ concentration in the dissolver at 6 M).

The dissolver vessel offgas was sampled and analyzed during the run. By separating the fuel fragment addition from the KE canister sludge addition, offgas data were generated for the dissolution of two different types of sludge material.

2.3 Summary Description of Test 3

Test 3 was conducted to examine the dissolution behavior of the KE Areas Sludge Composite. In addition to the sludge dissolution, approximately 2 ml of IX material (organic and inorganic) from KE Basin floor sample KES-H-08, contained within a stainless steel mesh module, were suspended in the dissolver solution to determine the uptake/release of radionuclides from IX material during dissolution. [For this report, the sludge material that contains a mixture of OIER and the inorganic ion exchange material, likely Zeolon-900, is referred to as IX material.] The module was constructed of a stainless steel screen to allow good exchange of the dissolved species in solution with the IX material. By keeping the IX material separated from the sludge, the need for complex bead/residual solids separation at the conclusion of the dissolution test was avoided.

The KE Areas Sludge Composite (~53 g, dry basis) was added to the dissolver in 10 incremental additions (4.6 to 6 g for each addition – dry basis) over a period of about 2 hr. After all sludge was added, the material was subjected to dissolution for 6 hr at 95°C. During the dissolution, several additions of 16 M HNO₃ were made to replenish the solution with acid consumed during the dissolution reactions (i.e., maintain the HNO₃ concentration in the dissolver at 6 M). Dissolver vessel offgas was continuously sampled and analyzed during the run.

During previous dissolution testing with the KE Areas Sludge Composite (Carlson et al. 1998b), significant gel formation was noted. In those tests at 6 M HNO₃, gel formation was observed after about 7 hr at boiling temperatures. By the time the test was completed (24 hr) a translucent precipitate (believed to be gel) coated the glass walls of the thermowell. In Test 3, a vigorous rate of stirring was maintained, a shorter dissolution (6 hr) period was used, and the dissolution was conducted at a lower temperature (95°C compared to boiling). Furthermore, in Carlson et al. (1998b), the 6 M HNO₃ test was conducted at an initial solids loading of 14 g/L, which is about 9-fold less than that used for Test 3. These test parameter differences were anticipated to have an impact on gel formation.

3.0 Materials, Equipment, and Approach

The materials, equipment, and approach used for the tests are detailed here.

3.1 Test Materials

Dissolution validation tests were conducted using two KE sludge composites, KE fuel fragments, and IX material. This section describes the sludge composites and preparation, the fuel fragments, and the IX material. Table 3.1 shows which KE Basin materials were used for each dissolution test.

Table 3.1. KE Sludge and Materials Used for Dissolution Tests

Dissolution Validation Test No.	Quantity of Material – dry basis, g (settled sludge, wet basis, g)			
	KE Canister Comp.	KE Areas Comp.	Fuel Fragments	IX Material
Test 1	71.3 (90.9)	--	--	--
Test 2	40.0 (50.3)	--	30.67	--
Test 3	--	52.7 (88.1)	--	1.98 - air dried

3.1.1 KE Canister Sludge Composite

The KE Canister Sludge Composite was prepared as described below. This composite contains a relatively high concentration of uranium (assumed to exist primarily in the form of UO₂) and high concentrations of radionuclides. Testing has shown that this sludge reacts rapidly with nitric acid.

Table 3.2 shows the individual KE canister samples used to prepare the KE Canister Sludge Composite. The individual samples used for the composite are described in detail, including physical, chemical, and radiochemical characterization results, in Makenas et al. (1997). Many of the individual samples were dry and were reconstituted with deionized water to restore the samples to an “as-settled” sludge basis before the composite was built. The final composite was a thick, brown slurry that flowed very slowly.

Table 3.2. Samples Used to Build the KE Canister Sludge Composite

Sample	Dry Mass, g	Wet Mass, g	Wt% Solids	Mass Water, g	Dry in Comp., g	Wet in Comp., g
96-01	61.92	84.37	73.39	22.45	61.92	84.37
96-05	62.92	87.03	72.30	24.10	62.92	87.03
96-06 L	74.05	96.04	77.10	21.99	74.05	96.04
96-06 M/L	57.37	74.83	76.67	17.46	57.37	74.83
96-08	45.45	88.62	51.28	43.17	39.03	76.11
96-13	124.54	158.14	78.75	33.61	124.54	158.14
96-15	57.37	93.47	61.39	36.09	57.37	93.47
Total	483.62	682.51	70.86	198.89	477.21	670.00

Significant differences were found in the concentrations of radionuclides in duplicate aliquots used to characterize the KE Canister Sludge Composite (Table 3.3). These differences indicate that its composition, even after extensive mixing, is not homogeneous. Thus, it cannot be assumed that the KE Canister Sludge Composite used for the dissolution tests contained radionuclides at the same concentration as the aliquots used to characterize the composite. Therefore, unless indicated otherwise, the composite characterization data for the evaluation of the dissolution test results were not used. Rather, for each test, the quantities of the radionuclides in the starting material were calculated by summing the quantities of radionuclides measured in the individual dissolution fractions (i.e., quantities of radionuclides in the residual solids and final dissolver solution plus the quantities of radionuclides in all of the samples).

Table 3.3. Concentrations of Key Radionuclides and Chemical Constituents in KE Canister Sludge Composite (Dry Basis)

Analyte	Composite Sample	Duplicate Sample	RPD, %	Composite Average
U	619	752	19.4	685
Fe	12.0	12.1	0.83	12.0
Al	19.2	17.7	8.15	18.4
Si	7.66	7.55	1.45	7.60
Ca	1.14	1.22	6.79	1.18
¹³⁷ Cs	718	901	22.6	809
²⁴¹ Am	87.8	103	16.9	95.3
^{239/240} Pu	111	131	16.6	121

All results are in mg/g or $\mu\text{Ci/g}$.

RPD = Relative Percent Difference between duplicate analyses.

3.1.2 KE Areas Sludge Composite

The KE Areas Sludge Composite used in this testing was prepared from sludge samples obtained from the KE floor and Weasel Pit as described below. From a volume basis, the KE floor and Weasel Pit sludge account for approximately 60% of the total K Basin sludge inventory. This sludge contains relatively high concentrations of iron and silicon compounds.

For the KE Areas Sludge Composite, Weasel Pit and floor composites were first prepared individually, then combined. Tables 3.4 and 3.5 show the samples used to prepare the Weasel Pit composite and the KE floor composite, respectively. The individual samples used to build the composites are described in detail, including physical, chemical and radiochemical characterization results, in Makenas et al. (1996).

Both composites were dry sieved to remove OIER beads present in some of the samples. After sieving, deionized water was added to the composites to reconstitute the dry sludge to a wet "settled sludge." To make the final areas composite, 148.91 g of reconstituted KE floor composite were added to 144.42 g of reconstituted KE Weasel Pit composite. Table 3.6 shows the calculated quantities of each sample that comprises the KE Areas Sludge Composite. The resulting material was a brown slurry that flowed very easily.

Table 3.4. KE Weasel Pit Sludge Composite

Sample	Dry Solids Mass, g	After Sieving Mass, g
KES-P-16	54.79	51.97
KES-Q-17	13.04	12.37
KES-R-18	117.18	111.14
KES-S-19	57.39	54.43
KES-T-20	55.00	52.16
Total Solids	297.40	282.07
Water		114.39
Wt fraction Solids		0.71

Table 3.5. KE Floor Sludge Composite

Sample	Dry Solids Mass, g	After Sieving Mass, g
KES-A-02	0.59	0.48
KES-B-03	2.11	1.73
KES-C-04	0.58	0.48
KES-F-10	15.82	12.99
KES-G-07	1.88	1.54
KES-I-15	2.40	1.97
KES-K-12	2.47	2.03
KES-L-01	0.54	0.44
KES-N-05	9.72	7.98
KES-E-11	26.52	21.77
KES-J-06	45.50	37.36
KES-D-14	11.64	9.56
Total Solids	119.77	98.34
Water		85.19
Wt fraction Solids		0.54

Due to the inhomogeneity observed in the KE Areas Sludge Composite, unless otherwise indicated, throughout this report all comparisons will be made using the sum of the analyte in solution plus the analyte in the residual solids. Table 3.7 shows the comparison of the duplicate analyses for the composite material, the average concentrations, and the relative percent differences (RPDs) between the duplicate analyses. The species with the highest RPDs are ^{137}Cs and ^{241}Am .

Table 3.6. KE Areas Sludge Composite

Sample	Mass, g
KES-A-02	0.39
KES-B-03	1.41
KES-C-04	0.39
KES-F-10	10.54
KES-G-07	1.25
KES-I-15	1.60
KES-K-12	1.65
KES-L-01	0.36
KES-N-05	6.48
KES-E-11	17.67
KES-J-06	30.31
KES-D-14	7.75
KES-P-16	18.93
KES-Q-17	4.51
KES-R-18	40.49
KES-S-19	19.83
KES-T-20	19.00
Total Solids	182.54
Water	110.79

Table 3.7. Concentrations of Key Radionuclides and Chemical Constituents in KE Areas Sludge Composite

Analyte	Composite Sample	Duplicate Sample	RPD, %	Composite Average
U	54.8	53.3	2.8	54.0
Fe	307	291	5.4	299
Al	47.1	46.0	2.4	46.6
Si	60.0	61.1	1.8	60.5
Ca	11.5	13.0	12.3	12.2
¹³⁷ Cs	410	1240	101	825
²⁴¹ Am	29.4	81.1	93.7	55.2
^{239/240} Pu	11.9	16.3	31.2	14.1

All results are in mg/g or $\mu\text{Ci/g}$.

RPD = Relative Percent Difference between duplicate analyses.

3.1.3 Fuel Fragments

Fuel fragments used for dissolution testing were taken from spent fuel element SFEC 09-94-04 (2540E), which was stored in the KE Basin. The element, considered badly corroded, broke while being handled during fuel element characterization activities. Information on fuel element 2540E, and its associated fuel fragments, was obtained from Test Instruction SNF-CT-093, "Examination Requirements for Fuel Element 2540E" [Duke Engineering & Services Hanford (DESH)]. The KE fuel fragments used for the dissolution testing were stored in an inert atmosphere. Some of the fuel fragments had surfaces that appeared to be corroded (i.e., most likely covered with a layer of uranium oxide). Zircaloy-2 cladding (zirconium-1.5% tin) was bonded to some of the fuel fragments; however, the quantity of cladding associated with the fuel fragments could not be determined before the dissolution test. The quantities of radioactive fission and activation products also were not known. The fuel had been irradiated to about 2600 megawatt-days per metric ton of uranium (i.e., fuels grade; ~18% ²⁴⁰Pu). It was 0.95% ²³⁵U enrichment before irradiation.

Fragments that could pass through a ¼-in. (open area) screen were desired for the dissolution testing, and a number of existing fuel fragments (0.4 g to 6 g) were used. Additionally, to provide the required quantity, some larger fuel fragments were cut into smaller pieces using bolt cutters in an inert atmosphere. Figure B.1 (Appendix B) shows examples of fuel fragments used in Test 2.

3.1.4 Ion Exchange Material

Sample KES-H-08 was collected from the KE Basin floor near the north Load Out Pit. Sieving work showed this sample was approximately 75 wt% round OIER beads. In addition to the round OIER beads, other material, including white particulates between 355 µm and 1180 µm, was observed (see Appendix C). These white particulates appeared similar to Zeolon-900, an inorganic mordenite used as an ion exchange material at KE Basin. Results from an X-ray diffraction (XRD) analysis of sample KES-H-08 showed the presence of mordenite [nominally $(Ca,Na_2,K_2)Al_2Si_{10}O_{24} \cdot 7H_2O$]. The XRD pattern was practically identical to that found for as-received Zeolon-900 (Schmidt et al. 1998).

The IX material used in this work was excess material prepared for leaching investigations (Delegard and Rinehart 1998). Material from KES-H-08 was sieved and rinsed prior to testing to remove entrained sludge. Sieving was performed to remove oxide sludge and obtain a sample primarily containing OIER beads. Manufacturer specifications for the beads indicate that <2% of the beads are smaller than 400 µm. Given this lower limit for the bead diameter, a Tyler 42 sieve with 355-µm openings was used for the separation. The KES-H-08 sample was placed on the Tyler 42 sieve, and KE Basin supernatant was flowed over the sample until no more small dark particulates were visible and the rinse passing through the sieve appeared to be clear. The white particulates (~1 mm) could not be separated from the beads via sieving. Again, these particulates appeared to be similar in shape and color to Zeolon-900, and could be the mordenite identified in the bulk sample by XRD (see Figure C.6, Appendix C). Following sieving, the IX material was collected and the material was designated H-08 Bead G, and two sample aliquots were taken for radiochemical analysis (Table 3.8).

For the testing described in this report, the sample of IX material was air dried at room temperature since oven drying temperatures (105°C) could cause physical or functional damage to the OIER.

Table 3.8. Concentrations of Key Radionuclides and Chemical Constituents in IX Material (Sample H-08 Bead G)

Element Concentrations, $\mu\text{g/g}$					
Al	Ca	Fe	Na	Si	U
23600	20100	7630	55900	86200	2180
Radionuclide Concentrations, $\mu\text{Ci/g}$					
^{60}Co	^{137}Cs	$^{239,240}\text{Pu}$	^{241}Am	$^{238}\text{Pu}/^{241}\text{Am}$	Total Alpha
0.0403	103	0.168	0.148	0.186	0.362

3.2 Equipment Description

Table 3.9 lists the functional requirements for the test system, based on the actual K Basin Sludge Pretreatment Process. The key parameters that can influence nitric acid dissolution of sludge, and whose effects can be assessed by dissolution testing, include:

- sludge composition
- sludge addition rate
- nitric acid concentration
- excess nitric acid
- dissolution temperature
- dissolution time
- stirring
- sludge/acid solution ratio.

The test system (shown in Figure 3.1) was designed to evaluate these key parameters and address the functional requirements. A description of each component in the test system and how it meets the functional requirements (*see italics*) is provided below.

Figure 3.1 is a schematic diagram that shows the test system arrangement used for Test 3. For Test 2, an identical system arrangement was employed, except the mesh module for the IX materials was not used. In Test 1, the following items shown in Figure 3.1 were not used: Ne/He purge, sludge addition valve, offgas system (i.e., in Test 1, offgas from the condenser was vented into the hot cell), the mesh module, and stainless steel clad stir bar (for Test 1, a glass-coated stir bar was used).

3.2.1 Dissolver Vessel Size

1-L glass dissolution vessel. The K Basin Sludge Pretreatment Process will target a dry solids concentration in the feed material of approximately 120 g/L (Westra et al. 1998); therefore, the experimental dissolver was sized for operation at this target as well. For an alkali-treated actual dissolver batch containing very high concentrations of uranium (i.e., canister and fuel wash sludge), 120 g/L is near the limit that can be effectively and consistently pumped (J. L. Ryan. PNNL. "Neutralization of Uranyl Nitrate Solutions." Letter Report to Westinghouse Hanford Company, December 1992.).

Table 3.9. Functional Requirements for K Basin Sludge Dissolution Test System

Function/Item	Description/Qualification
Dissolver Vessel Size	Vessel must be sized to accommodate required functions and with consideration of quantity of available sludge material.
Heating System	System design must include a mechanism to heat and control the temperature of the slurry (up to boiling).
Agitation System	System design must include a stirring mechanism capable of providing a high shear rate to slurry.
Liquid/Slurry Sampling Port	System must include a port and mechanism for intermittent liquid and/or slurry sampling.
Liquid/Solid Addition	System must include a port and mechanism for introducing liquid, sludge, and solid to the dissolver vessel.
Purge/Cover Gas Injection	System must include a port for introducing a purge or cover gas to the dissolver head space.
Offgas Condenser	System must include a jacketed condenser on the offgas line, with closed-loop chilled (i.e., < 20°C) cooling fluid. All condensate will be returned to dissolution vessel.
Gas Sampling Port	The system must include a port for continuous offgas sampling.
Offgas Analysis System	The dissolution test vessel system must be integrated with an online offgas analysis system to detect and quantify offgas flow rate, O ₂ , NO, NO ₂ , N ₂ (or other appropriate means for air leak check), H ₂ , CO ₂ , CO. (Possibility to continuously monitor Xe and Kr is to be examined.)
Conductivity Measurement	The system must include provisions for continuous measurement of solution electrical conductivity.

Nominally, for the test system, each test run was conducted with 60 g (dry basis) of K Basin sludge/fuel fragments and 500 ml of dissolver solution (i.e., 6 M HNO₃). Additionally, with the conductivity probe selected for this system, the dissolver vessel must contain a minimum of 475 ml of solution to provide valid conductivity measurements.

A flat-bottom glass vessel was selected to allow visual monitoring of the reaction (all dissolution validation tests were videotaped). Also, glass is compatible with nitric acid at 95°C. The flat-bottom vessel design provided stability and compatibility with a flat hot plate/stirrer.

A five-port glass reactor head was clamped to the 1-L dissolver vessel. Five ports are necessary to accommodate the functional requirements given in Table 3.9 and shown in Figure 3.1.

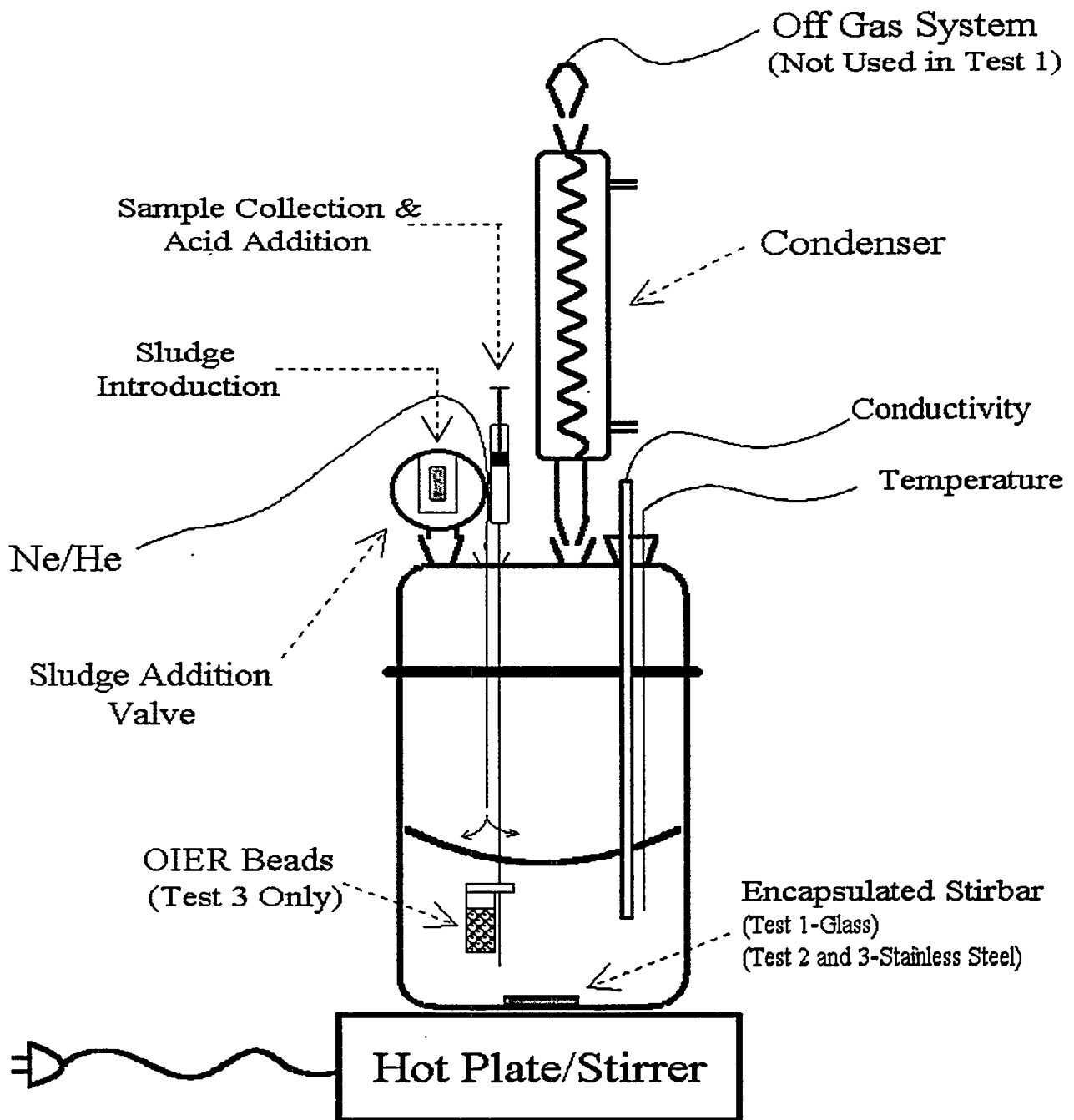


Figure 3.1. Schematic of Experimental Dissolver

3.2.2 Heating System

Hot plate. The dissolver vessel was heated to 95°C using an acid-resistant hot plate/stirrer. The hot plate (unlike a heating mantle) did not interfere with visual monitoring of the dissolution behavior. The high shear rates that were achieved with the stirrer resulted in a uniform temperature throughout the dissolver solution.

3.2.3 Agitation System

Stir plate and glass-coated or stainless steel clad stir bar. The initial plan was to agitate the dissolver solution with a stainless steel impeller connected to a motor drive system. However, during shakedown testing, the use of the magnetic stir bar provided very good agitation and significantly reduced the complexity of the dissolver system. Using the stir bar minimized vibrations to the system, and simplified assembly and operation in the hot cell.

3.2.4 Liquid/Slurry Sampling Port

Valved Luer-Lok sampling port with wide bore needle extending below the liquid surface. Liquid samples were collected using a standard Luer-Lok syringe. After a sample was collected, the syringe was removed from the system, and a 0.2- μm polyvinylidene fluoride (PVDF) syringe filter was used to filter the solution into a clean vial.

3.2.5 Sludge/Solid Feed Addition

Sample addition valve. Aliquots of sludge were loaded into syringes and submerged in a bath of liquid nitrogen. The frozen sludge pellets were added to the dissolver solution through a rotating ball-type valve that contained a sample chamber. Fuel fragments were also added to the dissolver through the sample addition valve. The material to be added to the dissolver was loaded into the sample chamber. Next, the valve was rotated 180 degrees, and the chamber contents dropped into the dissolver. While material was being discharged to the dissolver, the other side of the valve was sealed to the atmosphere to prevent air from being introduced into the dissolver system.

3.2.6 Liquid Addition

Valved Luer-Lok sampling port with wide bore needle extending below the liquid surface. The system used to collect liquid and slurry samples was also used for liquid (nitric acid) addition. Liquid addition through the sampling port was found to be less complicated than liquid addition through the sample addition valve.

3.2.7 Purge/Cover Gas Injection

Gas inlet with a tube extending ~2 in. above the liquid surface. The gas inlet was used to introduce a cover gas (e.g., He, N₂, O₂, air, etc.) mixed with a tracer gas (e.g., Ne) to the system and sweep off any gas generated by the dissolution. The swept gas was then carried through the condenser and collected at the gas sampling port. The inlet was plumbed such that standard gas mixtures (e.g., for calibration of gas analysis equipment) could be fed into the reactor to test the absorption/loss of any analytes of interest by the system.

3.2.8 Offgas Condenser

Graham-type condenser. The solution vapors were cooled and condensed using a Graham-type condenser supplied with recirculating chilled water. The cooling water from the condenser discharged into an open recirculation bath where it was pumped for return to the condenser. With dry ice addition to the recirculation bath, the recirculating cooling water could be maintained to a temperature of approximately 4°C.

3.2.9 Offgas Sampling Port

Gas sampling port at the top of the Graham-type condenser. The gas sampling port was used to collect the gas swept from the vessel by the cover gas. This gas was then sent to the offgas analysis system. By collecting the offgas sample downstream of the condenser, most of the water vapor in the offgas was removed, which resulted in more stable operation of the offgas analysis equipment.

3.2.10 Offgas Analysis System

The offgas analysis system included both a gas chromatograph with thermal conductivity detector (GC/TCD) and a mass spectrometer (MS). With this system, all gases of interest (O₂, NO, NO₂, N₂O, N₂, H₂, CO, CO₂, Xe, and Kr) could be quantified to measure the rate and extent of reaction. The quantification limits for O₂, N₂O, N₂, CO, and CO₂ are estimated to be on the order of 10 ppm. The quantification limits for NO and NO₂ are estimated to be in the range of 10 to 100 ppm. For H₂ the quantification level is estimated to be on the order of 1000 ppm. The preliminary estimates for the Kr detection limit with the MS is 10⁻⁷ to 10⁻⁵ g/ml. [According to ORIGEN2 calculations, the level of ⁸⁵Kr anticipated in a Mark IA spent fuel element (type of fuel fragment tested here) is approximately 3.9 g/MTU for a burnup of 3600 MWD/MTU. Assuming a 19-g U metal fuel chunk was introduced into the reactor with a cover gas flow of 20 ml/min, with a uniform dissolution over a 5-hr period, then the ⁸⁵Kr concentration should be 1.2⁻⁸ g ⁸⁵Kr /ml of offgas.] The offgas analysis system, including calibration procedures, is further described in Section 5.0.

3.2.11 Conductivity/Temperature Measurement

Conductivity/temperature probe with associated meter. The YSI Incorporated Model 3200 conductivity instrument was used to monitor the acid in the dissolution apparatus. The conductivity probes used (YSI Model 3440) have a cell constant of 10 cm⁻¹ (for high conductivity solutions). A new probe was used in each experiment. The probes subsequently were shortened (to accommodate the solution volume) and recalibrated, and were modified with a 24/40 glass joint so only the glass stem and electrodes contacted the solution or head space. Because temperature is critical to the conductivity measurement, as well as a key process parameter, this probe was operated with a thermistor or thermocouple (depending on the test), which was used to measure the temperature in the reactor.

3.3 Test Approach

For each dissolution validation test, a detailed test instruction was prepared, reviewed, and approved by cognizant staff from PNNL and NHC. Additionally, concurrence on the test instructions was obtained from the DESH Sludge Characterization Group, stewards of the sludge samples used for the testing. The test instructions identified the test objectives, summarized the approach, specified the test conditions, detailed the test procedures, and identified sampling and analytical requirements. An overview of the testing is provided below.

3.3.1 Feed Preparation

Before each run, the feed material was selected and the required quantity prepared. For the sludge composites, since wet, or as-settled, sludge was used, the percent moisture was determined by drying (105°C) two aliquots of the composite material. From the percent moisture value, the total quantity of sludge composite in the tests was calculated on a dry sludge basis.

For the actual K Basin Sludge Pretreatment Process, it is planned to continuously feed sludge to the dissolver for a period of time (Westra et al. 1998). Therefore, to simulate the process, 0.25- to 10-g portions of the "as-settled" sludge were loaded into preweighed, modified, 10-ml plastic syringes (i.e., the tops of syringes were cut off and beveled to allow insertion of a second plunger into the barrel of the syringe). The second plunger was inserted to confine the sludge. The loaded syringes were weighed, and the mass of "as-settled" sludge in each syringe was calculated. Just before the dissolution tests began, the loaded syringes were submerged into a liquid nitrogen bath to freeze the sludge. The frozen sludge pellets were then fed to the dissolver vessel through the sample addition valve (see Section 3.3.4).

For Test 2, additional small irradiated uranium metal fuel fragments were obtained as-received or by shearing larger pieces with a steel bolt cutter. The large fragments were positioned in the bolt cutter, and a plastic bag was placed around the cutters. Argon gas was flowed into the bag for several minutes to displace the air in the bag, and the pieces then were sheared. Some sparks were observed during the shearing. All fuel fragments used for the testing were placed in weigh boats, videotaped, and weighed. The fuel fragments were kept in the weigh boats for ~12 hr before being added to the dissolver vessel.

IX material was placed in the stainless steel module that was submerged in the dissolver solution during Test 3. The mesh screen allowed good contact between the IX material and the dissolver solution and kept the IX material from dispersing into the vessel. The IX material used in this test was air-dried sample H-08 Bead G (Section 3.1.4).

3.3.2 System Startup

For each test, the masses of the dissolver vessel body and the stir bar (glass coated or stainless steel clad) were determined. The test system was completely assembled, including installation of the condenser and cooling water system and the conductivity and temperature probes. For Tests 2 and 3, the purge gas line and offgas sampling line were installed (offgas sampling and analyses were not performed for Test 1).

Following system assembly, generally 500 ml of 6 M HNO_3 were added to the dissolver vessel, and the acid solution was heated to 95°C. For Test 1, sludge was added shortly after the acid temperature reached 95°C; however, it took several hours for the system temperature to stabilize. Consequently, for Tests 2 and 3, the acid solution was first held at 95°C for several hours to ensure that temperature stability was achieved throughout the tests.

Conductivity data and temperature data were collected once every 5 s for the entire duration of each test. A section of the glass was removed from the conductivity probe to decrease the level of the acid solution necessary to immerse the probe. Extensive calibration of the conductivity probe was performed using various solutions. The cell constant for the probe was determined before each test. During Test 1, gas bubbles collected within the protective glass sheath around the conductivity probe causing some erroneous conductivity measurements. The probes used in the subsequent dissolution tests were modified to mitigate this problem.

3.3.3 Offgas Analysis

Dissolver offgas was sampled and analyzed continuously during Tests 2 and 3. A cover gas of 10% Ne in a balance of He was flowed into the system at a rate of 500 ml/min through a piece of 1/16-in. stainless tubing. The tubing extended into the dissolver and down to ~2 in. above the surface of the dissolver solution. The dissolver was sealed, with the exception of a ¼-in. line running from the top of the condenser through the cell wall and into the hood containing the gas analysis system.

The dissolver offgas was analyzed using the GC/TCD and the MS. The GC was equipped with two columns and detectors and was primarily used to analyze the gas mixture for nonreactive components. The GC/TCD provided results every 2-3 min. The MS primarily analyzed the offgas for reactive components. While the MS is capable of providing results several times/second, signal averaging was used to provide a result every 5 to 10 s. Each instrument can analyze a number of the same gas components. This overlapping capability served to confirm the analytical results.

3.3.4 Sludge/Feed Addition

After the acid solution temperature stabilized at ~95°C, the sludge was added. For Test 1, since the offgas was not analyzed, frozen pellets of sludge were added directly into the dissolver by removing a glass stopper on the reactor head. For Tests 2 and 3, the sample addition valve was used to add the frozen sludge pellets and fuel fragments.

For Test 1, 15 frozen sludge pellets were added at 10- to 15-min intervals. The initial sludge additions were quite small (< 0.5 g). Once the sludge was observed to dissolve in a manageable manner, the quantity of the sludge per addition was increased to ~8 g.

For Test 2, fuel fragments and sludge were added sequentially. First, approximately 31 g of fuel fragments were added in 11 separate additions through the sample addition valve. The masses of the fuel fragments in the initial three additions were small (to verify that the dissolution behavior was manageable within the test system), then larger fragments were added. Once the dissolver had been maintained at 95°C for about 14 hr, the frozen sludge pellets were added.

For Test 3, approximately 53 g – dry basis (90 g as-settled) sludge were added to the dissolver through the sample addition valve in a series of 10 separate additions over a period of 2 hr and dissolved at 95°C for about 7 hr after the last sludge addition. The IX material in the module was placed into the dissolver vessel while the system was being assembled.

3.3.5 Acid Addition

In the actual K Basin Sludge Pretreatment Process, it is planned to operate the dissolver at a constant HNO_3 concentration of 6 M (Westra et al. 1998) with the sludge and HNO_3 added simultaneously. Therefore, to mimic the actual process, in Test 2 and 3, HNO_3 (16 M) was added to the dissolver solution once during feed addition and once after completion of feed addition. The purpose of these additions was to boost the HNO_3 concentration back up to 6 M, to replace the acid consumed in dissolution reactions. Acid was added with syringes through the liquid/slurry sampling port.

3.3.6 Sample Collection

3.3.6.1 Liquid Samples

Liquid samples (9 or 10 per test) were collected in plastic syringes through the liquid sampling port at specified times during the dissolution tests. These samples were then analyzed for key species to evaluate the effectiveness of the sludge dissolution as a function of dissolution time. Before each liquid sample was collected, agitation (stir bar) was turned off. The sample syringe was then attached to the Luer Lok fitting on the sampling port. Dissolver solution was pulled into the syringe and ejected back into dissolver two to three times to purge the sample line. Next, the sample was collected (~3 ml), and the syringe was disconnected from the sampling port and immediately filtered through a 0.2- μm PVDF Acrodisc filter (Gelman P/N 4406).

3.3.6.2 Slurry Samples

During Test 1, a slurry sample was collected 6 hr after the last frozen feed pellet was added. This sample was collected by lowering a glass bulb through one of the glass joints on the head of the dissolver vessel. In Tests 2 and 3, slurry samples were collected through the liquid/slurry sampling port 4 hr after the last sludge additions. The objective of the slurry sampling was to collect sufficient solids for chemical and radiochemical analyses to evaluate the level of decontamination that was achieved for the residual solids at an intermediate time during dissolution. The solids collected from the slurry sample were washed and rinsed as described in Section 3.3.7.

3.3.7 Collection of Residual Solids

When the specified dissolution period was completed, heating and agitation to the dissolver was stopped and the dissolver solution allowed to settle. After settling, the supernatant was decanted and filtered. A series of washes were performed on the insoluble residual solids: two washes with 2% HNO_3 and a final wash with deionized water. This procedure was also used to wash the solids associated with the slurry samples (Section 3.3.6). The decanted dissolver solution and the wash solutions were filtered.

3.3.8 Sample Analysis

Table 3.10 lists the procedures used for sample analyses.

Table 3.10. Analytical Procedures

PNNL Procedure Number	Procedure Title
Test Plan	Chemical Baseline Conditions
PNL-ALO-115	Solubilization of Metals from Solids Using a KOH-KNO ₃ Fusion
PNL-ALO-211	Determination of Elements by Inductively Coupled Argon Plasma Atomic Emission Spectroscopy
PNL-ALO-212	Determination of Inorganic Anions by Ion Chromatography
PNL-ALO-228	Determination of Hydroxyl (OH) and Alkalinity of Solutions, Leachates, & Supernates
PNL-ALO-268	Solids Analysis: X-Ray Diffraction Analysis
PNL-ALO-445	Solutions Analysis: Uranium by Laser-Excited Fluorescence
PNL-ALO-450	Gamma Energy Analysis (GEA) and Low-Energy Photon Spectrometry (LEPS)
PNL-ALO-417	Separation of Am & Pu and Actinide Screen by Extraction Chromatography
PNL-ALO-420	Solutions Analysis: Preparation of Alpha Sources by Direct Evaporation
PNL-ALO-421	Total Alpha Counting and Analysis
PNL-ALO-422	Solutions Analysis: Alpha Spectrometry
PNL-ALO-496	Precipitation Plating of Actinides for High-Resolution Alpha Spectrometry

3.3.8.1 Liquid Samples

The liquid samples collected during the runs were analyzed for U, Fe, Al, Ca, Si, Na, and other bulk metals using inductively coupled plasma (ICP), for NO₃⁻ and NO₂⁻ using ion chromatography (IC), and for H⁺ using titration. The final liquid samples (collected after completion of the dissolution) were analyzed for total alpha using alpha counting; for ^{239,240}Pu and ²³⁸Pu/²⁴¹Am using alpha energy analysis (AEA); for ¹³⁷Cs and ²⁴¹Am and others using gamma energy analysis (GEA); for U, Fe, Al, Ca, Si, Na, and other bulk metals using ICP; for NO₃⁻ and NO₂⁻ using IC; and for H⁺ using titration.

The rinse/wash solution from washing the IX material in Test 3 was analyzed for total alpha; for ^{239,240}Pu and ²³⁸Pu/²⁴¹Am using AEA; for ¹³⁷Cs and ²⁴¹Am using GEA; for U, Fe, Al, Ca, Si, Na, and other bulk metals using ICP; and for U using laser fluorimetry.

3.3.8.2 Residual Solid/Slurry Samples

All or a large fraction of the undissolved residual solids from the slurry samples were fused and analyzed for total alpha; for ^{239,240}Pu and ²³⁸Pu/²⁴¹Am using AEA; for ¹³⁷Cs and ²⁴¹Am using GEA; for U, Fe, Al, Ca, Si, Na, and other bulk metals using ICP; and for U using laser.

The residual solids remaining after completion of the sludge dissolution were analyzed as follows: 1) fusion followed by total alpha, AEA, GEA (for ¹³⁷Cs and ²⁴¹Am), ICP (for U, Fe, Al, Ca, Si, and other bulk metals), and U using laser; 2) drying (i.e., air drying); and 3) XRD.

The particle size distributions of the residual and intermediate slurry solids were measured by the use of the Microtrac X-100 Particle Analyzer and Ultrafine Particle Analyzer (UPA). The X-100 measures particle diameter in the range of 0.12 to 700 μm by light scattering from a laser beam projected through a stream of the sample particles dispersed in solution (1 M HNO_3 was the dispersant used in the present studies.) The UPA measures particle diameter by Doppler-shifted scattered light in the diameter range between 0.003 and 6.5 μm . Instrument performances were checked using NIST-traceable standards.

4.0 Results and Discussion

Results from the dissolution validation testing are provided in this section. First, a description of the equipment and protocol shakedown testing is presented, along with the key accomplishments of this work. Next, the three validation dissolution tests conducted with actual K Basin sludge materials are discussed. For each test, a description of the qualitative results is provided, including a table that summarizes the sequence of events. Results for the analysis of liquid and solids samples are also presented. The interpretation of the analytical results includes comparisons with previous testing.

4.1 Shakedown Testing

Before the dissolution tests with radioactive materials were initiated, an extensive shakedown testing process was conducted to develop testing protocols, validate the test configurations, and confirm the measurement techniques (i.e., conductivity and offgas analysis). Shakedown testing was expected to provide information on the capability of the apparatus to handle the actual test mixtures and to collect the information needed to prepare test instructions.

During the shakedown testing, protocols and equipment for sludge and solid addition, dissolver agitation, and sampling were investigated. Also, since the new dissolution testing apparatus had not yet been used, and because certain difficulties were observed with the previous experimental setup for dissolution tests (Carlson et al. 1998a, b), cold shakedown testing was required before the apparatus could be set up in the hot cells. This testing was used to identify needed modifications and provide operational experience for preparing the test instructions. Three types of tests were planned for the apparatus: 1) testing with a physical simulant and water, 2) testing with a gel-forming simulant and nitric acid, and 3) testing with a chemical simulant (for the generation of offgas to test the offgas analysis system). The planned testing with a gel-forming simulant was not conducted due to time constraints and since related gel formation/mitigation testing was inconclusive (Beck 1998).

4.1.1 Physical/Uranium Sludge Simulant Shakedown Tests

The shakedown tests to evaluate sample introduction, sample collection, and stirring techniques used several K Basin sludge physical simulants. Most of this testing involved a physical simulant (Prescott 1996), provided by the DESH K Basin Sludge Characterization group, that consisted of 17% tungsten powder, 8% flyash, 75% Hanford sand (by weight), and discrete pieces of tungsten metal (density = 19.4 g/cc). This simulant was representative of the high-density uranium sludges found in the K Basins. A physical simulant (Simulant 6) provided by Numatec's 222-S Laboratory was also tested (Duncan 1998).

The key accomplishments and findings from the physical shakedown testing are provided below:

- Neither a mechanical agitator nor a stir bar could suspend tungsten particles (density = 19.4 g/cc).
- Both a mechanical agitator and a stir bar successfully suspended and mixed the K Basin sludge physical simulants.
- While both the mechanical agitator and the stir bar would provide equivalent mixing, the stir bar was selected for the dissolution tests because of its simplicity (especially for hot cell applications). Additionally, use of the stir bar provides greater assurances that air in-leakage to the dissolver system can be minimized during testing with continuous offgas analysis.

- A technique was developed to add discrete quantities of sludge to the dissolver as frozen pellets. An apparatus (modified 10-ml syringe) was designed for loading and freezing sludge in the hot cells. The addition of frozen sludge minimizes the potential for sludge holdup/loss during feed addition.
- A sample addition valve was designed and fabricated for adding frozen sludge pellets to the dissolver without introducing air into the system; that is, the system remains sealed during sludge addition, which avoids perturbations to the offgas composition.
- A method for collecting liquid/slurry samples was developed and demonstrated. A wide-bore needle submerged in the dissolver solution allows samples to be collected without opening the system to air.
- A module was design and fabricated for introducing IX material, retrieved from the KE Basin floor and containing radionuclides, into the dissolver. With this module, the radionuclide uptake and elution of the IX material during dissolution can be measured.

4.1.2 Chemical Simulant Shakedown Testing

A chemical simulant (i.e., iron wire and iron powder) in nitric acid was used to test the offgas collection/analysis system. Secondary goals included determining the response/lag time for an event in the dissolver to be registered by the offgas analysis system.

The key accomplishments and findings from the chemical shakedown testing are provided below:

- Functionality and performance of the offgas analysis system were demonstrated. It was shown that NO and NO₂, the two most important offgas components in the K Basin Sludge Pretreatment Process, could be quantified.
- The system response/lag time was determined by injecting a slug of air into the dissolver vessel head space and measuring the time for its signal to appear on the MS.
- It was demonstrated that the test system could handle a reasonable offgas surge. A large offgas surge, from the addition of ~1 to 2 g of iron powder, disrupted the system (i.e., loosened glass fittings on the reactor head), but did not damage the test system. Iron wire dissolution offgas could be handled by the system.

4.1.3 Shakedown, Demonstration, and Calibration of the Conductivity Probe

The objectives of this testing were to validate the efficacy of the conductivity instrumentation and to determine the contributions of dissolved ferric nitrate [Fe(NO₃)₃] and aluminum nitrate [Al(NO₃)₃] to the total conductivity of the nitric acid dissolver solutions.

The conductivity probe (YSI Model 3440) measures the electrical conductance through solution between two cylindrical platinum black electrodes. The conductivity of 1.00, 4.00, and 6.00 M nitric acid solutions were measured at temperatures in the range 25°C to 95°C. The values were compared with published values to determine any bias in the instrument calibration.

The contribution of dissolved salt to the conductivity of acid solutions is low, on a mole basis (compared with that of the acid itself), because of the high conductance of the hydrogen ion. For example, the contribution of 0.2 M uranyl nitrate in 1 M HNO₃ to total conductivity is negligible and *decreases* the conductivity about 10% in 4 M HNO₃ (Schmieder and Kuhn 1972). Over this same range of HNO₃ concentration, the conductivity of HNO₃ itself increases over 2-fold from 0.3 to 0.7 ohm⁻¹-cm⁻¹. The conductivity of UO₂(NO₃)₂-HNO₃ solutions also increases about 1.3% per °C (derived from Slepyan and Karpacheva 1960). Thus, to a first approximation, with temperature compensation and some knowledge

of the sludge solids loading (expected not to exceed 120 grams per liter), electrical conductivity can provide a direct measure of acid concentration in $\text{UO}_2(\text{NO}_3)_2\text{-HNO}_3$ solutions.

After uranium and nitric acid, iron and aluminum nitrate will be the other major contributors to the dissolver solution electrolyte inventory. Therefore, tests were run to determine the conductivities of 0.20, 0.50, and 1.00 M $\text{Fe}(\text{NO}_3)_3$ and separate 0.10, 0.20, and 0.50 M $\text{Al}(\text{NO}_3)_3$ solutions in 1 and 4 M HNO_3 as a function of temperature in the range 25°C to 95°C. Results of the conductivity testing with the iron and aluminum nitrate solution are provided in Appendix G.

The key accomplishments and findings from the conductivity shakedown/calibration testing are provided below:

- The effects of a number of dissolved ions (at a range of concentrations and temperatures) on the solution conductivity were examined. The technical feasibility of using conductivity to track dissolution behavior in the nitric acid dissolver solution was demonstrated. From the shakedown testing, it was found that with the 1-L dissolver vessel, a minimum of 670 ml of dissolver solution was necessary to provide valid conductivity measurements with the YSI Model 3440 conductivity probe (due to the probe length). Therefore, the probe was shortened, its cell constant determined by use of solutions with known conductivities, and the required volume of dissolver solution was decreased to ~475 ml.

4.2 Test 1

Feed:	KE Canister Sludge Composite, 71.3 g
Acid:	498 ml, 6 <u>M</u> HNO_3
Temperature	95°C
Dissolution Time:	20 hr
Offgas Analysis:	none

4.2.1 Qualitative Results

Photographs from Test 1 (captured from the videotapes) are provided in Appendix A. The dissolution behavior of the KE Canister Sludge Composite was examined in 6 M HNO_3 . Approximately 490 ml of nitric acid were loaded into the dissolver and heated to approximately 95°C (Figure A.1). During the dissolution, the solution was stirred using a glass-coated magnetic stirrer. Gas analyses were not conducted during this test, nor was a cover gas used. The system was open to the air through the condenser.

The condenser was maintained between approximately 4°C and 15°C by additions of dry ice to the water recirculation bath. The temperature of the recirculation bath was monitored and recorded on a paper strip, but not captured on an electronic acquisition system.

During the sludge addition and for several hours afterwards, gas nucleated on the platinum electrodes within the conductivity probe and accumulated in the upper chamber of the probe. Although the upper chamber was equipped with a slit for the release of gas, it was not effective in preventing the accumulation of some gas in a pocket. The pocket that formed in the upper chamber caused a drop in the measured conductivity. By shaking the probe, it was possible to remove this gas and get a correct

reading. However, since the probe could not be shaken continuously, the initial few hours of the test show many spikes in the conductivity plot.

The temperature during the first several hours of Test 1 ranged from 86°C to 102°C. After several hours, the temperature stabilized and remained at ~95°C ±3°C.

A summary of sludge additions, sample collections, and other events is provided in Table 4.1. Run time (i.e., each test starting at time = 0:00) and actual clock time for the events are also included in Table 4.1. Actual clock time was included to allow the events to be correlated to the time scale recorded on the videotapes.

Table 4.1. Event History for Dissolution Test 1

Run Time	Clock Time	Event	Sample Mass, g (settled sludge basis)
0:10	11:20	Feed Sludge Addition #1	0.2787
0:19	11:28:40	Feed Sludge Addition #2	0.4157
0:29	11:39	Feed Sludge Addition #3	0.2832
0:41	11:51	Feed Sludge Addition #4	2.0692
0:51	12:01:27	Feed Sludge Addition #5	2.1437
1:07	12:17	Collect Solution #1	
1:17	12:26:50	Feed Sludge Addition #6	8.8136
1:30	12:39:30	Feed Sludge Addition #7	8.2384
1:50	12:59:50	Feed Sludge Addition #8	8.5281
2:12	13:22	Collect Solution #2	
2:17	13:27	Feed Sludge Addition #9	8.1454
2:30	13:40	Feed Sludge Addition #10	8.3651
2:53	14:03	Feed Sludge Addition #11	9.1588
3:10	14:20:00	Feed Sludge Addition #12	8.5957
3:29	14:39:00	Feed Sludge Addition #13	8.8551
3:52	15:02:40	Feed Sludge Addition #14	8.9820
4:14	15:24:21	Feed Sludge Addition #15	8.0324
4:40	15:50	Collect Solution #3	
5:19	16:29	Collect Solution #4	
6:25	17:35	Collect Solution #5	
10:07	21:17	Collect Slurry Sample	
16:10	3:20	Collect Solution #7 (skips #6)	
23:58	11:08	Collect Solution #8	
24:08	11:18	Heater off – Run Completed	
26:05	13:15	Collect Solution #9	

The frozen pellets (0.28 g to 9 g on a settled sludge basis) were introduced into the dissolver through one of the 24/40 glass joints. The first several additions (< 0.5 g each) were uneventful, and gas generation was not seen. The remaining additions were accompanied by gas bubbles observed in the solution and NO_x observed in the reactor head space. The offgas in the reactor head space was visible through the hot cell window, but difficult to see on the videotape of the run. The frozen pellets dissolved rapidly (15 to

60 s), and the NO_x lingered in the head space for as long as minutes after the sludge additions. Most sludge additions were made after the agitation to the dissolver (i.e., stir bar) was stopped; however, several additions were made with solution being stirred. Stirring did not appear to affect the rate at which the sludge pellets dissolved.

Dissolver solution samples were collected through the sampling port. The solution samples were blue-green, while the slurry in the dissolver appeared to be orange-brown. The solutions were collected through a valve that was later determined to be made from chrome-plated brass. Partial dissolution of this valve is a possible explanation of the blue color of the solutions.

At about 5 hr after the last sludge pellet addition, 9:15 (run time), the dissolver solution appeared to be yellow-green. The green coloration of solution produced by dissolving UO_2 pellets in nitric acid has been attributed to a combination of the yellow color of uranium(VI) and the blue color of dissolved N_2O_3 , the anhydride of nitrous acid, HNO_2 (Herrmann et al. 1984). At 20 hr after the last sludge addition, 24:00 (run time), it was noted that the particles in the dissolver solution appeared much larger and settled more rapidly (Figure A.2). These particles were more "floc-like" in nature than those observed 15 hr earlier.

Six hr after the last frozen sludge pellet addition, a slurry sample (~5 ml) was collected using a glass bulb lowered into the dissolver through one of the 24/40 joints. Settled solids were visible immediately after collecting the sample. Small, gel-like particulates were also observed in the sample.

When the test was completed, the dissolver solution was allowed to cool and settle. Significant quantities of a light gel-like particulate were suspended in the dissolver solution. This material was circulating in the solution on the thermal convection currents created during cooling. Within the first 10 min of cooling, a gel precipitate was observed on the dissolver vessel walls and vessel bottom (Figure A.3). After the insoluble solids were allowed to settle for about 3 hr, the dissolver solution, which appeared to be reasonably clarified (Figure A.4), was decanted and vacuum filtered (Filter No.1). The filtration rate slowed, and before reaching 1 hr of filtration time, Filter 1 was removed and replaced with a second filter (Filter No. 2). The mass of air-dried solids on Filter No.1 was 0.5775 g.

The remaining insoluble solids (settled in the reactor vessel) were rinsed with ~100 ml of 2% HNO_3 and settled. The gel precipitate on the vessel walls was easily rinsed off. Most of the solids appeared to be settled within 2 min. The solution was decanted onto Filter No. 2. The solids were rinsed again with 2% HNO_3 , settled (most solids settled in 7 min), and the solution was decanted again onto Filter No. 2. The solids were then rinsed with deionized water, and the entire slurry was transferred to Filter No. 2. The time required for filtration of the two 2% HNO_3 rinses and the single deionized water rinse was about 30 min each (each about 100 to 150 ml). Additional deionized water was used to transfer the remaining solids onto the filter. The residual solids formed a uniform filter cake composed of fine particles (Figure A.6). The mass of air-dried solids on Filter No. 2 was 0.8843 g. The filters used for this work were 47 mm diameter, 0.45- μm pore size, and were made of cellulose acetate.

After the solids were removed, the dissolver body was rinsed, air dried, and weighed. The mass at the end of the run (710.41 g) agreed with the initial dissolver body mass (710.54 g), which showed that little or no solids adhered to the dissolver vessel walls. During disassembly of the dissolver, it was also observed that no solids stuck to the sample syringe, which had been submerged in the solution during the run. A coating of gel was observed on the submerged portion of the conductivity probe (Figure A.6). When the conductivity probe was shaken, some material was observed to slough off it. Other solids on the conductivity probe were easily rinsed off.

The slurry sample collected at 16:10 was allowed to settle, and the associated dissolver solution was decanted onto a filter (Filter No. 3). A small, glass-coated stirrer was added to the settled solids, and 10 ml of 2% HNO₃ were added to the vial. The solids were stirred and then allowed to settle. However, the solution did not settle, so the slurry was decanted onto Filter No. 3. The solids on the filter were then rinsed a second time with 2% HNO₃, and the solution was decanted onto the filter. The solids were then rinsed with 10 ml of deionized water. The filter was dried in air. The mass of air-dried solids on Filter No. 3 was 0.0142 g. The entire filter with solids was fused for the analytical work. Filter No. 3 was 25 mm diameter, 0.45- μ m pore size, and was made of cellulose acetate.

4.2.2 Temperature and Electrical Conductivity

Temperature and electrical conductivity were measured for the duration of Test 1. These data were recorded automatically every 5 s in a spreadsheet file (17,280 data pairs in a 24-hr day). Unfortunately, however, gas bubbles produced during the dissolution collected in the conductivity cell (a vented 1-cm internal diameter glass tube) and decreased the values of the conductivity readings in an erratic manner. Therefore, valid readings only could be obtained when the cell was freed of the bubbles.

To evaluate these results, valid conductivity data (at apparent high conductivity periods), and the accompanying temperature data, were taken manually from the spreadsheet records. These data are presented in Figure 4.1 and begin at a "time zero" that is 10 min before the addition of the first sludge pellet (i.e., run time 0:00 = 11:10, Table 4.1) on July 23, 1998.

Though the conductivity data are intermittent, the values decrease distinctly in the first 4 hr of the test. All 15 feed sludge pellets were added during this time. Thereafter, the conductivity remained relatively constant until the heating was stopped at about 24:00, with the resulting concomitant decrease in conductivity. The sludge dissolution reactions consume the hydrogen ion and place metal nitrate salts (such as uranyl nitrate and ferric nitrate) in solution. Both these effects decrease the electrical conductivity of the solution. Because the hydrogen ion is the primary conductor in the acid solution, consumption of the hydrogen ion directly decreases conductivity. The dissolution of metal nitrate salts decreases the solution conductivity by suppressing HNO₃ dissociation by the common ion effect of nitrate. The conductivity data alone indicate that the dissolution reactions go to completion almost instantly.

As shown in Figure 4.1, the temperature generally was maintained between about 95°C and 98°C over the duration of the test, except for a downward spike between about 2:00 and 3:00. This cooling evidently was caused by not giving the test system sufficient time to establish a steady-state temperature before feed addition.

4.2.3 Hydrogen Ion and Metal Concentration Analyses

The hydrogen ion concentrations of the Test 1 solutions were measured by titration with standardized NaOH solution to a phenolphthalein endpoint (pH 8.2 to 10). With this technique, hydrolyzable metals ions (primarily Al, Fe, Ca, and U in these solutions) also are titrated in amounts proportional to their ionic charges (three for Al and Fe; two for Ca and U). This is because the metals precipitate as their hydroxides at the phenolphthalein endpoint. The contributions of the metal ions to the apparent H⁺ concentration were deducted based on their respective concentrations as determined by ICP.

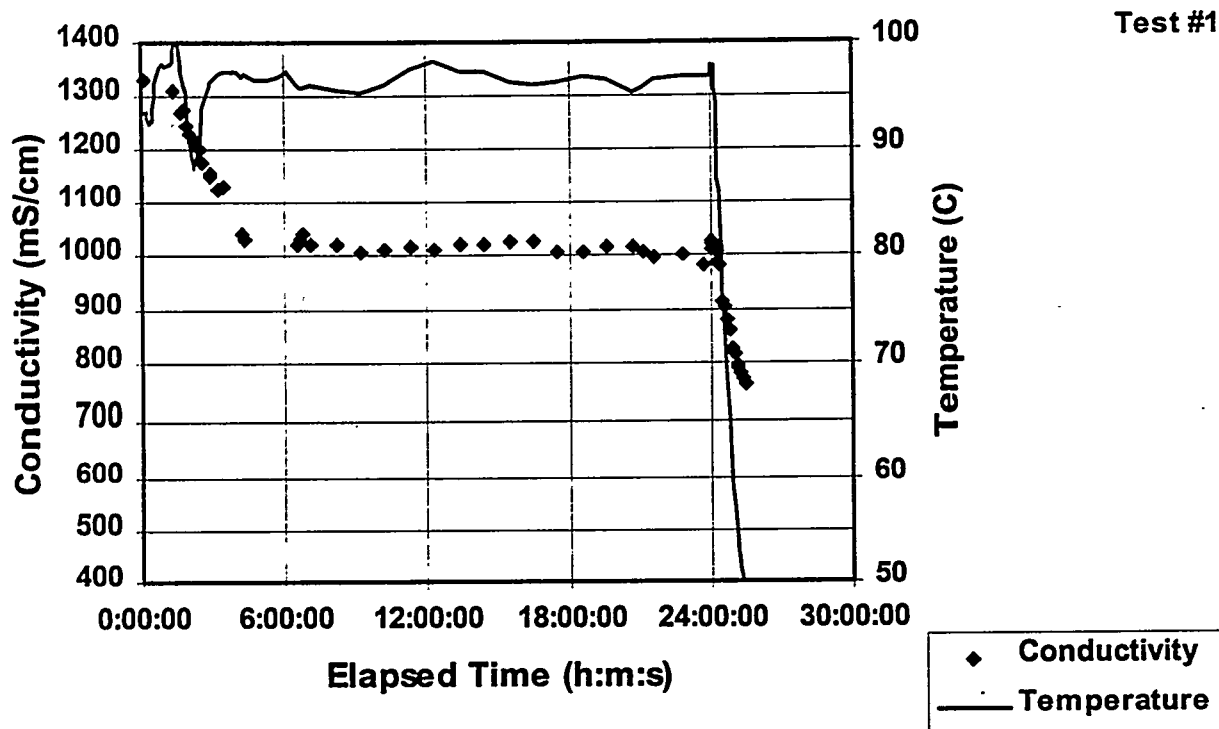


Figure 4.1. Conductivity and Temperature Measurements of Test 1

The concentrations of H^+ , U, Fe, Al, Ca, Si, and Na found in the Test 1 solutions as functions of time are shown in Table 4.2. The metal concentration data show that equilibrium dissolution of the KE Canister Sludge Composite was rapidly reached. The third sampling was taken at 4:40 or about 25 min after the final sludge addition. It is evident that by this time nearly all the uranium that ultimately would dissolve had dissolved. The kinetic behaviors of uranium and the other metals are considered in more detail in a subsequent section.

Unexpectedly, the H^+ concentrations were not stable until about 10:00 (run time) or about 6 hr after the final sludge addition and actually increased between 2:00 and 10:00. The H^+ trends are inconsistent with the conductivity data presented in Section 4.2.2. Further refinements in the H^+ analyses may be required.

The silicon concentration of the dissolver solutions was about 0.008 M, a factor of ~5 higher than that expected for the solubility of amorphous silica in similar concentration 95°C nitric acid (Elmer and Nordberg 1958). It was also a factor of ~15 above the expected solubility in 25°C nitric acid (Felmy et al. 1994). This apparent supersaturation could affect subsequent processing as the excess silica precipitates.

4.2.4 Residual Solids Concentrations

The quantity of KE Canister Sludge Composite added to the dissolution test was 71.36 g (dry basis). The total amount of dry residual solids remaining was 1.476 g or about 2.1% of the original weight. Samples of the residual solids from the dissolution were taken for analysis about 10:00 (run time) (6 hr after the

Table 4.2. Chemical Concentrations in Test 1 Dissolver Solutions

Time (h:m:s)	Concentration (M)						
	Al	Ca	Fe	Na	Si	U	H ⁺
1:07:00	0.0033	0.0002	0.0010	0.0012	0.0016	0.0235	4.84
2:12:00	0.0243	0.0011	0.0063	0.0027	0.0032	0.165	4.11
4:40:00	0.0619	0.0037	0.0170	0.0029	0.0083	0.424	4.11
5:19:00	0.0634	0.0023	0.0181	0.0027	0.0087	0.437	4.21
6:25:00	0.0637	0.0025	0.0186	0.0025	0.0117	0.433	4.24
10:07:00	0.0660	0.0025	0.0199	0.0027	0.0074	0.450	4.44
16:10:00	0.0667	0.0025	0.0206	0.0036	0.0078	0.445	4.47
23:58:00	0.0667	0.0025	0.0208	0.0029	0.0087	0.445	4.54
26:05:00	0.0678	0.0025	0.0208	0.0031	0.0087	0.445	4.42
	Concentration (μCi/ml)						
	⁶⁰ Co	¹³⁷ Cs	¹⁵⁴ Eu	²⁴¹ Am	^{239,40} Pu	²³⁸ Pu/ ²⁴¹ Am	Alpha
26:05:00	4.58E-02	1.19E+02	1.13E+00	1.09E+01	1.38E+01	1.17E+01	2.55E+01

final sludge addition) and at the end of the test, ~24:00 (22 hr after the final sludge addition). The solids were analyzed for bulk and radionuclide concentrations.

The chemical and radionuclide concentrations of the two residual solids are shown in Table 4.3. The residual solids were not analyzed by XRD to identify crystalline solid phases. However, residual solids taken from Test 2 (from fuel fragments and KE Canister Sludge Composite) were found to contain quartz [SiO₂, powder diffraction file (PDF) number 46-1045], anorthite (sodium calcium aluminosilicate, PDF number 20-0528 and/or CaAl₂Si₂O₈, PDF number 05-0528), and muscovite (a mica-like mineral, PDF number 07-0042). The same minerals previously were identified in surface soil samples taken 200 ft west of the KE Basin roll-up door (Makenas 1999). Similar phases would be expected for the residual solids from the dissolution of KE Canister Sludge Composite alone, because the fuel fragments themselves should have negligible residual solids except for incidental Zircaloy cladding. The residual solids compositions, with their relatively high silicon concentrations, reflect the presence of the quartz, anorthite, and muscovite phases. Needle-like particles of Zircaloy cladding also were visually observed on the residual solids (Figure A.3). Residual solids were found (by ICP) to contain 0.37 wt% zirconium.

Comparison of the compositions of the 10:00 and 24:00 solids shows that extending exposure to hot nitric acid increased the leaching of iron, sodium, and, particularly, uranium. The extra 14 hr leaching time also decreased the radionuclide concentrations in the residual solids uniformly by a factor of ~3.

4.2.5 Residual Solids Particle Size Distribution

The particle size distributions of Test 1 residual solids in a 1 M HNO₃ suspension were measured by a laser light scattering technique. Two different samples of residual solids were taken after the end of the dissolution test (~24:00). The distribution was measured on solids agitated at two different recirculation rates (40 and 70 ml/s) in the 1 M HNO₃ medium and on recirculated solids after 90 s treatment by a 40-W ultrasound source. Particle size analysis results, presented in Table 4.4, show that increased agitation (caused by increased flow rates of the particle suspensions) decreases the volume percentage of particles around the 600-μm size with a corresponding increase in the 200-μm size. The lower particle size

categories were not significantly affected. With sonication, a strong increase in the ~0.15- μm fraction is observed, seemingly arising at the expense of the ~5- μm fraction.

Specific examination of the lower particle size region was performed. The focus on smaller particles is achieved by settling the larger particle sizes and analyzing the smaller suspended particles by a laser Doppler technique. The results are presented in Table 4.5. The data confirm that up to half of the ~1-5 μm particle fraction is composed of aggregates that can be dispersed into sub-micron particles by sonication.

Table 4.3. Chemical and Radionuclide Concentrations in Test 1 Residual Solids

Solid	Chemical Concentration (wt%) ^a						
	Al	Ca	Fe	Na	Si	U	Zr
10:07	1.69	0.77	2.95	2.64	24.4	7.04	0.14
24:08	1.81	1.09	1.27	1.83	35.0	0.647	0.374
Solid	Radionuclide Concentration ($\mu\text{Ci/g}$)						
	⁶⁰ Co	¹³⁷ Cs	¹⁵⁴ Eu	²⁴¹ Am	^{239,40} Pu	²³⁸ Pu/ ²⁴¹ Am	Alpha
10:07	1.13E+00	8.53E+01	4.86E-01	5.59E+00	1.49E+01	5.47E+00	2.05E+01
24:08	3.59E-01	3.36E+01	1.51E-01	1.73E+00	4.65E+00	1.83E+00	6.83E+00

^a 24:08 sample also contains 0.37 wt% Zr.

Table 4.4. Overall Particle Size Distribution for Test 1 Residual Solids

Agitation	Sample	Volumetric Particle Size, %					
		~600 μm	~200 μm	~60 μm	~20 μm	~5 μm	~0.15 μm
40 ml/s	1	49	32	14	5	0	0
	2	26	26	26	16	6	0.5
70 ml/s	2	12	59	17	8	4	0.5
70 ml/s with ultrasound	1	15	48	25	7	5	2
	2	0	69	15	10	4	2

Table 4.5. Particle Size Distribution Below 6 Microns for Test 1 Residual Solids

Agitation	Sample	Volumetric Particle Size, %	
		~1-5 μm	~0.15 μm
40 ml/s	1	74	26
	2	100	0
70 ml/s with ultrasound	1	58	42
	2	55	45

4.2.6 Fractional Dissolution

The quantities of material that dissolve as a function of time can be monitored by multiplying the concentrations found in the solution and residual solids samples by their respective volumes and weights. In Figure 4.2, the quantities reporting to solution are compared with the fraction of KE Canister Sludge Composite added as a function of test time.

The plots in Figure 4.2 again show that most uranium dissolution occurs very rapidly. Uranium dissolution reaches 99.98%, as shown by assay of the residual solids remaining after 24 hr of leaching. Dissolution of aluminum is slower than uranium, and iron is slower yet. Only about 97% of both aluminum and iron dissolve by the end of the test. Sodium, calcium, and silicon dissolve incompletely, reflecting the stabilities (low solubilities) of quartz, anorthite, and muscovite in hot nitric acid.

Though the dissolution of the sludge was about 98%, radionuclide dissolution was much higher. In fact, with the exception of ^{60}Co , the fraction of radionuclides dissolved was 99.9% or more.

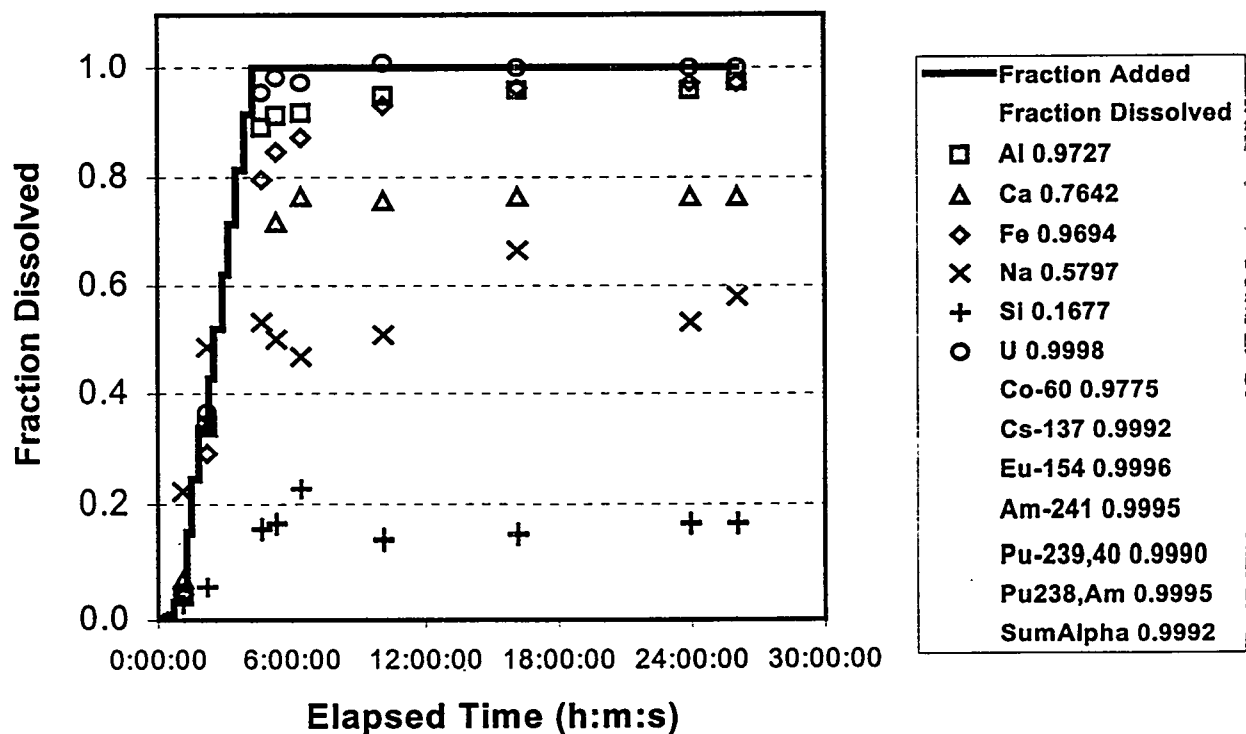


Figure 4.2. Fractions of Analytes Dissolved in Test 1 as a Function of Time (fraction dissolved at end of test given in legend box)

4.2.7 Material Balance

The quantities of bulk chemical and radiochemical components found in the dissolver solution and residual solids may be compared with the quantities expected from analyses of the starting KE Canister Sludge Composite (Table 3.3) to derive the material balance. The material balance for Test 1 (presented in Table 4.6) includes the elements measured by ICP and the principal radiochemicals. Material balances for nitrogenous and carbon dioxide offgas species are addressed in Section 5.0 of this report.

4.3 Test 2

Feed: Fuel Fragments, 30.7 g
 KE Canister Sludge Composite, 40.0 g
 Acid: 6 M HNO₃, 580 ml -- total (500 ml to start + 80 ml 16 M during test)
 Temperature 95°C
 Dissolution Time: 21 hr – fuel fragments; 6 hr – KE Canister Sludge Composite
 Offgas Analysis: yes

4.3.1 Qualitative Results

Photographs from Test 2 [captured from the videotapes plus a scanning electron microscope (SEM) image of a cladding residue] are provided in Appendix B. The dissolution behavior of N Reactor fuel fragments and KE Canister Sludge Composite was examined in 6 M HNO₃. Fragments of spent N Reactor fuel were added to the dissolver first and digested for approximately 14 hr before the sludge addition. The sludge and fuel were then digested for approximately 6 hr more. Gas analyses were conducted during Test 2. A cover gas of 10% Ne in a balance of He was flowed into the system at a rate of 500 ml/min.

Table 4.6. Material Balance for Test 1

	Quantity, µg				
	Al	Ca	Fe	Si	U
Sludge (Feed)	1.31E+06	8.42E+04	8.56E+05	5.42E+05	4.89E+07
Dissolver Solution	9.50E+05	5.20E+04	6.02E+05	1.04E+05	5.51E+07
Residual Solids	2.67E+04	1.60E+04	1.90E+04	5.15E+05	1.05E+04
Diss.&Res.	9.76E+05	6.80E+04	6.21E+05	6.19E+05	5.51E+07
Recovery,%	74.4	80.8	72.5	114.1	112.6
	Quantity, µCi				
	¹³⁷ Cs	²⁴¹ Am	^{239,240} Pu	²³⁸ Pu/ ²⁴¹ Am	Alpha
Sludge (feed)	2.70E+01	6.80E+03	8.63E+03	7.11E+03	1.58E+04
Dissolver Solution	2.35E+01	5.60E+03	7.09E+03	6.01E+03	1.31E+04
Residual Solids	5.03E+01	2.61E+00	7.01E+00	2.75E+00	1.03E+01
Diss.&Res.	2.41E+01	5.60E+03	7.10E+03	6.01E+03	1.31E+04
Recovery,%	89.2	82.4	82.2	84.5	83.2

Nitric acid, 500 ml, was loaded into the dissolver and heated to approximately 95°C. The dissolver was held at 95°C for several hours to establish a steady-state temperature. The temperature of the dissolver was monitored using an Omega type T thermocouple. The temperature of the cooling water recirculated through the condenser was monitored using a type K thermocouple. A section of glass was removed from the bottom of the conductivity probe to decrease the amount of acid needed to immerse the probe. However, just before the test, the entire protective glass sheath broke off, and the probe was recalibrated. Because there was no protective sheath on the conductivity probe capable of trapping exsolved gas, the plot of conductivity versus time for Test 2 does not show the spikes observed in Test 1.

For the duration of the test, the condenser was maintained between approximately 1°C and 15°C by additions of dry ice to the recirculation bath. In general, the bath temperature was below 5°C. The low temperature was maintained to condense the water vapor, which could have an adverse effect on the offgas analysis equipment, and to maintain dissolver solution volume.

During the dissolution, the solution was stirred using a stainless steel encapsulated magnetic stirrer. The stirrer weighed 7.8207 g before and after the test. No significant etching or erosion of the dissolver body was observed during the test.

Fuel fragments (Figure B.1) were added to the dissolver by placing them directly into the sample addition valve and rotating the valve. When the fuel fragments contacted with the dissolver solution, a period of rapid dissolution and bubbling/offgassing occurred for 2 to 60 s (depending upon the size of the fragment) (Figure B.2-A). This period was followed by relatively little activity as the fuel fragments slowly dissolved (Figure B.2-B). During the slow dissolution, gas bubbles formed around the fuel fragments and rose in a steady stream through the dissolver solution; however, this could have been the result of the fragments serving as nucleation points. The initial burst of offgas is suspected to have been caused by the rapid dissolution of uranium oxide associated with and possibly coating the fuel fragments. After the black coating was dissolved, the fuel fragments appeared as silver-gray metal covered with gas bubbles. After introduction of some fuel fragments, the dissolver solution developed a pale yellow-green color indicative of uranium(VI) and N_2O_3 , but remained fairly clear during the fuel fragment dissolution (before sludge addition). The condensate in the dissolver head space developed a yellow-brown color, indicative of NO_x .

Fifty milliliters of concentrated nitric acid were added to the dissolver 30 min after the last fuel fragment had been added. A solution sample was collected just before the addition of the first KE Canister Sludge Composite sample (i.e., ~14 hr after the last fuel fragment addition). NO_x was observed in the head space of the syringe used to collect this solution sample.

Most of the mass associated with the fuel fragments had dissolved before sludge addition was initiated; however, some metallic uranium was clearly visible even ~14 hr after all fuel fragments had been added (Figures B.3 and B.4). Zircaloy cladding fragments also were clearly distinguishable prior to sludge addition.

Sludge samples were frozen in the plastic syringes under liquid nitrogen and added to the dissolver through the sample addition valve. To avoid hitting the stirrer or damaging the exposed conductivity probe, stirring was stopped during sludge sample addition. Sludge sample #1 was dropped on the hot cell deck, and consequently was not added to the dissolver. Sludge sample #2 was added to the dissolver at 16:26 (run time). During the addition of sample #3, the sample addition valve broke and air was introduced into the dissolver. A clean pair of tongs was used to add sample #3, and then a 24/40 plug was installed. About 30 min after the first sludge sample addition, the plug was removed, and a new sample

addition valve was installed. After the addition of sludge sample #6, a burst of NO_x was observed. In general, the canister sludge dissolution in Test 2 was similar to Test 1. A summary of the fuel fragment and sludge additions and other events is given in the Table 4.7.

A slurry sample (~60 ml) was collected at 21:37 through the liquid sampling port. The dissolver solution was allowed to cool and settle. Settling progressed slowly, and after about 1 hr, a gel-like precipitate was visible along the vessel wall, and the solution remained slightly cloudy (Figure B.5). Upon filtering (using cellulose acetate filters with vacuum), approximately 5 ml of solution passed through Filter No. 1

Table 4.7. Event History for Dissolution Test 2

Run Time	Clock Time	Event	Sample Mass, g
0:10	19:25:35	Fragment PM2-1 Addition	0.4461
0:21	19:36:38	Fragment PM2-2 Addition	0.5922
0:30	19:45:35	Fragment PM2-3 Addition	0.2854
0:40	19:55:57	Fragment PM05-1 Addition	2.8257
1:02	20:17:24	Fragment PM05-2 Addition	2.4435
1:36	20:51:16	Fragment E1A Addition	2.9813
1:49	21:04:47	Fragment PM3 Addition	6.2503
2:00	21:15:26	Fragment K4-1 Addition	4.5016
2:10	21:25:32	Fragment K4-2 Addition	2.0571
2:20	21:35:21	Fragment A7-1 Addition	5.8409
2:38	21:53:19	Fragment A7-2 Addition	2.4471
3:08	22:24	Concentrated Nitric Acid Addition	
3:11	22:26:50	Concentrated Nitric Acid Addition	
3:12	22:28:00	Concentrated Nitric Acid Addition	
16:07	11:22:20	Collect Solution #1	
16:26	11:41:21	Sludge Sample #2 (sludge samples start at #2) Addition	8.4352
16:44	~12	Solid Addition Valve Broke	
16:48	12:03:12	Sludge Sample #3 Addition	7.2615
16:58	12:13:50	New Solid Addition Valve installed	
17:06	12:21:16	Sludge Sample #4 Addition	7.2974
17:11	12:27:03	Sludge Sample #5 Addition	8.3303
17:20	12:35:10	Sludge Sample #6 Addition	10.1821
17:28	12:43:37	Sludge Sample #7 Addition	9.7735
17:37	12:52:30	Collect Solution #2 Addition	
17:52	13:08:00	Collect Solution #3 Addition	
18:09	13:24:45	Collect Solution #4 Addition	
18:27	13:42	Concentrated Nitric Acid Addition	
18:27	13:43	Concentrated Nitric Acid Addition	
19:40	14:56	Collect Solution #5	
20:30	15:45:35	Collect Solution #6	
21:29	16:45	Collect Solution #7	
21:37	16:53	Collect Slurry Sample	
23:32	18:48	Collect Solution #8	
23:32	18:48	Heater off – Run Completed	
25:44	~21:00	Collect Solution #10 (Solution #9 not collected)	

before it plugged. The solution was removed from the filter housing and transferred to a poly bottle for storage. The mass of air-dried solids on Filter No. 1 was 0.0707 g. After an additional 24 hr of settling time, the clarified dissolution solution (~500 ml) was filtered through Filter No. 3. After 7.5 min of filtering, all but 30 ml of solution passed through the filter. The filtration of the remaining 30 ml of liquid was completed by vacuum filtering (Filter No. 4) the solution over ~48 hr. When Filter No. 4 was removed from the filter housing, it broke into many pieces. The filter pieces were transferred to a vial; however, some pieces, ~25%, were lost during the transfer.

Most of the mass associated with the residual solids appeared to consist of Zircaloy cladding pieces (Figure B.6). A large amount of gray solids were attached to the stirrer. The residual solids (and the stirrer) remaining in the dissolver vessel were rinsed and washed with two ~100-ml aliquots of 2% HNO₃ and one ~100-ml aliquot of deionized water as described for Test 1. The wash solutions and solids were decanted onto Filter No. 2. Wash solution was used to flush material off the vessel walls by a pipette. The material on the walls was easily removed with this technique. Between washes, the solid particles quickly settled (5 to 25 min), and the decanted wash solutions were readily filtered (i.e., no evidence of filter blinding). Additional deionized water was used to transfer the remaining solids onto the filter. The wet weight of the material on Filter No. 2 was 2.56 g. Filter No. 2 was air dried, and the mass of air-dried solids was 1.9569 g.

The solids from the slurry sample collected at 21:37 were filtered and rinsed as described in Section 3.3.7. The mass of air-dried solids on the filter was 0.0251 g. The entire filter and solids were fused for the analytical work.

4.3.2 Temperature and Electrical Conductivity

The temperature and the electrical conductivity of the dissolver solution were measured for the entire 26-hr duration of Test 2. As noted, the outer glass insulating sheath of the conductivity probe was inadvertently broken just before the test began, but the broken probe was quickly recalibrated (no new probe was available) and used in Test 2. While the loss of the outer sheath allowed steadier conductivity results to be obtained because bubbles could not collect near the electrodes, the well-defined solution conduction path provided by the glass sheath was lost. This made the probe much more sensitive to the shape and volume of the solution surrounding it (for example, proximity to vessel walls and solution volume). Thus, the calibration for the broken probe, which was performed in a 50-ml graduated cylinder, was not valid for the 1-L dissolver vessel. Evidence of this discrepancy was shown by the conductivity of the initial 6 M HNO₃ measured at about 96°C prior to the addition of any sludge or metal fragments. The indicated conductivity was 1078 mS/cm; 1360 mS/cm was expected. Therefore, the conductivity values obtained in Test 2 were adjusted upward by a factor of 1.26 (1360/1078) to correct for the calibration change caused by vessel geometry.

The "time zero" for Test 2 was 19:16, 10 min before introduction of the first fuel fragment at 19:26 on August 5, 1998. Again, conductivity and temperature data were gathered and recorded every 5 s. To obtain a manageable file size for graphical presentation, these data were taken only at 5- to 30-min intervals (Figure 4.3).

About 30.67 g of fuel fragments (28.92 g after deducting the cladding) were added in the first 2.5 hr of Test 2. As expected, and as shown in Figure 4.3, the indicated conductivity also decreased in that interval. Taking into account the temperature fluctuations, the conductivity continued to decrease, though at a lower rate, through about 7:00 (run time). At 3:00, an aliquot of concentrated nitric acid was added.

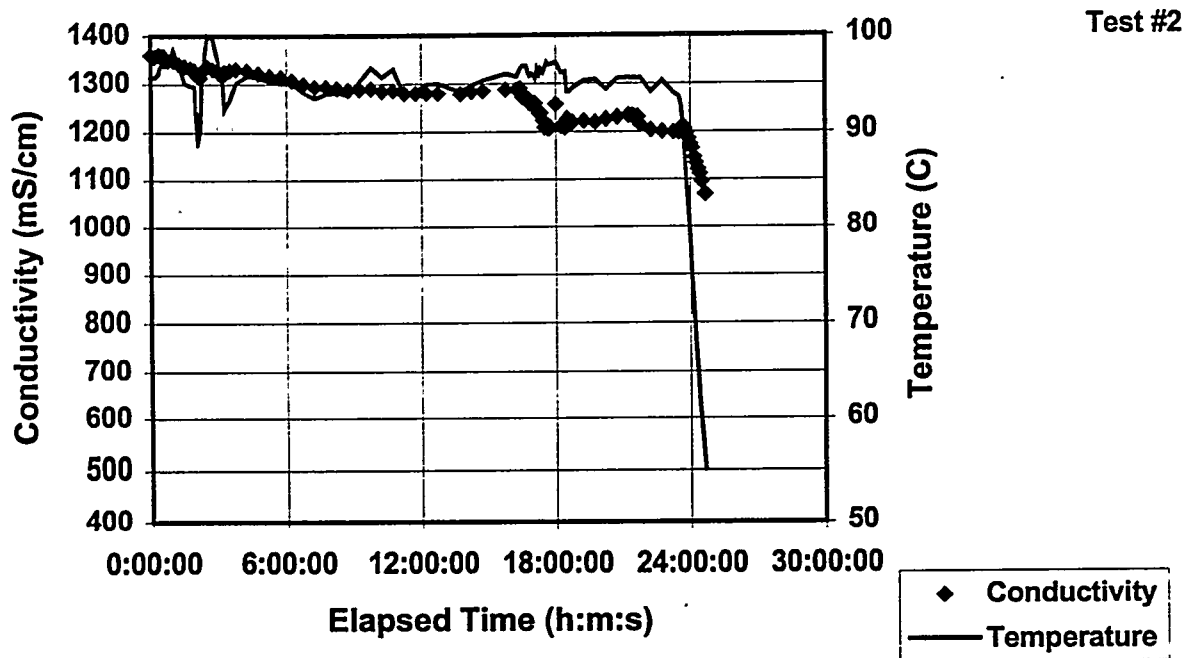


Figure 4.3. Conductivity and Temperature Measurements of Test 2

No corresponding increase in conductivity was registered, but the rate of conductivity decrease became even lower such that the conductivity remained relatively constant from that point until about 16:00.

Visual observation showed that, at 16:00, one piece of uranium metal still was not completely dissolved. That is, at least one piece of metal required more than 13.5 hr to dissolve. The heaviest piece added was about 6.25 g. A spherical piece of this mass would require the longest dissolution time and would be about 8.6 mm in diameter based on a uranium density of 19.1 g/cm^3 . The maximum linear corrosion rate thus would be 4.3 mm per 13.5 hr or 0.32 mm/hr. Based on studies by Swanson et al. (1985), the corrosion rate of uranium in 97°C 6 M HNO_3 is about 0.22 mm/hr. The observed rate ($\leq 0.32 \text{ mm/hr}$) thus is consistent with prior observations.

Over the next hour (at about 16:26 to 17:28), 40.05 g (dry basis) of KE Canister Sludge Composite were added in six frozen pellet additions. Similar to Test 1, a corresponding decrease in conductivity also occurred in that interval. The amount of conductivity decrease, about 80 mS/cm, was somewhat less than would be expected based on the Test 1 results (a decrease of 300 mS/cm for about 71 g dry sludge). Another aliquot of concentrated nitric acid was added at 18:28, about 1 hr after the final sludge addition. This addition caused little change in the conductivity reading. A noticeable decrease in conductivity occurred at about 22:00. This time corresponded to the taking of a large slurry sample (about 10% of the total solution volume). The apparent conductivity decrease may have been caused by the change in conductor solution geometry and the sensitivity to this caused by the unsheathed conductivity cell. Cooling caused the conductivity decrease after 23:30. The dissolver temperature generally was maintained at $95 \pm 1^\circ\text{C}$, except at the beginning when the metal pieces were added.

Despite the problems caused by the broken cell and the resulting suspect accuracy of the conductivity values, these data still show that the reaction progress was reflected by the conductivity measurements. The results confirm that strict control of the conductive environment around the electrodes (no bubbles, fixed conduction path) is required to obtain accurate and reliable data.

4.3.3 Hydrogen Ion and Metal Concentration Analyses

The concentrations of H⁺, U, Fe, Al, Ca, Si, and Na found in the Test 2 solutions as functions of time are shown in Table 4.8. A small piece of uranium fuel still remained undissolved before the first solution sample was taken at about 16:00. The sludge additions occurred between the first and second solution samplings. The dissolution kinetics of uranium and the other metals are considered in more detail in Section 4.3.6.

The silicon concentration was about 0.012 M for those solutions taken after introduction of the KE Canister Sludge Composite. As in Test 1, supersaturation in silica was indicated because the equilibrium solubility of amorphous silica is about 0.0004 to 0.001 M in room temperature and 95°C nitric acid, respectively.

The H⁺ concentrations decreased overall during the test, as expected. However, the data trends were not consistent with the acid addition after the fourth sampling and the expected sequential decrease in H⁺ concentration for the first through fourth and fifth through ninth samples. Further work is required to better understand the H⁺ analysis and data.

4.3.4 Residual Solids Concentrations

The quantity of fuel metal fragments added to the Test 2 dissolver was 30.67 g. Of this amount, about 1.75 g were found in the residual solids to be Zircaloy cladding. Thus, no more than 28.92 g of uranium were included in this material. About 40.05 g (dry basis) KE Canister Sludge Composite subsequently were added to the Test 2 dissolution. A sample of the residual solids was taken as slurry about 21:37 or about 4 hr after the final sludge addition. The mass of residual solids, not including Zircaloy, remaining at the end of the test (at 23:30) was about 0.32 g. Some residual solids from the 21:37 sampling were observed not to dissolve after the KOH/KNO₃ fusion digest. On this basis, from the results of the digestate analyses, and from video images of Zircaloy needles from Test 1 (Figure A.3), it is suspected that small Zircaloy particles (which resist alkali fusion) were present in the residual solids.

Table 4.8. Chemical and Radionuclide Concentrations in Test 2 Dissolver Solutions

Time (h:m:s)	Concentration (M)						
	Al	Ca	Fe	Na	Si	U	H ⁺
16:06:45	0.0013	0.0001	0.0017	0.0019	0.0057	0.215	6.22
17:36:55	0.0404	0.0022	0.0098	0.0040	0.0144	0.424	4.46
17:52:25	0.0393	0.0021	0.0100	0.0034	0.0139	0.405	4.13
18:09:10	0.0348	0.0016	0.0107	0.0032	0.0100	0.450	5.41
19:40:25	0.0335	0.0025	0.0115	0.0027	0.0091	0.445	4.57
20:20:00	0.0391	0.0070	0.0135	0.0021	0.0121	0.523	5.49
21:25:25	0.0415	0.0048	0.0145	0.0025	0.0131	0.555	4.84
23:32:25	0.0407	0.0047	0.0145	0.0019	0.0115	0.538	4.48
25:44:25	0.0439	0.0046	0.0157	0.0015	0.0146	0.584	4.38
25:44:25	Concentration (μCi/ml)						
	⁶⁰ Co	¹³⁷ Cs	¹⁵⁴ Eu	²⁴¹ Am	^{239,40} Pu	²³⁸ Pu/ ²⁴¹ Am	Alpha
	6.59E-01	4.57E+03	2.39E+01	1.98E+02	1.92E+01	2.16E+01	4.09E+01

Four dilute acid-rinsed residual solids were analyzed: the particulate slurry solids taken at 21:37, the solid particulate residual solids remaining at the end of the test at about 23:30, solids found on the magnetic stir bar, and the Zircaloy cladding. All solids (except the stir bar solids) were analyzed to determine radiochemical concentrations (including uranium); the two particulate samples (i.e., not the Zircaloy pieces or stir bar solids) also were analyzed by ICP. The final residual solids and stir bar solids were analyzed by XRD to identify solid phases, and a Zircaloy fragment was examined by SEM.

As expected, the zirconium-based cladding survived the baseline nitric acid dissolution. Prior studies have shown that interdiffusion of zirconium into uranium and uranium into zirconium occurs in the fuel fabrication process. The uranium trapped in the Zircaloy cladding will undergo fission and activation during irradiation. The activation and fission products, likewise, will remain trapped in the Zircaloy matrix and will not be released unless the Zircaloy itself has dissolved. Nitric acid-treated cladding from irradiated N Reactor fuel has been found to contain TRU activity at about 200 to 400 nCi/g (Swanson et al. 1985). The disposal pathway of the leached cladding will be to ERDF. Analyses of cladding in the present tests were undertaken to determine if the ERDF disposal criteria (Bechtel 1998) for radionuclide concentration are met.

The cladding residue in Test 2 originated from N Reactor fuel that had been irradiated to about 2600 MWD/MTU and thus the plutonium produced was fuels grade (estimated 18% ²⁴⁰Pu). Results of the radiochemical analyses of two separate pieces of residual cladding from Test 2 are presented in Table 4.9. The concentrations are compared, where data exist, with concentrations found for cladding hulls produced in studies of low irradiated (weapons grade; nominally 6% ²⁴⁰Pu) and unirradiated N Reactor fuels dissolution and subsequent leaching in nitric acid (Swanson et al. 1985).

The radioelement concentrations found for the two Test 2 cladding pieces agree closely. It is seen that plutonium and americium concentrations remaining in the cladding after acid treatment are much higher in Test 2 than in the prior tests. The higher TRU concentrations can be attributed to the higher irradiation, which would have produced more TRU isotopes by neutron capture. This is especially evident in comparing the ²³⁸Pu/²⁴¹Am concentrations (which primarily arise from ²⁴¹Am). The 20-fold higher concentrations found in Test 2 reflect both the higher irradiation and the longer cooling time which allows ²⁴¹Am to grow-in from decay of ²⁴¹Pu ($t_{1/2}$ of ²⁴¹Pu is 14.4 years). The higher ¹³⁷Cs concentrations in the

Table 4.9. Radioelement Concentrations in Zircaloy Cladding Residues from Test 2 and from Previously Reported Tests

Cladding Item	Concentration							
	U (wt%)	⁶⁰ Co (μCi/g)	¹³⁷ Cs (μCi/g)	¹⁵⁴ Eu (μCi/g)	²⁴¹ Am (μCi/g)	^{239,240} Pu (μCi/g)	²³⁸ Pu/ ²⁴¹ Am (μCi/g)	Alpha (μCi/g)
Test 2, #1	0.0322	1.68	55.2	0.267	1.11	0.741	1.06	1.81
Test 2, #2	0.0337	1.66	56.3	0.265	1.11	0.711	1.05	1.77
Fuel Diss'n. ^a	0.12	6.7	20	NR	NR	0.37	0.050	0.42
Fuel Diss'n. and Leach ^a	0.06	6.2	16	NR	NR	0.25	0.034	0.28
Unirradiated Fuel Diss'n. and Leach ^a	0.17	--	--	--	--	--	--	--

^a Results from Swanson et al. (1985); dissolution from "6% ²⁴⁰Pu"; NR = not reported.

Test 2 pieces also reflect the higher irradiation; the half-life of ^{137}Cs is about 30 years and thus radioactive decay is not a dominant factor in comparing the concentrations. The ^{60}Co concentrations are lower in the Test 2 items because of the significant cooling time compared with its 5.3-year half-life. The N Reactor last operated in 1986.

The uranium concentrations in the Test 2 cladding pieces are significantly lower than found in the previous testing both for the irradiated and unirradiated materials. The lower concentrations may reflect some greater irradiation-induced diffusion of the captured uranium out of the Test 2 cladding aided by cracking along grain boundaries. This also would enhance subsequent uranium removal by dissolution in nitric acid. However, these explanations are speculative and require literature or laboratory studies to confirm. The Pu/U weight ratio in the cladding from Test 2 is about 0.029 compared with a ratio of about 0.003 found in K Basin sludges containing high uranium concentrations. The 10-fold higher ratio in the cladding reflects the expected higher thermal neutron flux and capture experienced at the fuel periphery. The Pu/U ratio in the prior tests with the weapons grade material is about 0.005. A sample of cladding retrieved from the Test 2 residual solids was examined by SEM and energy dispersive spectrometry (EDS); results are shown in Figures B.7 and B.8. The images show a smooth outer (coolant) side and a striated (uranium metal) fuel side. The uranium seems to be associated with aluminum and silicon on the fuel side in scaly patches.

The chemical and radionuclide concentrations for the two particulate solids streams from Test 2 are summarized in Table 4.10. As noted previously, the solid phases identified by XRD for the residual solids remaining at the end of the dissolution test were quartz, anorthite, and muscovite. The stir bar solids also contained these phases, but had significant amorphous (X-ray indifferent) bands that likely arise from silicic acid. The solids chemical analysis is consistent with the XRD assignment of these Hanford soil phases. Significantly, the residual solids also contained about 0.6 wt% zirconium, although no diffraction peaks attributable to zirconium metal, zirconium hydride, or zirconium oxide were discovered at this low concentration. Thus, finely particulate zirconium will be present in the sludge residual solids. It is noted that metallic zirconium needles have been identified by SEM and EDS of dissolver residual solids from acid processing of K Basin sludge (one needle was about 4 mm long), Figures B.7 and B.8, and were identified in Test 1 residual solids (Figure A.3). As shown in Table 4.8, extending the leaching time by 2 hr decreased the iron and uranium concentrations in the residual solids 2- to 3-fold. Similar diminution of fission product and americium concentrations also occurred. The plutonium concentration decreased about 4-fold with the additional leaching time.

Table 4.10. Chemical and Radionuclide Concentrations in Test 2 Particulate Residual Solids

Solid	Chemical Concentration (wt%)						
	Al	Ca	Fe	Na	Si	U	Zr
21:37	1.13	0.943	5.30	1.09	26.4	1.54	0.518
23:30	1.77	0.946	2.81	1.96	20.9	0.467	0.590
Solid	Radionuclide Concentration ($\mu\text{Ci/g}$)						
	^{60}Co	^{137}Cs	^{154}Eu	^{241}Am	$^{239,240}\text{Pu}$	$^{238}\text{Pu}/^{241}\text{Am}$	Alpha
21:37	6.12E-01	2.03E+02	8.88E-01	1.65E+01	1.91E+01	1.78E+01	3.73E+01
23:30	4.70E-01	8.64E+01	3.31E-01	6.83E+00	4.73E+00	5.54E+00	1.08E+01

4.3.5 Residual Solids Particle Size Distribution

Particle size distributions of samples of Test 2 residual solids in a 1 M HNO₃ suspension were determined by a laser light scattering technique. The samples were obtained from the dissolution slurry retrieved at 21:37 (4 hr after the final sludge addition) and from the solids remaining at the end of the test at 23:30. The distribution was measured on solids agitated by 40 ml/s recirculation in the 1 M HNO₃ medium and on recirculated solids after 90 s treatment by a 40-W ultrasound source. Results of the particle size analyses presented in Table 4.11 show that increased processing time decreased the particle size distribution for the solids both before and after sonication. Sonication apparently decreased the 100-μm population and shifted it to the 60-μm size. Sonication had little effect on the 23:30 sample size distribution.

Specific examination of the lower particle size region (achieved by excluding the larger particle sizes by settling) was performed using a laser Doppler technique (Table 4.12). Unfortunately, because insufficient sample quantities prevented acquisition of conclusive data for most conditions, meaningful comparisons of the effects of test duration and agitation could not be made.

4.3.6 Fractional Dissolution

The quantities of material that dissolve in Test 2 as a function of time were derived based on the solution and solids analyses. Figure 4.4 displays the quantities of the major elements reporting to solution in comparison with the nominal amount of uranium added to the dissolver vessel. This amount of uranium was based on the metal fragments mass, the assumption that the metal fragments are pure uranium (except for the cladding), and on the mass and assay of the KE Canister Sludge Composite. The time scale in Figure 4.4 commences at 15:00 because the first sampling occurred at about 16:00.

Table 4.11. Overall Particle Size Distribution for Test 2 Residual Solids

Agitation	Sample	Volumetric Particle Size, %				
		~100 μm	~60 μm	~20 μm	~8 μm	~2 μm
40 ml/s	21:37	92	0	0	8	0
	23:30	0	2	29	55	14
40 ml/s with ultrasound	21:37	0	97	0	3	0
	23:30	0	0	39	49	12

Table 4.12. Particle Size Distribution Below 6 Microns for Test 2 Residual Solids

Agitation	Sample	Volumetric Particle Size, %	
		~1-5 μm	~0.15 μm
40 ml/s	21:37	--	--
	23:30	--	--
40 ml/s with ultrasound	21:37	--	--
	23:30	80	20

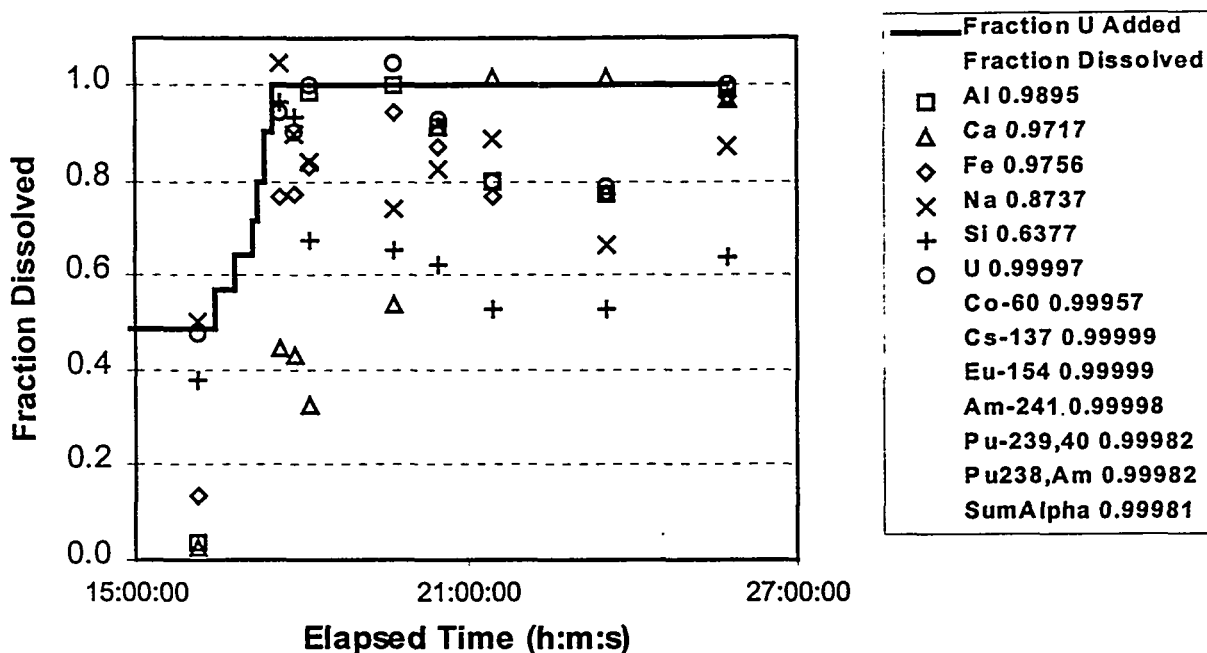


Figure 4.4. Fractions of Analytes Dissolved in Test 2 as a Function of Time (fraction dissolved at end of test given in legend box)

The uranium dissolution from the KE Canister Sludge Composite did not proceed nearly as rapidly in Test 2 (Figure 4.4) as it did in Test 1 (Figure 4.2). It appears that at least 4 hr are required to reach the uranium dissolution asymptote. This, however, may have been an artifact of a relatively high uranium concentration in the last solution sample (see Table 4.7). Recall, however, that a small piece of uranium metal still was present at 16:00. Nevertheless, over 99.99% of the uranium dissolved by the end of the test. Iron dissolution also proceeded asymptotically to attain about 98% dissolution. Aluminum dissolution was more rapid and complete. Sodium and silicon dissolutions were incomplete as further shown by the presence of quartz, anorthite, and muscovite in the residual solids. Most significantly, radionuclide dissolution was 99.9% or greater for all measured isotopes.

4.3.7 Material Balance

The quantities of bulk chemical components found in the dissolver solution and residual solids may be compared with the quantities expected from analyses of the KE Canister Sludge Composite (Table 3.3) and the mass of uranium metal to arrive at a material balance (Table 4.13). Radiochemical material balance is not possible because the radionuclide quantities in the irradiated uranium metal fuel pieces are not known. The quantities presented for Test 2 include the elements (measured by ICP) and the radiochemicals found in the dissolver solution and residual solids. Material balances for nitrogenous and carbon dioxide offgas species are addressed in Section 5.0 of this report.

Table 4.13. Material Balance for Test 2

	Quantity, μg				
	Al	Ca	Fe	Si	U
Metal&Sludge	7.37E+05	4.73E+04	4.81E+05	3.04E+05	5.64E+07
Dissolver Soln.	5.21E+05	1.04E+05	3.88E+05	1.21E+05	5.92E+07
Residual Solids	5.54E+03	3.05E+03	9.68E+03	6.87E+04	1.78E+03
Diss.&Res.	5.26E+05	1.08E+05	3.97E+05	1.90E+05	5.92E+07
Recovery,%	71.4	227.5	82.6	62.3	105.1
	Quantity, μCi				
	^{137}Cs	^{241}Am	$^{239,240}\text{Pu}$	$^{238}\text{Pu}/^{241}\text{Am}$	Alpha
Metal&Sludge	--	--	--	--	--
Dissolver Soln.	2.50E+06	1.08E+05	1.05E+04	1.18E+04	2.23E+04
Residual Solids	3.08E+01	2.44E+00	1.88E+00	2.09E+00	4.14E+00
Diss.&Res.	2.50E+06	1.08E+05	1.05E+04	1.18E+04	2.23E+04
Recovery,%	--	--	--	--	--

4.4 Test 3

Feed: KE Areas Sludge Composite, 52.7 g; IX material, 1.98 g
 Acid: 6 M HNO₃, 700 ml – total (550 ml to start + 150 ml 16 M during test)
 Temperature: 95°C
 Dissolution Time: 7 hr
 Offgas Analysis: yes

4.4.1 Qualitative Results

The dissolution behavior of the KE Areas Sludge Composite was examined in 6 M HNO₃ in the presence of IX material. Images of Test 3, taken from videotape records and SEM images, are shown in Appendix C.

Before the test, a section of glass was removed from the bottom of a new conductivity probe (YSI Model 3440, same model number as used earlier) to decrease the amount of acid needed to immerse it. In addition, holes were drilled in sections of the probe to allow trapped gas to be released. The modified conductivity probe was calibrated before the run. At the start of the run, the conductivity probe was not fully immersed; therefore, an additional 80 ml of 6 M HNO₃ were added to the dissolver (i.e., it was planned to start the test with only 470 ml of 6 M HNO₃). The holes drilled in the glass sheath were effective in allowing gas bubbles to release, as indicated by the lack of conductivity spikes as were observed during Test 1. Gas analyses were conducted during this test. A cover gas of 10% Ne in a balance of He was flowed into the system at a rate of 500 ml/min. The offgas condenser was maintained between approximately 1°C and 10°C by additions of dry ice to the recirculation bath. In general, the bath temperature was below 5°C.

The temperature of the dissolver was monitored using an Omega type T thermocouple. The temperature of the cooling water recirculated through the condenser was monitored using a type K thermocouple.

During the dissolution, the solution was stirred using a stainless steel encapsulated magnetic stirrer. The magnet was sealed in a piece of 300 series stainless steel tubing with welded end-caps. The stirrer was weighed before and after the dissolution test. No mass gain or loss was recorded. A summary of sludge additions, sample collections, and other events is provided in Table 4.14.

A sample of IX material, 1.9788 g, from sample KES-H-08 was suspended in the dissolver solution in the stainless steel module (i.e., mesh bag). The starting IX material is depicted in Figure C.6. The nitric acid, 530 ml, was loaded into the dissolver and heated to approximately 95°C. The IX material was submerged in the dissolver for about 1 hr at ambient temperatures plus 2 hr at ~95°C before the first sludge sample was added (Figure C.1-Before). During this time, while the reactor was being preheated and temperature being stabilized, it was observed that the acid was discoloring and gas bubbles were being produced from the stainless steel mesh module. Therefore, just before sludge was introduced into the dissolver, a solution sample was collected (run time = 00:00) to determine which components were being leached from the IX material. Brown gas, most likely NO₂, was observed in the head space of the syringe used to collect the solution sample.

Table 4.14. Event History for Dissolution Test 3

Run Time	Clock Time	Event	Sample Mass, g
0:00	10:34	Collect Solution #0 (before first sludge addition)	
0:10	10:44:19	Sludge Sample Addition #1	8.8302
0:22	10:56:23	Sludge Sample Addition #2	8.7701
0:32	11:06:26	Sludge Sample Addition #3	8.6577
0:42	11:15:45	Sludge Sample Addition #4	8.6704
0:51	11:25:26	Sludge Sample Addition #6 (Sample #5 Added Last)	8.7597
1:02	11:36:26	Concentrated Nitric Acid	
1:34	12:08	Concentrated Nitric Acid	
1:48	12:22:15	Sludge Sample Addition #7	9.9958
1:58	12:31:58	Sludge Sample Addition #8	9.1244
2:06	12:40:29	Sludge Sample Addition #9	8.3983
2:12	12:45:37	Sludge Sample Addition #10	9.1090
2:18	12:52:08	Sludge Sample Addition #5	7.7625
2:28	13:02	Collect Solution #1	
2:48	13:22	Collect Solution #2	
3:18	13:52	Collect Solution #3	
3:26	14:00	Concentrated Nitric Acid Addition	
4:32	15:03	Collect Solution #4	
5:26	16:00	Collect Solution #5	
6:33	17:07	Collect Solution #6	
6:37	17:11:15	Collect Slurry Sample #1	
6:37	17:10:30	Collect Slurry Sample #2	
8:28	19:02	Collect Solution #7	
9:06	19:40	Lost Condenser	
9:28	20:02	Collect Solution #8	
9:29	20:03	Heater off - Run Completed	
10:41	21:15	Collect Solution #9	

KE Areas Sludge Composite samples were prepared in plastic syringes and frozen in liquid nitrogen. The sludge samples were between 7 and 10 g each (settled sludge basis). During sample preparation, two samples of the KE Areas Sludge Composite were placed in 20-ml vials for weight percent solids determinations. However, these two samples had noticeably dried before the initial weights could be measured, so a second set of samples was collected on September 1, 1998, for weight percent solids determination. The samples were placed in an oven at 105°C until a stable mass was reached. The weight percent solids were calculated at 59.8% (59.7% and 59.8%). The frozen pellets were introduced into the dissolver using the sample addition valve connected to one of the 24/40 glass joints. During previous experiments it was noted that turning off the agitator during sludge addition caused an increase in the acid temperature in the dissolver. To avoid fluctuation in acid temperature, the agitator was left on throughout the experiment, including during sludge additions.

All solution samples and the slurry sample were collected through the liquid sampling port. The solution samples were immediately filtered through a 0.2- μ m PVDF Acrodisc filter (Gelman P/N 4406). Liquid sample #5 and all subsequent liquid samples were found to be significantly easier to filter (i.e., required less force and time) than the previous liquid samples. During the collection of solution sample #1, some unfiltered solution may have dripped into the clean sample vial.

At 9:06 (run time), 6 hr and 40 min after addition of the last sludge, the cooling line became disconnected from the pump and sprayed cooling water into the hot plate, which dropped the temperature in the dissolver to ~85°C. The line was reattached to the pump, but it disconnected again 13 min later. The line could not be reattached, so the hot plate was turned off at 19:57, 7 hr after the last addition of solids. The agitator was turned off at 9:29 (run time).

The mesh module was removed from the dissolver and placed in a 50-ml centrifuge tube containing ~30 ml of 2% HNO₃. This volume of acid completely immersed the module. The module was removed from the acid several days later and disassembled and rinsed twice in ~25 ml of 2% HNO₃. After each rinsing, the acid was decanted off the beads and vacuum filtered. The mesh module was disassembled, and the beads were rinsed into a clean centrifuge cone, labeled "DVT3OIER" using 2% HNO₃. The acid was decanted and filtered. Finally, the beads were rinsed with ~25 ml of deionized water, and the water was then decanted and filtered.

The IX material was left in the centrifuge cone to air dry. The mass of air-dried solids in centrifuge cone DVT3OIER was 1.2919 g. This represents a mass loss of 35% over the starting mass of air-dried IX material.

Following the dissolution, some gray solids were attached to the stirrer, but not as much as in Test 2. Solids coated the thermocouple and conductivity probe. These solids were readily washed off with deionized water.

After completion of the run, the dissolver solution was allowed to cool and settle. The dissolver solution was too dark (nearly opaque), and there was too much scum on the vessel walls to clearly observe the settling behavior. From close inspections with the video camera, it appeared that significant gel-precipitate/floc formed in the solution and on the vessel walls. Although not apparent from the videotape, the insoluble solids/gel settled, and a clarified supernatant was produced within 3 hr. Approximately 250 ml were decanted into a filter apparatus, but, due to a mechanical failure, this solution was lost. The solution remaining in the dissolver was remixed with the stirrer, and the solution was allowed to settle overnight. The mixing removed the scum from the vessel walls, allowing the settling behavior to be

clearly observed. Within 10 min, approximately half the solution volume partially clarified, and a distinct sludge layer was visible.

After several hours, the supernatant clarified. Several hundred milliliters of sludge were also observed. The supernatant was decanted and vacuum filtered (Filter No. 1). The remaining residual solids/sludge were rinsed with ~100 ml of 2% HNO₃ and settled. Good separation of the solids and supernatant was achieved in less than 30 min (Figure C.2). The solution was decanted onto Filter No. 1 (i.e., 47 mm, PVDF filter with 0.45- μ m pore size). The solids were rinsed again with 2% HNO₃, settled, and the solution was decanted again onto Filter No. 1. The solids were then rinsed with deionized water, and the entire slurry was allowed to settle for several hours (monitored via camera) (Figure C.3). Within about an hour, a highly clarified supernatant was generated. The solids were slurried, and then transferred to Filter No. 1. Additional deionized water was used to transfer the remaining solids onto the filter. Vacuum filtration of this slurry (~400 ml) took about 1 hr. During the filtration, a translucent gel with a consistency similar to "Jello" was formed (Figure C.4-A). As vacuum filtration continued, the gel dewatered and formed a gelatinous filter cake. Continued filtration caused the filter cake to continue dewatering to the point it cracked into several pieces (Figure C.4-B). The wet weight of the material on Filter No. 1 was 25.21 g. The mass of air-dried solids on Filter No. 1 was 8.8156 g (Figure C.4-C). Although the acid solutions and deionized water were used to rinse the dissolver vessel, a "bath-tub" ring remained adhered to the vessel walls (Figure C.4-D).

One of the slurry samples collected at 6:37 was filtered (PVDF filter) in a manner similar to that used for the residual solids/sludge (filtered and rinsed as described in Section 3.3.7). The filter cake material was gelatinous and was quite similar to the filter cake described above. The filter was dried in air (Figure C.4-D). The mass of air-dried solids on the filter was 0.2067 g. The entire filter with solids was fused for the analytical work.

4.4.2 Temperature and Electrical Conductivity

The dissolver solution temperature and the electrical conductivity were measured continuously over the entire 11-hr duration of Test 3. A new conductivity probe (YSI Model 3440, same model number as previous probes) was used in this test. Before it was used in Test 3, the probe's conductivity cell was shortened to decrease the required immersion depth, and a larger vent hole was drilled into the top to allow ready escape of collected gas. After these physical changes, the cell was recalibrated. The "time zero" for Test 3 was 10:34 on August 19, 1998. This was 10 min before the introduction of the first sludge pellet to the dissolver solution (not counting the IX material held in the module) at 10:44 and coincided with the first solution sampling. The KE Areas Sludge Composite was added in two nearly equal-mass groups of five pellets each. The first group of five was added between 0:10 and 0:51 time with 10-min intervals between additions. A concentrated nitric acid aliquot was added at around 1:02. The second group of five sludge pellets was introduced between 1:48 and 2:18.

The numerous conductivity and temperature data again were abstracted to produce a manageable file size for graphical presentation. These data for Test 3 are presented in Figure 4.5.

The two sets of sludge additions, separated by an addition of concentrated nitric acid, are identifiable in the conductivity data. The conductivity decreases markedly with each group of sludge additions. In contrast to prior tests with KE Canister Sludge Composite, which showed that conductivity changes effectively ceased when sludge additions stopped, the conductivity for Test 3 with the KE Areas Sludge Composite continued to decrease until about 3 hr elapsed time, 40 min after the last sludge addition. Sharp, but slight, conductivity increases were observed when concentrated nitric acid additions were

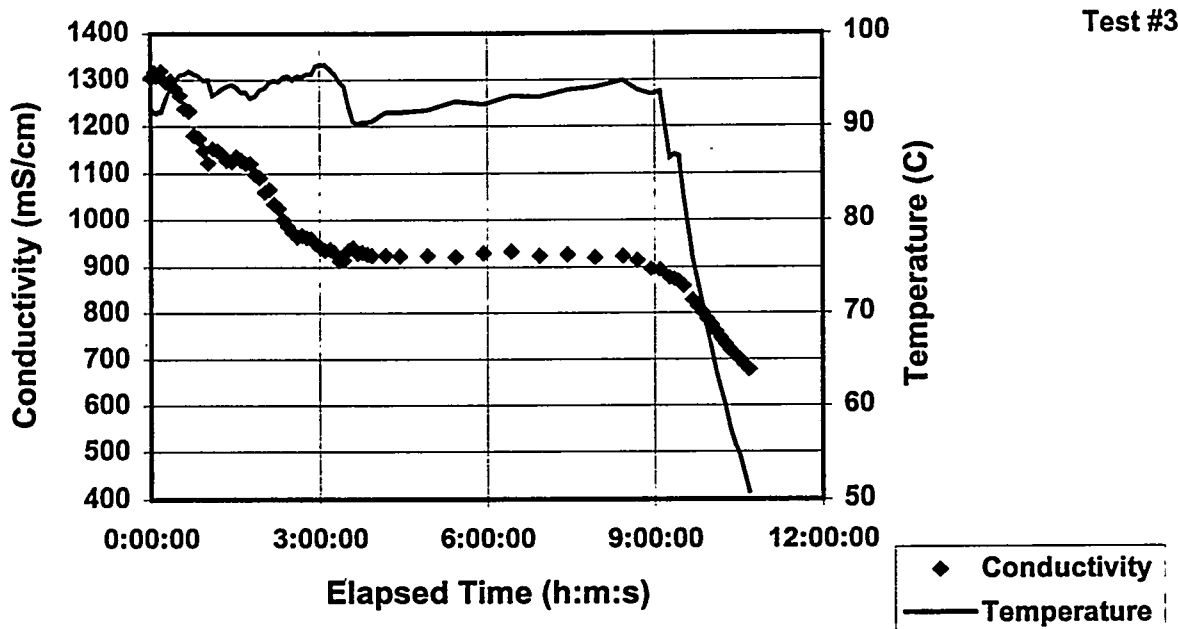


Figure 4.5. Conductivity and Temperature Measurements of Test 3

made at 1:00 and again at about 3:26. After the second acid addition, the conductivity remained relatively steady until the heating ceased at about 9:30 and the solution cooled.

The solution temperature generally was held within one degree of the 95°C target during the sludge additions, but dropped to about 90°C just after that. The temperature then slowly returned to 95°C over the following 5 hr before heating was stopped.

4.4.3 Metal Concentration Analyses

The concentrations of the metal ions found in the Test 3 dissolver solution samples are presented in Table 4.15. The concentrations of H^+ were not measured for this test. The initial solution sample was taken before any KE Areas Sludge Composite was added. However, the IX material was present in the module.

The silicon concentrations were observable by ICP but were about half of the lower detection limit set by data quality requirements. The reported results given in Table 4.15 are relatively constant, at about 0.0015 M Si, and are near the expected solubility of amorphous silica, 0.001 M at 95°C (Elmer and Nordberg 1958). The dissolution kinetics of uranium and the other metallic sludge components are considered later in this section. Note, however, the high concentrations of iron (about 0.52 M) and aluminum (about 0.16 M) in the dissolver solution and relatively low uranium concentration (0.025 M). In Test 1, these concentrations were about 25-fold lower for iron and 2-fold lower for aluminum, whereas the uranium concentration was about 25 times higher.

Table 4.15. Chemical and Radionuclide Concentrations in Test 3 Dissolver Solutions

Time (h:m:s)	Concentration (M)						
	Al	Ca	Fe	Na	Si ^a	U	H ²¹⁸
0:00:00	0.0013	0.0009	0.0004	0.0046	0.0010	0.0000920	--
2:28:00	0.166	0.0264	0.385	0.0070	0.0012	0.0259	--
2:48:00	0.173	0.0267	0.458	0.0061	0.0022	0.0269	--
3:18:00	0.165	0.0250	0.467	0.0061	0.0017	0.0244	--
4:29:00	0.152	0.0233	0.457	0.0052	0.0017	0.0233	--
5:26:00	0.144	0.0220	0.437	0.0052	0.0013	0.0220	--
6:33:00	0.158	0.0249	0.487	0.0057	0.0015	0.0240	--
8:28:00	0.156	0.0244	0.487	0.0057	0.0014	0.0237	--
9:29:00	0.159	0.0244	0.492	0.0057	0.0020	0.0241	--
10:41:00	0.165	0.0254	0.519	0.0061	0.0010	0.0250	--
	Concentration (μCi/ml)						
	⁶⁰ Co	¹³⁷ Cs	¹⁵⁴ Eu	²⁴¹ Am	^{239,240} Pu	²³⁸ Pu/ ²⁴¹ Am	Alpha
10:41:00	1.09E-01	1.85E+01	1.63E-01	1.38E+00	1.46E+00	1.55E+00	3.02E+00

^a Concentrations observable but about 50% below analytical detection limit.
^b Not measured.

4.4.4 Residual Solids Concentrations

The quantity of KE Areas Sludge Composite added to the dissolver in Test 3 was 52.67 g (dry basis). The mass of dry residual solids remaining after leaching (about 9½ hr of acid contact at elevated temperature) was 9.02 g or about 17% of the starting mass. The quantity of organic and inorganic (primarily Zeolon-900, mordenite) IX material present in the module initially was 0.918 g (oven-dry basis); after testing, the air-dried mass was 1.292 g. The mass increase likely reflects water uptake by the resin. A sludge residual solids sample also was retrieved from the dissolver at 6:37, about 3 hr and 22 min after the last sludge addition.

The residual solids from the acid processing conducted in Test 3 were rinsed in dilute nitric acid and water. The rinsed residual solids then were digested and analyzed for chemical and radionuclide concentrations. Four materials were analyzed: the residual solids taken at 6:37, the residual solids taken at the end of the acid treatment (~9:30), the starting IX material, and the IX material after dissolver treatment. A special mechanical separation technique was used to fractionate the IX material as the spherical OIER and the irregular-shaped mordenite and similar granular inorganic materials.^(a) The separated IX materials (Figure C.5) were analyzed individually. Their compositions were determined, and the compositions of the combined IX material calculated.

^(a) In the separation technique, the organic beads were rolled away from the inorganic solids by gentle shaking on a slightly inclined surface. The separation was imperfect, however. Because some organic beads were split and would not roll, they remained with the inorganic solids. Likewise, some inorganic solid was retained in the organic fraction as fine particles stuck on the beads or rounded particles which rolled with the beads. Nevertheless, a distinct difference in the visual appearance and composition of the separated fractions was evident (see Figures C.5 and C.6, Appendix C).

The solid phases present in the final residual solids were identified by XRD to be quartz and anorthite. Although the phases were similar to those identified for the KE Canister Sludge Composite residual solids, the quartz pattern in the KE Areas Sludge Composite residual solids was much more prominent. The chemical and radionuclide concentrations of the sludge residual solids samples are presented in Table 4.16. The data show that the additional 3 hr of acid treatment decreased iron concentration in the residual solids about 30% and the uranium concentration about a factor of 6. The TRU concentrations decreased about 30% overall, mostly due to plutonium. Concentrations of ^{137}Cs and ^{241}Am were not strongly affected by the extended leaching.

The chemical and radionuclide concentrations of the IX materials before and after contact with the dissolver solution for the separate organic and inorganic fractions and the combined materials are given in Table 4.17. The fractional amounts of the organic and inorganic portions were adjusted to give identical silicon concentrations (8.64 wt%) in the combined material both before and after exposure to the dissolver solution. This calculation was based on the assumption that the silicon concentration in the OIER is negligible compared with that of the inorganic fraction and the fact that silicon dissolution from the inorganic fraction by nitric acid is negligible (as shown in the present sludge treatment tests). With that assumption, the inorganic fraction comprises about 35.4 wt% of the starting IX material and about 29.9 wt% of the leached IX material.

The concentrations of various chemical and radionuclide components in the IX material before and after exposure to the dissolver solution given in Table 4.15 may be compared. It is seen in Table 4.17 that exposing the IX material to the dissolver solution decreases monovalent cation (Na^+ and Cs^+) concentrations, has little effect on divalent cation (Co^{2+} and UO_2^{2+} but not Ca^{2+}) concentrations, and increases trivalent cation (Fe^{3+} , Eu^{3+} , and Am^{3+} but not Al^{3+}) and tetravalent cation (Pu^{4+}) concentrations.

The correlation of metal charge to metal distribution on the combined IX material overlooks important distinctions found between the organic and inorganic fractions, however. Most significantly, plutonium concentrations in the IX material increase sharply by exposure to the dissolver solution. The plutonium concentration increases a factor of 9 for the inorganic fraction and increases a factor of 275 for the organic resin to give an overall 100-fold increase in the IX material. The expected loading of plutonium on the OIER thus is observed. It is significant that plutonium also absorbs to some degree on the inorganic fraction. Cesium concentration is significantly higher in the initial inorganic solid than in the organic resin. By exposing the IX material to the acidic dissolver solution, the ^{137}Cs concentration decreases about 7-fold on the organic resin and about 120-fold in the inorganic fraction to give about a 100-fold decrease overall. Americium concentrations in the organic and inorganic fractions are about equal initially. On exposure to the dissolver solution, the concentration on the organic fraction increases

Table 4.16. Chemical and Radionuclide Concentrations in Test 3 Residual Solids

Solid	Chemical Concentration (wt%)						
	Al	Ca	Fe	Na	Si	U	Zr
6:37	2.72	0.912	7.14	1.05	33.0	0.0331	0.101
9:30	2.81	0.786	5.00	1.02	33.9	0.00492	0.116
Solid	Radionuclide Concentration ($\mu\text{Ci/g}$)						
	^{60}Co	^{137}Cs	^{154}Eu	^{241}Am	$^{239,40}\text{Pu}$	$^{238}\text{Pu}/^{241}\text{Am}$	Alpha
6:37	4.49E-01	1.59E+01	1.68E-02	2.09E-01	8.76E-01	2.95E-01	1.17E+00
9:30	5.73E-01	1.53E+01	2.53E-02	1.79E-01	5.13E-01	2.56E-01	7.85E-01

about 10-fold, while the inorganic fraction remains unchanged. Uranium concentrations in both fractions are unaffected by exposure to the dissolver solution.

4.4.5 Residual Solids Particle Size Distribution

Particle size distributions of samples of Test 3 residual solids in a 1 M HNO₃ suspension were determined by a laser light scattering technique. The samples were from the dissolver slurry retrieved at 6:37 test duration and the residual solids remaining at the end of the test (~9:30). The distributions were measured on solids lightly agitated by 40 ml/s recirculation in the 1 M HNO₃ medium and on the solids after 90 s treatment by a 40-W ultrasound source. Results, presented in Table 4.18, show that longer processing time shifted the particle size distribution to larger overall size for the non-sonicated solids. The increased particle size may indicate agglomeration of flocs. However, this explanation is suspect because sonication only slightly decreased the 30- μ m population of the 9:30 sample, shifting it to the 8- μ m size. The particle size distribution of the 6:37 residual solids after sonication was not measured.

Table 4.17. Chemical and Radionuclide Concentrations in Test 3 Ion Exchange Materials

Solid	Chemical Concentration (wt%)						
	Al	Ca	Fe	Na	Si	U	
Start - Org	0.443	1.22	0.132	3.02	0.451	0.249	
Start - Inorg	4.69	0.537	1.12	2.78	22.9	0.0571	
Start - Combined	1.99	0.953	0.491	2.89	8.64	0.176	
Final - Org	0.225	0.047	2.28	0.144	0.302	0.266	
Final - Inorg	1.22	0.410	2.78	1.02	28.1	0.0514	
Final - Combined	0.522	0.156	2.41	0.406	8.64	0.200	
Solid	Radionuclide Concentration (μ Ci/g)						
	⁶⁰ Co	¹³⁷ Cs	¹⁵⁴ Eu	²⁴¹ Am	^{239,40} Pu	²³⁸ Pu/ ²⁴¹ Am	Alpha
Start - Org	4.32E-02	7.34E+00	2.26E-02	1.49E-01	1.07E-01	1.53E-01	2.63E-01
Start - Inorg	2.75E-02	4.96E+02	--	2.58E-01 ^a	4.50E-01	3.25E-01	7.78E-01
Start - Combined	3.69E-02	1.86E+02	--	1.79E-01	2.31E-01	2.14E-01	4.47E-01
Final - Org	2.05E-02	1.01E+00	1.29E-01	1.41E+00	3.11E+01	5.99E+00	3.71E+01
Final - Inorg	3.14E-02	4.09E+00	3.35E-02	2.63E-01	3.95E+00	8.42E-01	4.80E+00
Final - Combined	2.36E-02	1.93E+00	9.94E-02	1.06E+00	2.27E+01	4.40E+00	2.71E+01

^a Estimated by deducting the contribution of ²³⁸Pu from the combined ²³⁸Pu/²⁴¹Am alpha peak. The ²³⁸Pu activity is about 0.15 of the ^{239,240}Pu activity based on radionuclide concentrations found in the KE Areas Sludge Composite and IX material.

Table 4.18. Overall Particle Size Distribution for Test 3 Residual Solids

Agitation	Sample	Volumetric Particle Size, %		
		~30 μ m	~8 μ m	~2 μ m
40 ml/s	6:37	56	34	10
	9:30	89	11	0
40 ml/s with ultrasound	6:37	No	No	No
	9:30	82	18	0

Specific examination of the lower particle size region was performed; results are presented in Table 4.19. The populations for residual solids taken at both 6:00 and 9:00 centered around 1-2 μm . Sonication decreased the particle size distribution for the 9:30 residual solids but not that of the 6:37 solids. Again, however, difficulties in obtaining sufficient sample were encountered, possibly preventing the acquisition of a representative particle size distribution.

4.4.6 Fractional Dissolution

The quantities of materials that dissolve in the Test 3 treatment of KE Areas Sludge Composite to hot nitric acid are displayed in Figure 4.6. Uranium dissolution seemed to occur rapidly, ultimately attaining about 99.99%. Again, aluminum dissolution was slower than uranium, and iron dissolution slower still. Dissolutions of sodium, aluminum, and calcium were incomplete, reflecting the poor solubility of anorthite in nitric acid. The silicon solution concentrations were detectable, but somewhat below the analytical reporting threshold. The data were consistent, however, and indicate that silicon solution concentrations rapidly reached saturation with respect to amorphous silica. Total silicon dissolution was low based on these data, the high concentration of silicon found in the residual solids, and the presence of quartz and anorthite as found by XRD.

The TRU dissolutions were well over 99%. The lower extent of ^{137}Cs dissolution (about 98.9%) may reflect the presence of some mordenite in the sludge. Dissolution of ^{60}Co was lower yet. Retention of ^{60}Co in the iron solid phase may account for its relatively low dissolution.

4.4.7 Material Balance

The quantities of bulk chemical components found in the dissolver solution and residual solids may be compared with the quantities expected from analyses of the KE Areas Sludge Composite (Table 3.7) and the IX material (Table 4.17) to arrive at a material balance (Table 4.20). The material balance presented here for Test 3 includes the elements measured by ICP and the radiochemicals found in the dissolver solution and residual solids. Material balances for nitrogenous and carbon dioxide offgas species are addressed in Section 5.0. The low material balances found for ^{137}Cs and ^{241}Am seemingly reflect difficulties in obtaining representative samples of the radionuclide-rich, mixed organic resin and zeolitic IX material, and also may reflect the heterogeneity of the sludge as shown in Table 3.7.

Table 4.19. Particle Size Distribution Below 6 Microns for Test 3 Residual Solids

Agitation	Sample	Volumetric Particle Size, %		
		~1-2 μm	~0.15 μm	~0.004 μm
40 ml/s	6:37	100	0	0
	9:30	100	0	0
40 ml/s with ultrasound	6:37	100	0	0
	9:30	67	22	11

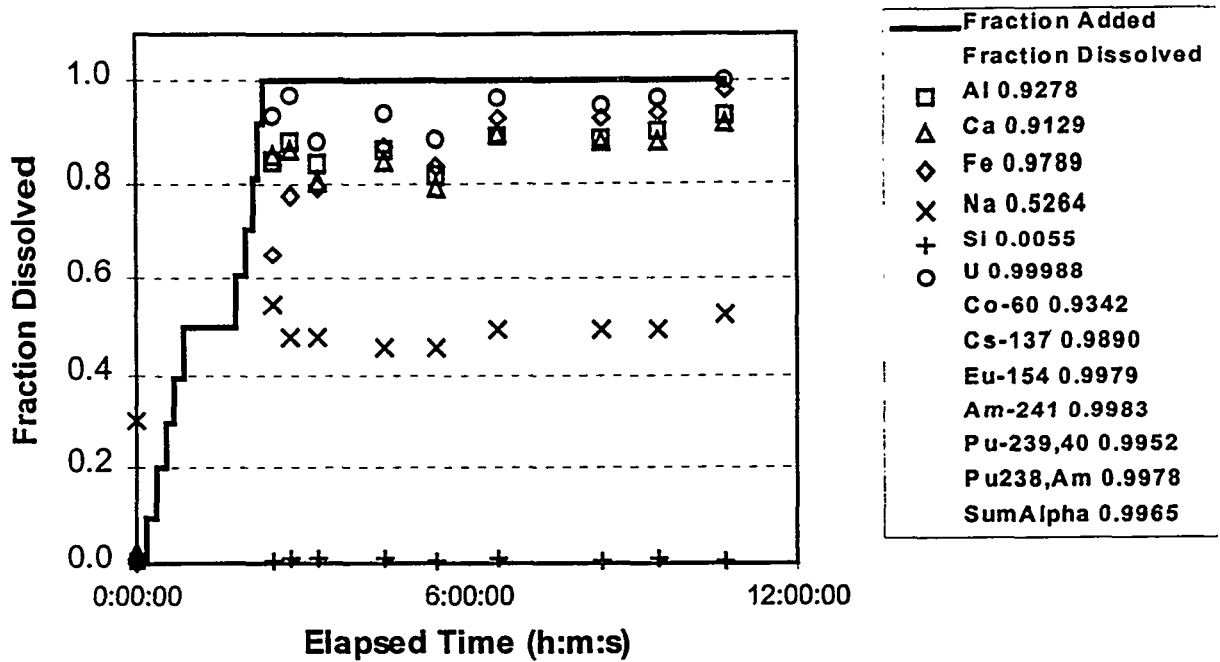


Figure 4.6. Fractions of Analytes Dissolved in Test 3 as a Function of Time (fraction dissolved at end of test given in legend box).

Table 4.20. Material Balance for Test 3

	Quantity, μg				
	Al	Ca	Fe	Si	U
Sludge&IX	2.48E+06	6.61E+05	1.58E+07	3.27E+06	2.85E+06
Dissolver Soln.	3.26E+06	7.51E+05	2.12E+07	1.80E+04	4.38E+06
Res. Solids	2.53E+05	7.12E+04	4.56E+05	3.06E+06	5.02E+02
IX	6.74E+03	2.01E+03	3.12E+04	1.12E+05	2.58E+03
Diss.&Res.&IX	3.52E+06	8.24E+05	2.17E+07	3.17E+06	4.39E+06
Recovery,%	142.3	124.7	137.4	97.6	154.1
	Quantity, μCi				
	¹³⁷ Cs	²⁴¹ Am	^{239,240} Pu	²³⁸ Pu/ ²⁴¹ Am	Alpha
Sludge&IX	4.35E+04	2.91E+03	7.43E+02	7.48E+02	1.01E+03
Dissolver Soln.	1.24E+04	9.28E+02	9.98E+02	1.04E+03	2.05E+03
Res. Solids	1.38E+02	1.62E+00	4.70E+00	2.32E+00	7.16E+00
IX	2.49E+00	1.36E+00	2.94E+01	5.69E+00	3.51E+01
Diss.&Res.&IX	1.26E+04	9.31E+02	1.03E+03	1.05E+03	2.09E+03
Recovery,%	28.8	32.0	138.9	140.7	206.7

4.5 Evaluation and Comparison of Residual Solids Compositions

The chemical and radionuclide concentrations in the residual solids produced by nitric acid processing of K Basin sludges in the validation tests may be compared with concentrations found from processing similar or identical materials in prior tests. The comparisons help identify the effects of process conditions on the chemical attack. The uranium and radionuclide concentrations in the solids also may be compared with the relevant ERDF disposal criteria. Comparisons of the residual solids compositions with the results from previous testing and with ERDF criteria are presented and discussed in this section.

4.5.1 ERDF Criteria

The compositions of the residual solids were compared against the ERDF Waste Acceptance Criteria (WAC) (Bechtel 1998) to determine whether, and to what extent, further washing/leaching would be necessary before the residual solids could be dispositioned ERDF. These comparisons provide insight into the ability of the nitric acid dissolution step to decontaminate the residual solids. However, for the following reasons, the comparison cannot be used to draw definitive conclusions on whether the residual solids generated within the K Basin Sludge Pretreatment Process will be acceptable for disposal to ERDF. First, in the comparisons below, the residual solids are compared to ERDF WAC on the basis of sludge type (i.e., KE Canister Sludge Composite and KE Areas Sludge Composite), whereas, in the baseline process, all residual solids from K Basin sludge dissolutions will be accumulated and mixed in one tank, which will effectively average the residual solids composition. This averaging will have a dramatic effect on the analyte concentrations in the residual solids from KE Basin, since the less contaminated KE Areas (i.e. floor and pit) residual solids will account for most of the residual solids mass. The more highly contaminated residual solids from the KE canisters and fuel washing will account for only about 1% of total mass.

Second, the baseline process includes a leaching step that will be performed to further decontaminate the residual solids. This leaching step has not been taken into consideration within the comparisons made below. Third, in the baseline process, the leached residual solids will be immobilized in a grout matrix before disposition to ERDF. In accordance with ERDF rules, compliance with the ERDF WAC will be based upon the concentrations of the analytes within the grout matrix (e.g., TRU activity per unit mass of grout). Therefore, while the ERDF criteria provide a benchmark for comparison and evaluation of nitric acid dissolution, for the reasons discussed, the comparisons cannot be used to make absolute judgments on the efficacy of the process.

The ERDF disposal criteria for the various elements or radionuclides are often stated in measurement values that do not directly correspond to the reported analytical concentrations. In Table 4.21, the ERDF criteria are recalculated and their corresponding values expressed in the same units as normally reported.

In addition to the comparison with individual analyte limits, the cumulative impact of the radionuclide concentrations in the residual solids, with respect to ERDF criteria, was evaluated with the "sum of fractions" method (10 CFR 61.55). When two or more radionuclides are present in a waste to be dispositioned to ERDF, the concentration of each constituent in the waste must be divided by the appropriate ERDF limit. The quotients are then summed, and the sum must be less than or equal to 1 for the waste to be acceptable for disposal. It should be noted that the sum of TRU and Pu/Am constitutes "double counting" in the sum of fractions analysis.

Table 4.21. Equivalent Concentrations for the ERDF Criteria

Analyte	ERDF Criterion	Equivalent Conc.	Rationale
²³⁸ U ²³⁵ U	0.012 Ci/m ³ ²³⁸ U and daughters 0.0027 Ci/m ³	0.0013 g U/g	²³⁸ U decays to stable ²⁰⁶ Pb by 8 alpha and 6 beta decays. The specific activity of ²³⁸ U is 3.36x10 ⁻⁷ Ci/g. Thus, the specific activity of the chain is 14 times higher or 4.7x10 ⁻⁶ Ci/g U. 0.012 Ci/m ³ is equivalent to 0.0026 g ²³⁸ U/ml or 0.0013 g ²³⁸ U/g solid (assuming a solids density of 2 g/ml) or 0.13 wt% uranium. The ERDF criterion for ²³⁵ U (0.0027 Ci/m ³ , daughters not included) is equivalent to 0.14 g U/g assuming 0.9% ²³⁵ U. The ²³⁵ U-based criterion is less restrictive than the ²³⁸ U-based criterion.
¹³⁷ Cs	32 Ci/m ³	16 μCi ¹³⁷ Cs/g	Solids density of 2 g/ml assumed.
²³⁹ Pu ²⁴⁰ Pu ²³⁸ Pu	0.029 Ci/m ³ 0.029 Ci/m ³ 1.5 Ci/m ³	0.022 μCi ^{239,240} Pu/g	The ERDF criteria for ²³⁹ Pu and ²⁴⁰ Pu are equal but ²³⁹ Pu represents about 3/4 of the combined measured ^{239,240} Pu activity in Hanford material. The ERDF criterion for ²³⁸ Pu is 1.5 Ci/m ³ and is not significant in the mix of Pu isotopes. Solids density of 2 g/ml assumed.
²⁴¹ Am	0.050 Ci/m ³	0.025 μCi ²⁴¹ Am/g	Solids density of 2 g/ml assumed.
TRU	100 nCi/g	0.100 μCi total α/g	

4.5.2 KE Canister Sludge Residual Solids

The bulk element and radionuclide concentrations found in residual solids from nitric acid processing of KE Canister Sludge Composite in Tests 1 and 2 are given in Table 4.22. These data are compared with residual solids concentrations found in similar tests by Carlson et al. (1998a) for the same sludge composite and Makenas (1999) for a single, iron-rich KE canister sludge sample (96-08).

The residual solids weights are similar for all tests with the KE Canister Sludge Composite, ranging from about 1% to 2% of the initial dry sludge amount. The iron concentrations in the residual solids decrease with increasing leaching time and increasing acid concentration. The primary residual solids component is silica (with aluminum and calcium), and the XRD data for the residual solids, where available, all show quartz, anorthite, and muscovite. The residual solids from the treatment of the iron-rich sample 96-08 residual solids is about 12 wt% of the starting material and remains relatively rich in iron and aluminum. Phases identified in the residual solids are anorthite and quartz. Two FeO(OH) phases, goethite and lepidocrocite, were found for residual solids leached at lower temperatures.

The residual solids also contain about 0.5 to 7 wt% uranium. The uranium concentrations in the residual solids decrease with leaching time and increase with increasing acid concentration. The presence of this relatively high uranium concentration in the acid-leached residual solids implies that acid-stable uranium phases (perhaps uranium silicates) are present. Particles rich in uranium and silicon have been identified on unwashed and acid-leached OIER taken from the floor of the KE Basin (sample H-08). The X-ray powder diffraction patterns obtained for the final residual solids samples taken at the ends of Tests 1 and 2 were examined closely for the presence of uranium silicate phases, but none were identified. Uranium concentrations were about 4 to 50 times the relevant ERDF criterion.

The concentrations of ¹³⁷Cs found in the residual solids ranged from about 15 to 85 μCi/g or about 1 to 5 times the ERDF criterion. Cesium concentrations decreased with increasing leach time and were lowest for the 6 and 7.8 M HNO₃ concentration tests.

Table 4.22. Chemical and Radionuclide Concentrations in KE Canister Sludge Residual Solids and Comparison to ERDF Criteria

Test	Solid	Conditions	Wt% Res.	Chemical Concentration (wt%)								
				Al	Ca	Fe	Si					
Test 1	KE Can. Comp.	143 g sludge/L, 95°C, 6 M, 10:07	--	1.69	0.77	2.95	24.4					
		143 g sludge/L, 95°C, 6 M, 24:08	2.1	1.81	1.09	1.27	35.0					
Test 2	Fuel & KE Can. Comp.	(50 g U metal fuel & 69 g sludge)/L, 95°C, 6 M, 21:37	--	1.13	0.94	5.30	26.4					
		(50 g U metal fuel & 69 g sludge)/L, 95°C, 6 M, 23:30	0.8	1.77	0.95	2.81	20.9					
	Zircaloy	(50 g U metal fuel & 69 g sludge)/L, 95°C, 6 M, 23:30	5.7 of fuel	--	--	--	--					
Carlson et al. (1998a)	KE Can. Comp.	217 g sludge/L, boil, 4 M, 11 hr	1.5	1.32	0.55	10.5	19.5					
		45 g sludge/L, boil, 6 M, 11 hr	1.0	1.60	0.89	1.04	31.3					
		58 g sludge/L, boil, 7.8 M, 11 hr	0.91	1.61	0.79	1.04	35.6					
		70 g sludge/L, boil, 10 M, 11 hr	1.0	1.65	1.19	1.23	33.2					
Makenas (1999)	96-08	58 g sludge/L, 95°C, 10 M, 6 hr	12	4.44	1.93	3.14	30.9					
Test	Cond.	Radiochemical Concentration and Fraction (Fr.) of ERDF Criterion										
		U		¹³⁷ Cs		^{239,240} Pu		²⁴¹ Am		Alpha		Sum
		Wt%	ERDF Fr.	μCi/g	ERDF Fr.	μCi/g	ERDF Fr.	μCi/g	ERDF Fr.	μCi/g	ERDF Fr.	Fract.
Test 1	10:07	7.04	54	85.3	5.3	14.9	550	5.59	220	20.5	205	1070
	24:08	0.647	5.0	33.6	2.1	4.65	170	1.73	69	6.83	68	320
Test 2	21:37	1.54	12	203	13	19.1	870	16.5	660	37.3 ^a	370	1920
	23:30	0.467	3.6	86.4	5.4	4.73	180	6.83	270	10.8	108	570
	Zircaloy	0.033	0.25	55.8	3.5	0.726	33	1.11	44	1.79	18	99
Carlson et al. (1998a)	4 M	5.08	39	82.7	5.2	26.9	1000	4.93	200	37 ^a	370	1510
	6 M	2.40	18	15.6	1.0	8.17	300	1.45	58	12 ^a	120	500
	7.8 M	3.70	28	14.9	0.9	11.0	410	1.57	63	16 ^a	160	660
	10 M	5.36	41	23.4	1.5	21.7	800	2.45	98	29 ^a	290	1230
Makenas (1999)	10 M	2.10	7.7	72.5	4.5	5.86	210	5.05	200	11.4	114	530

^a Sum of alpha activity with estimated contributions of ²³⁸Pu and ^{242,244}Cm.

Plutonium and americium, like uranium, had decreasing concentrations in the residual solids with increasing leach time and with decreasing leachate acid concentration. The higher concentrations of the actinides in the residual solids with acid concentration increasing above 6 M may reflect the increased stability (lower solubility) of silica with increasing acid concentration (Elmer and Nordberg 1958; Felmy et al. 1994). Thus, mineralization of plutonium and americium with silicate may be occurring in the K Basin sludge. Further solids characterization is required to confirm or refute this possibility.

The concentrations of plutonium found in the residual solids ranged from about 5 to 27 μCi/g or about 170 to 1000 times the ERDF criterion. Americium concentrations ranged from about 1.6 to 7 μCi/g or 60 to 270 times the ERDF criterion. The separate TRU criterion, which accounts for both the plutonium and americium, was exceeded by 70- to 400-fold. Thus, the radionuclides of most concern for disposal of the KE canister sludge residual solids are the transuranium isotopes, ^{239,240}Pu and ²⁴¹Am. The leaching and characterization data at least suggest that attack of the silicate component is required to dissolve the TRU.

4.5.3 KE Areas Sludge Composite Residual Solids

The bulk element and radionuclide concentrations found in residual solids from nitric acid processing of KE Areas Sludge Composite (KE floor and Weasel Pit sludge) in Test 3 are given in Table 4.23. These data are compared with residual solids concentrations found in similar tests by Carlson et al. (1998b) for the same sludge composite and by Makenas (1999) for a single KE floor sludge sample (T-20).

The residual solids weights from KE Areas Sludge Composite were about 17 wt% of the starting material's dry weight, except for one test using a relatively low 4 M HNO₃ concentration and high solids loading in which about 23 wt% was left in the residual solids. The residual solids remaining for the single KE floor sludge sample T-20 was about 50 wt% of the starting material. For the sludge from the KE Areas Sludge Composite, quartz and anorthite phases again were found. The quartz phase was more prominent. For the T-20 residue, quartz and goethite were found.

Again, the iron concentrations in the residual solids decreased with increasing leach time, acid concentration, and sludge loading in the dissolution. Iron concentrations range from about 1 to 21 wt% of the residue (about 16 wt% for the T-20 residue). Calcium concentrations were about 0.4 to 1 wt%; aluminum about 1.5 to 2.8 wt%. Calcium and aluminum, with silicon and oxygen, are present in anorthite. Silicon again was the prominent element in the residual solids.

The residual solids from the KE Areas Sludge Composite were much less concentrated in uranium and radionuclides than the KE canister sludge residual solids. The uranium concentrations ranged from 0.005 to about 0.5 wt% (0.04 to about 4 times the ERDF criterion). The uranium concentrations were lower for the Test 3 residual solids than for residual solids produced in prior testing. The lower concentrations may reflect the more thorough washing performed on the Test 3 residual solids.

Table 4.23. Chemical and Radionuclide Concentrations in KE Floor and Weasel Pit Sludge Residual Solids

Test	Solid	Conditions	Wt% Res.	Chemical Concentration (wt%)								
				Al	Ca	Fe	Si					
Test 3	KE Areas Comp.	75 g sludge/L, 95°C, 6 M, 6:37	--	2.72	0.91	7.14	33.0					
		75 g sludge/L, 95°C, 6 M, 9:30	17.1	2.81	0.79	5.00	33.9					
Carlson et al. (1998b)	KE Areas Comp.	115 g sludge/L, boil, 4 M, 24 hr	22.6	1.47	0.46	21.2	22.0					
		25 g sludge/L, boil, 4 M, 24 hr	18.9	1.93	0.63	2.44	32.6					
		43 g sludge/L, boil, 6 M, 24 hr	16.9	1.57	0.44	1.09	35.5					
		55 g sludge/L, boil, 7.8 M, 24 hr	16.6	2.02	0.62	1.54	33.4					
Makenas (1999)	T-20	~58 g sludge/L, 60°C, 10 M, 8 hr	49.9	1.77	0.61	15.6	25.6					
Test	Cond.	Radiochemical Concentration and Fraction (Fr.) of ERDF Criterion										
		U		¹³⁷ Cs		^{239,240} Pu		²⁴¹ Am		Alpha		Sum Fract.
		Wt%	ERDF Fr.	μCi/g	ERDF Fr.	μCi/g	ERDF Fr.	μCi/g	ERDF Fr.	μCi/g	ERDF Fr.	
Test 3	6:37	0.0331	0.25	15.9	1.0	0.876	40	0.209	8.3	1.17	12.0	62
	9:30	0.0049	0.04	15.3	1.0	0.513	23	0.179	7.2	0.785	7.9	39
Carlson et al. (1998b)	4 M, 115	<0.2	<1.5	64.5	4.0	2.99	140	0.592	24	4.1 ^a	41	210
	4 M, 25	<0.2	<1.5	12.2	0.8	0.432	20	0.370	15	0.95 ^a	9.5	46
	6 M	<0.2	<1.5	5.18	0.3	0.132	6.0	0.082	3.3	0.25 ^a	2.5	13
	7.8 M	0.21	1.6	10.2	0.6	0.454	21	0.385	15	0.95 ^a	9.5	47
Makenas (1999)	10 M	0.46	3.5	45.2	2.8	0.392	18	0.254	10	0.708	7.1	42

^a Sum of alpha activity with estimated contributions of ²³⁸Pu and ^{242,244}Cm.

The ^{137}Cs concentrations ranged from about 5 to 64 $\mu\text{Ci/g}$ or 0.3 to 4 times the ERDF criterion. The ^{137}Cs concentrations in the residual solids did not decrease with increasing leach time (for the two points tested) and were lowest at about 6 M HNO_3 .

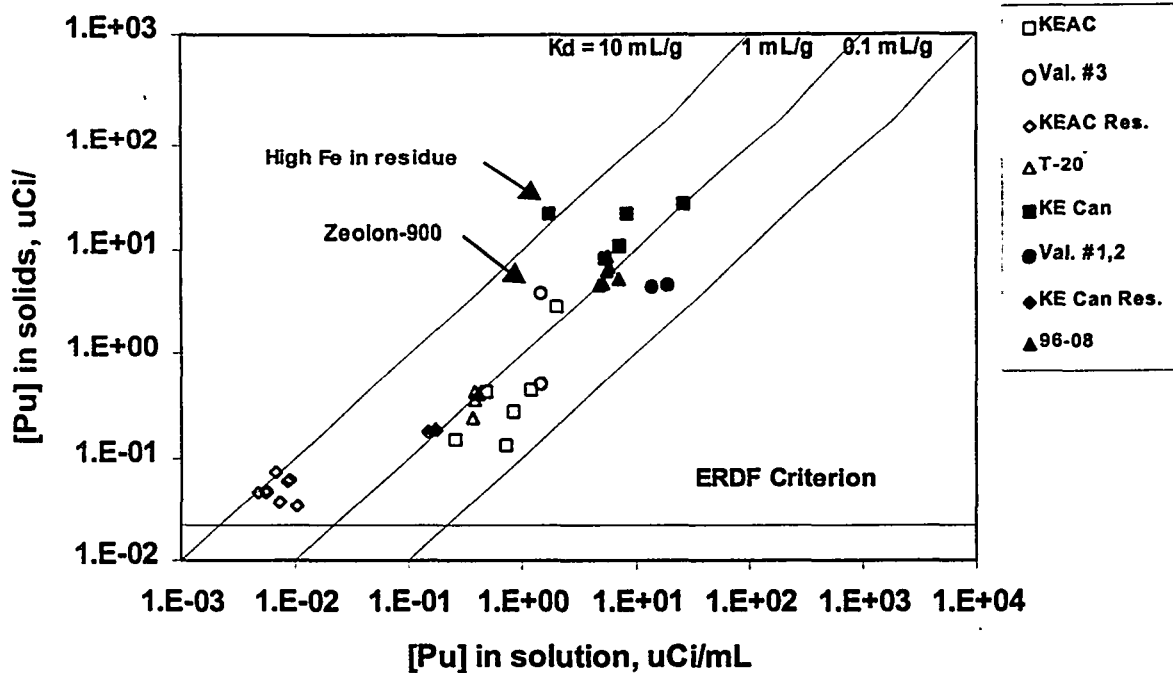
Although the effect of acid concentration was not strong, the plutonium and americium concentrations also were lowest at 6 M HNO_3 . Increasing leach time decreased plutonium and americium concentrations slightly. Plutonium was present at about 0.13 to 3 $\mu\text{Ci/g}$ or 6 to 140 times the ERDF criterion; americium was about 0.08 to 0.6 $\mu\text{Ci/g}$ or 3 to 24 times the ERDF criterion. The ERDF criterion for TRU was exceeded from 2.5- to 40-fold. Again, the radionuclides causing the most impact on reaching the ERDF criteria are ^{241}Am and, particularly, $^{239,240}\text{Pu}$.

4.5.4 Plutonium Concentrations on Residual Solids

As shown in Tables 4.16 and 4.17, the residual solids from single contact leaching of the KE canister and floor and Weasel Pit sludges are 6 to 1000 times the ERDF disposal criterion for plutonium. Separate tests have been performed to decrease the radionuclide (particularly plutonium) concentration in residual solids from single contact HNO_3 leaching of KE Canister and KE Areas Sludge Composites (Delegard et al. 1998a,b; 1999). Beginning with a 6 M HNO_3 solution, a variety of leachant additives targeting plutonium were tested on the KE Areas Sludge Composite residue. Oxidative dissolution of plutonium suspected to be present as Pu(IV) oxide was tested using strong oxidants [persulfate with silver ion catalyst and cerium(IV)]. To dissolve Pu(IV) oxide by fluoride complexation, or plutonium associated with silicate by attack of the silicate matrix, hydrofluoric acid additive was used. To dissolve plutonium possibly associated with iron oxides or hydroxides, hydrochloric acid additive was used. Of the four leachants tested, 6 M HNO_3 /0.3 M HF proved to be the most effective, not only for plutonium but also for uranium and americium, and nearly the most effective for cesium (Delegard et al. 1998a). The plutonium concentration in the solids decreased about a factor of 8 with 4-hr leaching at 95°C. Subsequent tests with a KE Canister Sludge Composite residue confirmed the efficacy of this leachant, and plutonium concentrations decreased about a factor of 35 (Delegard et al. 1998b).

As noted previously, the solid phases observed by X-ray diffraction of residual solids from nitric acid treatment in all instances for which XRD analyses are available include native Hanford soil minerals: quartz (SiO_2), anorthite ($\text{Ca}_2\text{Al}_2\text{Si}_2\text{O}_8$), and sometimes muscovite (a mica-like mineral). In addition, significant amounts of amorphous material, indicated by a large mound in the XRD patterns and qualitatively observed as difficult-to-filter gels in the leaching tests, are found in the silica-rich solids. Silica gels are known to form from acid treatment of certain silicate minerals, including anorthite (Terry 1983). Thus, silica gels are almost certainly present in the acid treatment residual solids.

In reviewing the technical literature, it was found that silica gel and high silica glass can sorb plutonium from strong acid solution (Cleveland 1970). Distribution coefficients, K_{ds} ($[\text{Pu}_{\text{solid}}]/[\text{Pu}_{\text{solution}}]$), of about 0.2 to 1 ml/g are reported. In the reported studies, plutonium K_{ds} were found to be relatively independent of nitric acid concentration in the range of 1 to 8 M , but increase sharply (stronger sorption) in less concentrated acid. Plutonium exchange rates with silica gel were low, requiring hours to reach equilibrium at 25°C to 40°C. Because of these findings, the concentrations of plutonium found in the various residual solids produced from acid treatment and leaching tests of K Basin sludge were plotted as a function of plutonium concentration in the associated supernatant solutions (Figure 4.7). All plutonium solid/solution data available from nitric acid processing tests of K Basin sludge were used to prepare Figure 4.7 (Carlson et al. 1998a, b; Makenas 1999; Delegard et al. 1998a, b; and the present validation testing).



KEAC data from Carlson et al. (1998b).
 KE Can data from Carlson et al. (1998a).
 Val. #1,2 and Val. #3 data from present report.
 KEAC Res. and KE Can Res. data from Delegard et al. (1998a) and (1998b), respectively.
 T-20 and 96-08 data from Makenas (1999).

Figure 4.7. Plutonium Concentrations in Solid Residues as a Function of Plutonium Solution Concentrations from Nitric Acid Treatment and Leaching of K Basin Sludge

It is seen that plutonium concentrations on K Basin sludge residual solids are roughly proportional to the plutonium solution concentrations regardless of the sludge origin (individual sludge samples, sludge composites, and residual solids from HNO_3 treatment), HNO_3 leachant concentration (2 to 10 M), sludge/solution ratio (25 to 143 g sludge/L), leachant additive [none, HF, HCl, $\text{Ag}^+/\text{S}_2\text{O}_8^{2-}$, Ce(IV)], leaching time (4 to 24 hr), leach temperature (25°C to boiling), and solid/liquid separation and rinsing technique (filtration/washing, centrifuge/decant) used in the testing. That is, the behavior of plutonium can be described by a K_d .

The corresponding ^{137}Cs concentrations on sludge residual solids are not proportional to the ^{137}Cs concentrations in solution and are not described by a K_d (Figure 4.8). Thus, the plutonium behavior is not simply a function of the thoroughness of solids washing.

Most plutonium K_d s in Figure 4.7 are around 1 ml/g and thus lie near the values observed in the previously cited studies of sorption on silica gel. In Figure 4.7, higher K_d s were observed for a KE Canister Sludge Composite treatment test which used 2 M HNO_3 and left high residual iron (18 wt% Fe; $K_d \cong 13$ ml/g) and for leached KE Areas Sludge Composite residual solids having low plutonium concentrations. A K_d of about 2.7 ml/g was found for the inorganic (mordenite) ion exchange material in Test 3.

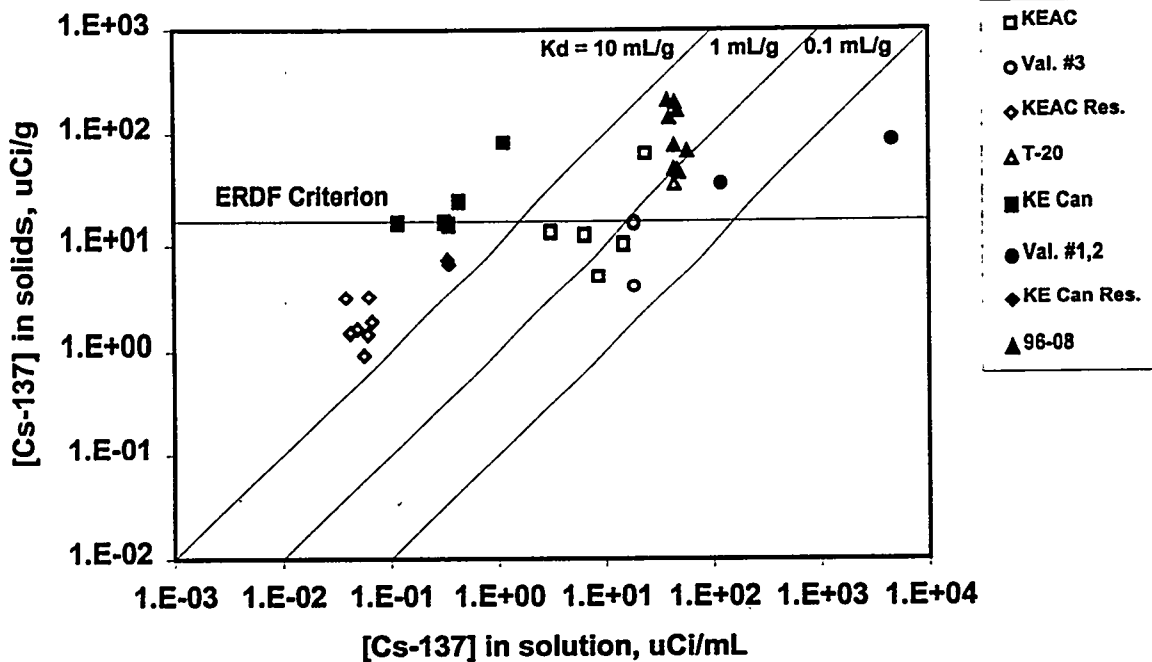


Figure 4.8. Cesium-137 Concentrations in Solid Residues as a Function of Cesium-137 Solution Concentrations from Nitric Acid Treatment and Leaching of K Basin Sludge

If ion exchange is the mechanism for plutonium retention on the siliceous solids, HNO_3/HF may have been the most effective leachant of the four tested because, in addition to its effect on dissolving silicates, PuF^{3+} (or other fluoride complexes that decrease cation exchange loading) was formed. Oxalate in dilute HNO_3 , however, may be a more effective leachant than fluoride. Oxalate will form charge-neutral $\text{Pu}(\text{C}_2\text{O}_4)_2^0$, which should have low ion exchange affinity. Oxalate with HF may be even more effective by providing a combination of plutonium complexing and silicate attack. Additional testing is required to determine if $\text{HNO}_3/\text{H}_2\text{C}_2\text{O}_4$ or $\text{HNO}_3/\text{H}_2\text{C}_2\text{O}_4/\text{HF}$ will leach residual solids better than HNO_3/HF .

5.0 Dissolver Offgas Analysis

Offgas analyses were performed online to quantify the rate and extent of reaction and to demonstrate the feasibility of offgas monitoring as a process control method. The design, operation, and calibration of the offgas analysis system are presented in this section. Also presented are results obtained for offgas analyses of Tests 2 and 3 (offgas analyses for Test 1 were not performed). These results are compared with results predicted based on quantities and compositions of the feed KE Basin materials.

5.1 Offgas Analysis, Sampling, and Instrumentation

The analysis of the dissolver offgas employed MS (Hewlett Packard 5972 instrument scanning from 1.2-300 atomic mass unit, amu) and GC/TCD (Microsensor Technology, Inc). The schematic of the analysis system is illustrated in Figure 5.1.

The MS was capable of detecting each of the anticipated gases produced during dissolution. The GC was used to analyze gases having similar masses. The low resolution MS used was unable to distinguish between gases having masses within 1 amu. The GC also had lower detection limits in some instances. Because the gas was directly introduced into the MS, it was anticipated that the MS would perform more consistently than the GC for reactive gases such as NO and NO₂. In addition, the MS was scanned over a sufficient mass range to allow detection of any unanticipated offgas components.

Throughout the analysis, a cover gas consisting of 90% helium and 10% neon was introduced into the dissolver head space at a rate of 0.50 L/min. The cover gas acted as a diluent (helium) and as an internal standard (neon). The offgas outlet from the dissolver was passed through a condenser having an approximate 30-cm path length at 4°C. The outlet of the condenser was connected by a 0.45- μ m Teflon filter to a 2-m section of high-density polyethylene tubing. The outlet of the filter connected to 0.25 in. x 3 m stainless steel tubing, passing through the hot cell wall to the sampling manifold. The sampling manifold is also illustrated in Figure 5.1.

Gas samples were introduced into the MS using a 2-m section of 0.10-mm-ID fused capillary tubing. One end of the fused silica tubing was attached to the sampling manifold; the other was connected directly to the MS analyzer. The sample gas flow into the MS was approximately 0.8 ml/min. The MS results were averaged to produce one data point (of all scanned masses) every 8 s.

Gas samples were introduced into the GC using a 1.5-m length of 1/16-in. stainless steel tubing. Approximately every 3 min, the GC sampling pump pulled sample gas from the sampling manifold at a flow of 10 ml/min past a semi-permeable hydrophobic membrane. The membrane was used to decrease water contained in the sample gas stream which, if introduced into the GC column, would have accumulated in the chromatographic column and eventually would have degraded the GC performance. The gas sampled by the GC then was directed through a sample loop and subsequently introduced into the GC columns. Two parallel columns, a 4-m molecular sieve and an 8-m Poropak Q, were used to separate the gas components. Each column used a separate TCD.

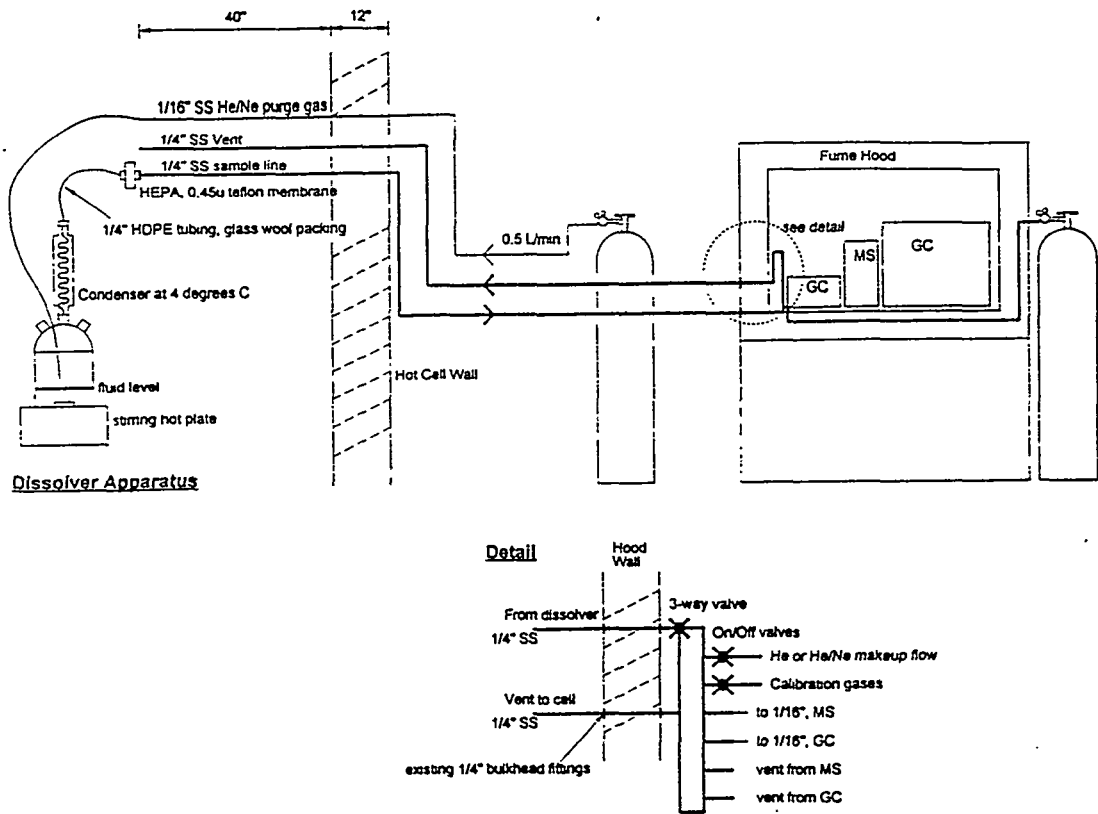


Figure 5.1. Schematic of Offgas Flow and Analysis System for K Basin Sludge Dissolution Testing

5.2 Calibration

The analytical instrumentation was calibrated using a series of 10 gas standards obtained from Norco, Inc. Each of the standards was analyzed by the vendor to be within $\pm 2\%$ of the stated value. The 10 bottles of standard gas, components, and their concentrations are listed in Table 5.1. The gas components and their concentration were chosen based on the anticipated offgas from the dissolver system and the cover gases chosen. The bottles used as cover gas during analysis are listed in Table 5.2.

Prior to the instrument calibration, the MS was first tuned using PFTBA (perfluoro-tetrabutylamine) tuning gas to ensure proper mass assignment and mass resolution was obtained. Calibration data were then obtained before and after each of the dissolution tests. Each of the calibration gases was introduced into the sampling manifold at a flow rate of 0.50 L/min. The sampling manifold inlet valve was switched to allow only calibration gas flow. With the valve in the calibration position, the standby cover gas (helium) for the MS was switched off, and the gas from the dissolver system bypassed the sampling manifold. For each calibration mixture, at least 3 min of data were obtained on the MS using the identical parameters as the actual dissolver offgas analysis. The GC obtained at least a duplicate set of analyses during calibration.

The GC was calibrated using an external standard method because the response to the internal standard was virtually unchanged throughout the time of data acquisition. The GC detector response to various concentrations of a specific gas was fit to a linear regression.

The MS responses to the various gas components were calculated relative to neon, which was used as the internal standard. The relative response factors (RRF) obtained were used to quantitate gases in the sample.

$$RRF = \frac{R_{(gas)}}{R_{(ISTD)}} \times \frac{C_{(ISTD)}}{C_{(gas)}}$$

where

$R_{(gas)}$ = response of the characteristic ion for the gas measured

$R_{(ISTD)}$ = response of the characteristic ion for the internal standard (neon)

$C_{(ISTD)}$ = concentration of the internal standard (neon)

$C_{(gas)}$ = concentration of the gas measured

Table 5.1. Calibration Gases Used As Standards

Level	High +	High	Med	Low
<u>Calibration Gas 1</u>				
Component		Cylinder 1	Cylinder 2	Cylinder 3
NO ₂	none	20000	2000	100
He	Balance			
<u>Calibration Gas 2</u>				
Component		Cylinder 4	Cylinder 5	Cylinder 6
NO	none	50000	2000	100
He	Balance			
<u>Calibration Gas 3</u>				
Component	Cylinder 7	Cylinder 8	Cylinder 9	Cylinder 10
O ₂	100000	10000	1000	100
H ₂	20000	2000	200	20
N ₂ O	none	2000	200	20
CO	20000	2000	200	20
CO ₂	100000	10000	1000	100
Ne (tracer)	100000	10000	1000	100
Xe	1000	100	10	1
He	Balance			

Table 5.2. Gases Used As Cover/Internal Standards During Testing

Component	Cylinder 11	Cylinder 12
Ne	100000	100000
He	Balance	

5.3 Data Acquisition

Before the offgas dissolution studies, the sampling system response time was evaluated. Immediately before Test 2, the dissolver vessel was filled with the initial amount of nitric acid solution, heated, and stirred. The cover gas was turned on and introduced into the dissolver vessel exactly as performed in the dissolution tests that followed. After the system had equilibrated for approximately 20 min, a 5-ml sample of air was injected into the dissolver vessel at the liquid sampling port. Data were obtained to evaluate the analytical system response time and peak width.

Following the response time evaluation, data for offgas of dissolution Test 2 were obtained on August 5-6, 1998. Dissolution Test 3 was performed on August 19, 1998. Throughout both of the tests, 0.50 L/min of cover gas was introduced into the dissolver vessel. Care was taken throughout the tests to minimize the quantity of air introduced into the vessel from fuel or sludge additions.

5.4 Quantitation

The amount of each gas present was determined after each dissolver run was completed. For Test 2, the concentration of each gas was determined by comparing the detector response with the best fit linear regression obtained while calibrating the GC. This calculation was performed for each set of data obtained throughout the dissolver run.

For Test 3, quantitation was performed in the same manner as in Test 2; however, because the GC had difficulty resolving CO₂ and NO₂, for Test 3 a single peak and retention time were obtained for both gases. To obtain concentrations of CO₂, the contribution of NO₂ was removed by using the concentration results obtained for NO₂ from the MS. The calculated NO₂ response on the TCD was subtracted after an adjustment was made to account for the differing thermal conductivities of the two gases. The thermal conductivity adjustment was verified by the ratio of response factors for the two gases obtained during calibration for Test 2.

Quantitation of the MS data was performed for each averaged mass scan obtained. The MS averaged 2⁷ (128) scans for each reported mass scan, which was obtained approximately every 8 s. A comparison of the response for a given gas relative to the response of the internal standard was obtained and compared with the ratio of responses obtained for the standard calibration gases at the appropriate concentrations during calibration. As is typical for mass spectrometers, internal standard adjustments were necessary due to drift of detector response with time.

The ion masses used for quantitation and any necessary adjustments to response or concentration are presented in Table 5.3.

Table 5.3. Mass Spectrometer Quantitation Ions and Corrections for Gas Components

Gas Component	Quantitation Ion Mass	Response Correction
Neon (Ne)	20	No correction required
Nitrogen (N ₂)	28	Subtract CO contribution using GC data. Subtract CO fragment ion contribution from CO ₂
Carbon Monoxide (CO)	28	Subtract N ₂ contribution using GC data
Nitric Oxide (NO)	30	Subtract NO fragment ion contributions from NO ₂ and N ₂ O
Oxygen (O ₂)	32	No correction required
Nitrous Oxide (N ₂ O)	44	Subtract CO ₂ contribution using GC data and adjust for ionization sensitivity
Carbon Dioxide (CO ₂)	44	Subtract N ₂ O contribution using GC data and adjust for ionization sensitivity
Nitrogen Dioxide (NO ₂)	46	No correction required
Xenon (Xe)	132	No correction required

5.5 Results and Discussion

Offgas monitoring was shown to be an effective online technique for tracking the progress of the sludge dissolution reactions. The gas chromatograms corresponded with the test events (e.g., sludge addition, acid addition, sample collection) and the results from the analyses of the solution samples (i.e., completion of dissolution reactions). Results from offgas monitoring for nitrogen oxides (NO_x, which includes NO, NO₂, and N₂O) are in good agreement with the sludge and fuel fragment dissolution reactions. The quantity of NO_x measured ranged from 50% to 90% of the quantity predicted. The monitoring of carbon dioxide in the offgas can also be used as an indication of the progress of the dissolution reactions.

Plots from the offgas analyses are contained in Appendix D (Test 2, MS), Appendix E (Test 2, GC), and Appendix F (Test 3).

5.5.1 System Response Time Tests

The results of monitoring the air components nitrogen, oxygen, and carbon dioxide (Figure D.1) showed the response time for the system was approximately 0.8 min from the time air was injected into the system until the MS began detection. While peak response for air was observed at 1.2 min, the elapsed time for overall response, the time it takes for the MS to return to within 10% of the baseline value, was 1.4 min. The system performance was monitored during the same time period using neon and relative moisture. This test was not performed for the GC because the sampling interval (~3 min) was too long to accurately measure the 1-2 min transit time.

5.5.2 Test 2 System Performance

The relative stability of both analytical systems was demonstrated by the response of each instrument to the internal standard (neon). The response of the MS to neon varied from the first portion to the end of the test by almost 90%. Figure E.4 shows the response for the GC was nearly unchanged throughout the

test. Although the data compare quite well, the conclusion can be made from the relative stability information that the GC data should take precedence over the MS data whenever possible. Retention time shifting on the GC indicated some instability, although it was not manifested in the neon response. However, other factors should be taken into consideration, such as comparability of the data sets for other gas components and comparison with expected results.

5.5.3 Test 3 System Performance

The ability of the GC to resolve components was compromised during Test 3. The NO and N₂O were unresolved and eluted as a single peak, as were NO₂ and CO₂. Therefore, NO₂ and NO data were not obtained from the GC for this test. However, their contributions were subtracted using the MS data in order to obtain results for N₂O and CO₂.

The MS stability for Test 3 was improved over Test 2, as seen by the relative stability of neon throughout the run (Figure F.1). The MS provided the only results for NO and NO₂ for this test.

5.5.4 Quantities of Gas Projected in Validation Testing

The quantities of offgas produced by the dissolution reactions may be estimated based on the compositions of the sludge materials being dissolved and the chemical reactions anticipated. The principal anticipated and observed product gases are CO₂, NO, and NO₂. Lesser amounts of N₂O may arise based on known reactions of nitric acid with UO₂ (Herrmann 1984); minor amounts of N₂ also form by reaction of nitric acid with uranium metal (Blanco and Watson 1961). The amounts of gaseous products projected in the validation testing are predicted and evaluated in the following sections.

5.5.4.1 Carbon Dioxide

Carbon dioxide may be produced by the decomposition of carbonate salts (inorganic carbon) from the sludge in acid and by the oxidation of carbon found as a trace component in uranium metal fuel and as organic carbon in the sludge. The speciation of organic carbon in the sludge is not known. However, cellulose, found in paper, cardboard, and plant life, is arguably the most credible and prevalent source of organic carbon in the K Basin sludge. The oxidation state of carbon in cellulose, (C₆H₁₀O₅)_x, is zero. Thus, for the purposes of this analysis, the organic carbon oxidation state is assumed to be zero. Nominal reactions that produce CO₂ are presented.

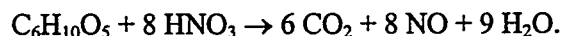
Acidification of carbonate salts:



Oxidation of carbon present in metallic fuel by nitric acid:



Oxidation of organic carbon (represented here as the cellulose monomer):



In Tests 1 and 2, the total inorganic carbon (TIC) concentration of the KE Canister Sludge Composite may be estimated based on the compositions (Makenas et al. 1997) and respective masses (Table 3.2) of

the individual samples used to prepare it. The derived TIC concentration in the dry KE Canister Sludge Composite is 0.002372 g/g. The concentration of inorganic carbon in the KE Areas Sludge Composite used in Test 3 is 0.002618 g C/g dry sludge. The TIC concentration in the KE Areas Sludge Composite was calculated based on the weighted average of the samples used to create it (Table 3.6) and the analyses of these samples on a dry basis (Makenas et al. 1996). Three of the 17 sludge samples used to prepare the composite were not analyzed for TIC, so estimates were made based on concentrations found for neighboring samples.

In Test 2, uranium metal also was dissolved. The concentration of carbon nominally present in the metal is 0.000330 to 0.000735 g/g (RHO 1980).

Organic carbon concentrations present in the KE Canister Sludge Composite and the KE Areas Sludge Composite were calculated based on characterization data (Makenas et al. 1997 and 1996, respectively) and sample masses (Tables 3.2 and 3.6). For the dry KE Canister Sludge Composite (Tests 1 and 2), the organic carbon concentration was calculated to be 0.001832 g/g; for the dry KE Areas Sludge Composite (Test 3), the total organic carbon concentration was found to be 0.003176 g/g. Test 3 also had about 1 g of OIER present in the stainless steel mesh module. Oxidation of the resin by nitric acid ultimately would produce CO₂, but likely would be too slow to be noticeable in Test 3. Although some attack of the organic resin by nitric acid probably occurred (as shown by the roughened surface of nitric acid-treated resin found by SEM), the organic resin largely would have survived the nitric acid treatment (Pool et al. 1998).

Carbon dioxide was evolved in Test 1 from the decomposition of carbonate (inorganic carbon) salts and oxidation of organic carbon in the KE Canister Sludge Composite (71.36 g of sludge, dry basis, were used). The amount of CO₂ from the inorganic carbon thus is $71.36 \times 0.002372 / 12.011 = 0.0141$ moles. The amount of CO₂ from the organic carbon is $71.36 \times 0.001832 / 12.011 = 0.0109$ moles.

In Test 2, CO₂ is produced from the carbon oxidized from the metallic uranium fuel pieces (28.92 g) and from inorganic and organic carbon in the KE Canister Sludge Composite (40.05 g, dry basis). Assuming a carbon concentration of 0.0005 g/g uranium metal, 0.0012 moles of CO₂ would evolve from the metal. The subsequent KE Canister Sludge Composite addition would yield 0.0057 moles of CO₂ from inorganic carbon decomposition and 0.0044 moles CO₂ from the organic carbon oxidation.

In Test 3, CO₂ is produced from inorganic and organic carbon in the KE Areas Sludge Composite (52.67 g, dry basis). The sludge was added in two nearly equal groups of five pellets. For the inorganic carbon, the first group contained 49.6% of the added sludge or 0.0057 moles CO₂; the second group contained the balance or 0.0058 moles CO₂. The CO₂ produced from the organic carbon oxidation would be 0.0069 moles from the first group of sludge pellets and 0.0070 moles from the second group.

5.5.4.2 Nitrogenous Offgas Products

The products of nitrate reduction caused by oxidation of organic carbon, carbon in uranium fuel, UO₂, and uranium metal itself are primarily NO and NO₂. Some lesser quantities of N₂O and N₂ also are produced. These are all gaseous products. Little or no dissolved species (except dissolved gases) are expected as products (Herrmann 1984). Nitrate, but not nitrite, was found in all test solutions. Nitrite disproportionates in acid to yield NO and NO₂. The reduction of nitrate to these various products involves changes in the oxidation state of the contained nitrogen. For example, the chemical reduction of nitrate [NO₃⁻, oxidation state (V)] to NO₂ [oxidation state (IV)] is a one-electron change. The chemical reductions of nitrate to NO [(II)], N₂O [(I)], and N₂ [(0)] are, respectively, three-, four-, and five-electron

changes. The diversity and potential distribution of the nitrogenous products complicate the prediction of offgas composition. Therefore, it is more useful to predict the change in chemical equivalents (the moles of total change in the nitrogen oxidation state).

The oxidation of organic carbon from cellulose to CO₂ is a four-electron change for each carbon. The oxidation of elemental carbon present in uranium metal fuel likewise is a four-electron change. Oxidation of UO₂ to the dissolved uranyl ion, UO₂²⁺, is a two-electron change, and the oxidation of uranium metal to UO₂²⁺ is a six-electron change. The number of nitrate reduction equivalents required to achieve the oxidations in the three validation tests may be predicted based on the amounts of organic carbon in the sludge, uranium (as UO₂) in the sludge, carbon in the uranium metal, and uranium metal used in the respective tests.

For Test 1, the total number of nitrate reduction equivalents is the amount required to oxidize the organic carbon (0.001832 g/g) and the UO₂ (0.685 g U/g) present in the KE Canister Sludge Composite (71.36 g). This amount would be $71.36 \times 0.001832 \times 4/12.011 = 0.0435$ equivalents for the organic carbon and $71.36 \times 0.685 \times 2/270.03 = 0.3620$ equivalents for the UO₂.

Test 2 was conducted in two stages: uranium metal fuel piece addition (28.92 g metal) followed by KE Canister Sludge Composite addition (40.05 g). The uranium metal oxidation would require $28.92 \times 6/238.0 = 0.7290$ equivalents. The oxidation of carbon in the uranium would require $28.92 \times 0.0005 \times 4/12.001 = 0.0048$ equivalents. The subsequent oxidation of the UO₂ in the KE Canister Sludge Composite would require 0.2032 equivalents and oxidation of the organic carbon would require 0.0176 equivalents.

In Test 3, 52.67 g of KE Areas Sludge Composite (5.4 wt% uranium) were treated with nitric acid. The sludge was added in two nearly equal portions consisting of five frozen pellets each. Oxidation of the contained UO₂ in the first portion would require 0.01014 equivalents; the second portion would require 0.0106 equivalents. Oxidation of the organic carbon would require 0.0276 and 0.0280 equivalents, respectively.

The projected quantities of CO₂ offgas and nitrate reduction equivalents are presented in Table 5.4.

Table 5.4. Projected Quantities of Offgas

Test	CO ₂ (moles) from				NO ₃ ⁻ Reduction (Equivalents) from Oxidation of				
	C in U Metal	TIC	TOC	Total	U metal	UO ₂ in Sludge	C in U Metal	TOC	Total
1	0	0.0141	0.0109	0.0250	0	0.3620	0	0.0435	0.4056
2, U metal	0.0012	0	0	0.0012	0.7290	0	0.0048	0	0.7338
2, sludge	0	0.0057	0.0044	0.0101	0	0.2032	0	0.0176	0.2208
2, metal & sludge				0.0113	2, metal & sludge				0.9546
3, 1 st group	0	0.0057	0.0069	0.0126	0	0.0104	0	0.0276	0.0381
3, 2 nd group	0	0.0058	0.0070	0.0128	0	0.0106	0	0.0281	0.0387
3, 1 st and 2 nd group				0.0254	3, 1 st and 2 nd group				0.0768

5.5.5 Comparison of Projected and Measured Offgas Quantities

The quantities of gas projected based on the K Basin material quantities and compositions may be compared with the actual measured quantities (offgas measurement results are presented in Appendices D through F).

The offgas quantities are reported for different periods in Tests 2 and 3 corresponding to the additions of the uranium metal pieces and the sludge pellets. In Test 2, the uranium metal additions occurred over about the first 2.5 hr of the run; sludge additions began about 17:06 into the run. Therefore, gas collected in the interval from 0:00 to 16:15 was quantified, representing that gas generated from metal dissolution (though some small quantity of metal still remained undissolved prior to sludge addition). The gas generated in the remainder of the test (interval from 16:20 to 22:30) also was quantified, representing the gas generated from the dissolution of the KE Canister Sludge Composite. In Test 3, the KE Areas Sludge Composite was added in two five-pellet portions. The offgas profiles were divided to identify quantities released in the two portions (i.e., approximately in the intervals 0:00 to 1:37 and 1:37 to 3:24). Overall offgas quantities also were determined for the entire 10-hr duration of Test 3 to quantify the gas that continued to evolve by exsolution from the dissolver liquor. These quantities proved to be significantly greater than the sum of the two 0:00-1:37 and 1:37-3:24 intervals, particularly for the oxides of nitrogen.

The CO₂ quantities found for Tests 2 and 3 (Figures E.5, E.6, F.5, and F.9) are presented in Table 5.5. It is seen that in Test 2, only about 10% of the predicted amount of CO₂ is found by either GC or MS. Most of the shortfall lay in the amount expected from the sludge addition. It is possible that the inorganic carbon originally present in the component samples of the KE canister sludge had been lost during storage by radiolytic or corrosion reactions. Such reactions could lower the solution pH and cause release of carbonates as CO₂ gas. The pH of KE Basin waters was reported to be 6.38 and 6.68 (Makenas et al. 1997). However, the pH of waters from canister cylinders sometimes was as low as 4.41, sufficiently low to decompose carbonate salts. Measurements of gases evolved from "bubbling" sludge samples (96-05, 96-06, 96-13, and 96-15) indicate CO₂ concentrations ranging from 0.049 to 0.90 mole percent (Makenas et al. 1997). The pH of the KE Canister Sludge Composite was measured to be 5.10 ± 0.10. At pH 5.10, calcium carbonate, the primary carbonate phase found in the K Basin sludges, readily dissolves and liberates CO₂. Though further analyses would determine the carbonate concentration in sludge, the pH measurements give strong evidence that the KE Canister Sludge Composite became depleted in carbonate during storage.

Table 5.5. Quantities of Carbon Dioxide in Tests 2 and 3

Test	Predicted, Moles	Gas Chromatography		Mass Spectrometry	
		Found, moles	Found/Pred.	Found, moles	Found/Pred.
2, U metal	0.0012	0.00077	0.64	0.00038	0.32
2, sludge	0.0101	0.00100	0.10	0.00059	0.06
2, total	0.0113	0.00177	0.16	0.00098	0.09
3, 1 st group	0.0126	0.00811	0.64	0.00801	0.64
3, 2 nd group	0.0128	0.01003	0.78	0.01113	0.87
3, total	0.0254	0.02327	0.92	0.02426	0.95

Much closer agreement is found between the predicted and analyzed quantities of CO₂ for Test 3; 92% to 95% of the predicted CO₂ was quantified in the offgas. The pH of the KE Areas Sludge Composite was measured to be 7.80 ± 0.01. At this pH, calcium carbonate is stable.

The quantities of nitrate reduction gas (NO₂, NO, N₂O) found by GC and MS (Test 2) and by MS alone (Test 3) can be compared with the predicted equivalents of electrochemical reduction of NO₃⁻. The comparisons are presented in Table 5.6. In addition, small quantities of xenon fission product gas were detected during the dissolution of the irradiated metal in Test 2 (Figure E.5).

Table 5.6. Equivalents of Nitrate Reduction Gases in Tests 2 and 3

Test	Pred., Equiv.	Gas Chromatography					Mass Spectrometry				
		Found, moles			Total Equiv.	Found/ Pred.	Found, moles			Total Equiv.	Found/ Pred.
		NO ₂	NO	N ₂ O			NO ₂	NO	N ₂ O		
2, U metal	0.7338	0.0190	0.1043	0.000241	0.3329	0.45	0.0399	0.1297	0.000241	0.4300	0.59
2, sludge	0.2208	0.0283	0.0840	0.000221	0.2812	1.27	0.0073	0.0219	0.000221	0.0738	0.33
2, total	0.9546	0.0473	0.1883	0.000462	0.6141	0.64	0.0472	0.1516	0.000462	0.5038	0.53
3, 1 st group	0.03081	--	--	--	--	--	0.00392	0.00309	3.26E-07	0.0148	0.39
3, 2 nd group	0.03869	--	--	--	--	--	0.00633	0.00477	8.90E-07	0.0238	0.61
3, total	0.07678	--	--	--	--	--	0.0174	0.0150	1.22E-06	0.0672	0.88

The material balance in Table 5.6 suggests that not all electrochemical reductions were reflected in the measured gas products. It is likely that some dissolved gas still remained in the dissolver solution and thus would not be detected in the offgas. This phenomenon is displayed in Figures E.1 and F.2, which show NO and NO₂ still being released from solution at the ends of Tests 2 and 3, respectively, even though the dissolution reactions are complete. Condensed water in the offgas train also would scrub and remove the NO and NO₂ products. Finally, as stated in Section 5.5.3, some ambiguities exist in the quantitation of the product gases (for example, N₂O and CO₂ have the same mass, confounding the MS analyses; other gases coelute, confounding the GC analyses).

Most of the nitrogenous product gas was found to be NO (Table 5.6). The high NO concentration indicates that the oxidation was relatively efficient in nitric acid (i.e., reduction of HNO₃ to NO provides three oxidation equivalents per mole of HNO₃; reduction to NO₂ only provides one oxidation equivalent). Another way of understanding the efficiency is to plot the NO₂/NO ratio against NO_x (NO₂ + NO) partial pressure. The NO₂:NO ratio observed at selected points over the duration of Tests 2 and 3 (derived from Figures D.2, E.1, and F.2) are presented in Figure 5.2.

As shown in Figure 5.2, the NO₂:NO ratios in Test 2 ranged from about 0.15 to 1; overall through Test 2, the NO₂:NO ratio averaged 0.25 and 0.31 by the respective GC and MS methods. The NO₂:NO ratio found in Test 3, which had lower NO_x partial pressure, was about 1.16 overall (by MS) and ranged from about 0.6 to 1.3. These observations qualitatively agree with prior studies of UO₂ dissolution in HNO₃, in which lower total NO_x concentration was found to increase the NO₂:NO ratio (Herrmann 1984).

Dissolution of UO₂ in HNO₃ also has been found to produce N₂O, which increases in quantity with increasing HNO₃ concentration, and constitutes about 2% of the nitrate reduction equivalents under conditions similar to those used in Tests 2 and 3 (Herrmann 1984). However, in Test 2, the analyzed amount of N₂O only represented 0.37% of the nitrate reduction equivalents and 0.0073% of the reduction observed in Test 3 (derived from data in Table 5.6 and Figures D.5, E.4, and F.8). Detection of nitrogen (N₂) evolved in the dissolution reactions was compromised by air in-leakage (see O₂ accompanying the N₂ in Figures D.5 and F.5). For this reason, the product N₂, if it existed, could not be quantified.

6.0 References

- Bechtel Hanford, Inc. 1998. "ERDF Waste Acceptance Criteria." BHI-00139, Rev. 3, Richland, Washington.
- Beck, M. A. 1998. "K Basin Gel Formation Studies." HNF-2911, Rev. 0, Numatec Hanford Corporation, Richland, Washington.
- Blanco R. E. and C. D. Watson. 1961. "Head-End Processes for Solid Fuels." In *Reactor Handbook*, 2nd Edition, Volume II, "Fuel Reprocessing." S.M. Stoller and R.B. Richards, editors. Interscience Publishers, Inc., New York, pp. 60-61.
- Carlson, C. D., C. H. Delegard, I. E., Burgeson, A. J. Schmidt, P. R. Bredt, and K. L. Silvers. 1998a. "K Basin Sludge Conditioning Testing: Nitric Acid Dissolution of K East Canister Sludge." PNNL-12110, Pacific Northwest National Laboratory, Richland, Washington.
- Carlson, C. D., C. H. Delegard, I. E., Burgeson, A. J. Schmidt, and K. L. Silvers. 1998b. "K Basin Sludge Conditioning Testing: Nitric Acid Dissolution of K East Area Sludge Composite, Small- and Large-Scale Testing." PNNL-12109, Pacific Northwest National Laboratory, Richland, Washington.
- Cleveland, J. M. 1970. *The Chemistry of Plutonium*. Gordon and Breach Science Publishers, Inc., New York, pp. 146-147.
- Delegard, C. H., and D. E. Rinehart. 1998. "Radionuclide Leaching from Organic Ion Exchange Resin." PNNL-12105, Pacific Northwest National Laboratory, Richland, Washington.
- Delegard, C. H., D. E. Rinehart, C. D. Carlson, C. Z. Soderquist, and S. K. Fadeff, 1998a, "Radionuclide Leaching from Residual Solids Remaining After Acid Dissolution of K East Area Sludge Composite." PNNL-12104, Pacific Northwest National Laboratory, Richland, Washington.
- Delegard, C. H., D. E. Rinehart, C.Z. Soderquist, and S. K. Fadeff. 1998b. "Radionuclide Leaching from Residual Solids Remaining After Acid Dissolution of K East Canister Sludge." PNNL-12106, Pacific Northwest National Laboratory, Richland, Washington.
- Delegard, C. H., D. E. Rinehart, and F.V. Hoopes. 1999. "Distribution of Components in Ion Exchange Materials Taken from the K East Basin and Leaching of Ion Exchange Materials by Nitric/Hydrofluoric Acid and Nitric/Oxalic Acid." PNNL-12111, Pacific Northwest National Laboratory, Richland, Washington.
- Duncan, J. B. 1998. Memorandum to T. L. Flament, "Sludge Simulant for Organic Ion Exchange Resin Separation." 80720-98-JBD-001 (April 1998), COGEMA, Richland, Washington.
- Elmer, T. H. and M. E. Nordberg. 1958. "Solubility of Silica in Nitric Acid Solutions." *Journal of the American Ceramic Society* 41(5):517-520.
- Felmy, A. R., C. C. Schroeder, and M. J. Mason. 1994. "A Solubility Model for Amorphous Silica in Concentrated Electrolytes." PNL-SA-25345, Pacific Northwest Laboratory, Richland, Washington.

- Flament, T. A. 1998. "Testing Strategy to Support the Development of K Basin Sludge Treatment Process." HNF-2574, Rev. 0, Numatec Hanford Corporation, Richland, Washington.
- Herrmann B. 1984. *Auflösung Unbestrahlter UO₂-Pellets in Salpetersäure*. KfK-3673, Kernforschungszentrum Karlsruhe, Karlsruhe, Germany.
- Herrmann, B., W. Bumiller, E. Henrich, and R. v. Ammon. 1984. Zur Chemie der Auflösung von UO₂ in Salpetersäure, *KfK Nachrichten* 16:87:93.
- Makenas, B. J. (Editor). 1999. "Supplementary Information on K-Basin Sludges." HNF-2367 Rev. 0, Fluor Daniel Hanford, Inc., Richland, Washington.
- Makenas, B. J., T. L. Welsh, R. B. Baker, D. R. Hansen, and G. R. Golcar. 1996. "Analysis of Sludge from Hanford K East Basin Floor and Weasel Pit." WHC-SP-1182, Westinghouse Hanford Company, Richland, Washington.
- Makenas, B. J., T. L. Welsh, R. B. Baker, E. W. Hoppe, A. J. Schmidt, J. Abrefah, J. M. Tingey, P. R. Bredt, and G. R. Golcar. 1997. "Analysis of Sludge from Hanford K East Basin Canisters." HNF-SP-1201, DE&S Hanford, Inc., Richland, Washington.
- Makenas, B. J., T. L. Welsh, R. B. Baker, G. R. Golcar, P. R. Bredt, A. J. Schmidt, and J. M. Tingey. 1998. "Analysis of Sludge from Hanford K West Basin Canisters." HNF-1728, Rev. 0, Fluor Daniel Hanford, Richland, Washington.
- Pearce, K. L., S. C. Klimper, and T. A. Flament. 1998. "105-K Basin Material Design Basis Feed Description for Spent Nuclear Fuel Project Facilities, Volume 2, Sludge." HNF-SD-TI-009, Vol. 2, Rev. 0, Numatec Hanford Corporation, Richland, Washington.
- Pool, K. H., C. H. Delegard, A. J. Schmidt, B. M. Thornton, and K. L. Silvers. 1998. "Results from Test 4, Acid Digestion of Mixed-Bed Ion Exchange Resin." PNNL-12107, Pacific Northwest National Laboratory, Richland, Washington.
- Prescott, R. D. 1996. "Test Report for K Basin Canister Sludge Sampling Equipment." WHC-SD-SNF-TRP-013, Rev. 0, Westinghouse Hanford Company, Richland, Washington.
- Rockwell Hanford Operations (RHO). 1980. Purex Technical Manual. RHO-MA-116, Richland Washington.
- Schmieder, H., and E. Kuhn. 1972. "Automatische Kontrolle und Steuerung von Aufarbeitungsprozessen für Kernbrennstoffe durch Spektralphotometrie und Leitfähigkeitsmessung." *Chemie Ingenieur Technik* 44:104-111.
- Schmidt, A. J., G. S. Klinger, and P. R. Bredt. 1998. "Evaluation of Ion Exchange Materials in K Basin Floor Sludge and Potential Solvents for PCB Extraction from Ion Exchange Materials." PNNL-12108, Pacific Northwest Laboratory, Richland, Washington.
- Slepyan, T. A., and S. M. Karpacheva. 1960. "Physicochemical Properties of Nitric Acid Solutions of Uranyl Nitrate and Determination of Their Composition by Density, Electrical Conductivity and Index of Refraction." *Radiochemistry USSR* 2:108-115.

Swanson, J. L., L. A. Bray, H. E. Kjarmo, J. L. Ryan, C. L. Matsuzaki, S. G. Pitman, and J. H. Haberman. 1985. "Laboratory Studies of Shear/Leach Processing of Zircaloy Clad Metallic Uranium Reactor Fuel." PNL-5708, Pacific Northwest Laboratory, Richland, Washington.

Terry, B. 1983. "The Acid Decomposition of Silicate Minerals." *Hydrometallurgy* 10:135-171.

U.S. Code of Federal Regulations. "Licensing Requirements for Land Disposal of Radioactive Waste." 10CFR61.55.

U.S. Environmental Protection Agency (EPA). 1997. "Approval to Conduct Research and Development Tests to Dispose of Polychlorinated Biphenyls – Battelle Pacific Northwest Laboratory – Removal of PCB Containing Insulation Materials, Painted Metal, Soil, Sludges, Debris and Oil Using the Base Catalyzed Decomposition Process (BCD) and the KPEG Process, Solvent Washing, Acid Digestion, Chemical Oxidation, Electrochemical Destruction, Plasma Arc Destruction, and Physical Separation." Issued December 17, 1997.

Westra, A. G., T. A. Flament, and L. de Lamartinie. 1998. "K Basin Sludge Treatment Process Description." HNF-2735, Rev. 0, Numatec Hanford Corporation, Richland, Washington.

Appendix A

Photographs from Test 1

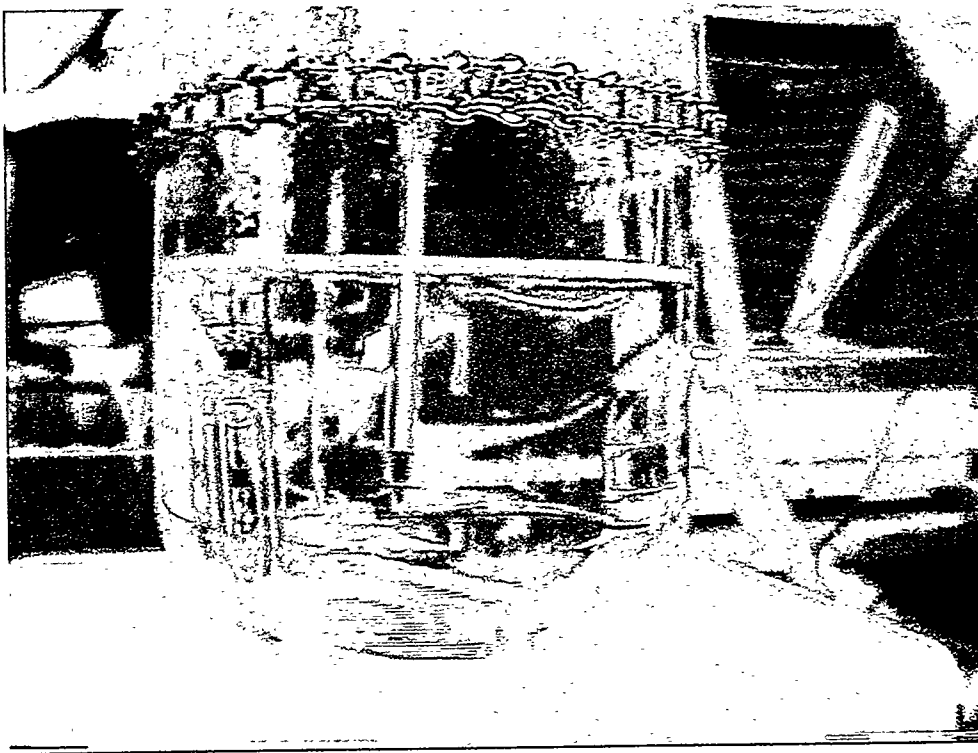
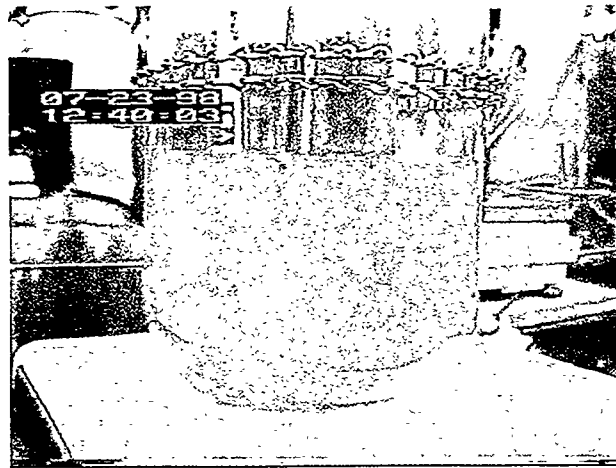


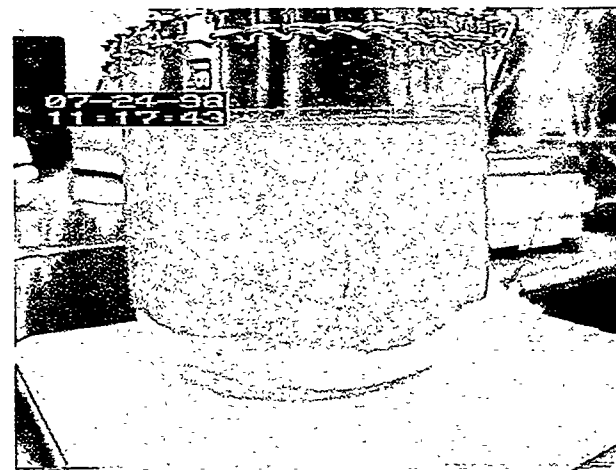
Figure A.1. Dissolver apparatus (1-liter) for Test 1 prior to sludge introduction. Entering the solution, from left to right, are the conductivity probe, the liquid sampling/addition needle, and the thermistor.



A



B



C

Figure A.2. Dissolver during Test 1.
A) After addition of sludge pellet #7 (run time = 01:30).
B) After 17 hours of digestion, gas color in reactor head visible (run time = 21:20).
C) End of run, agglomerated gel visible (run time = 24:08).

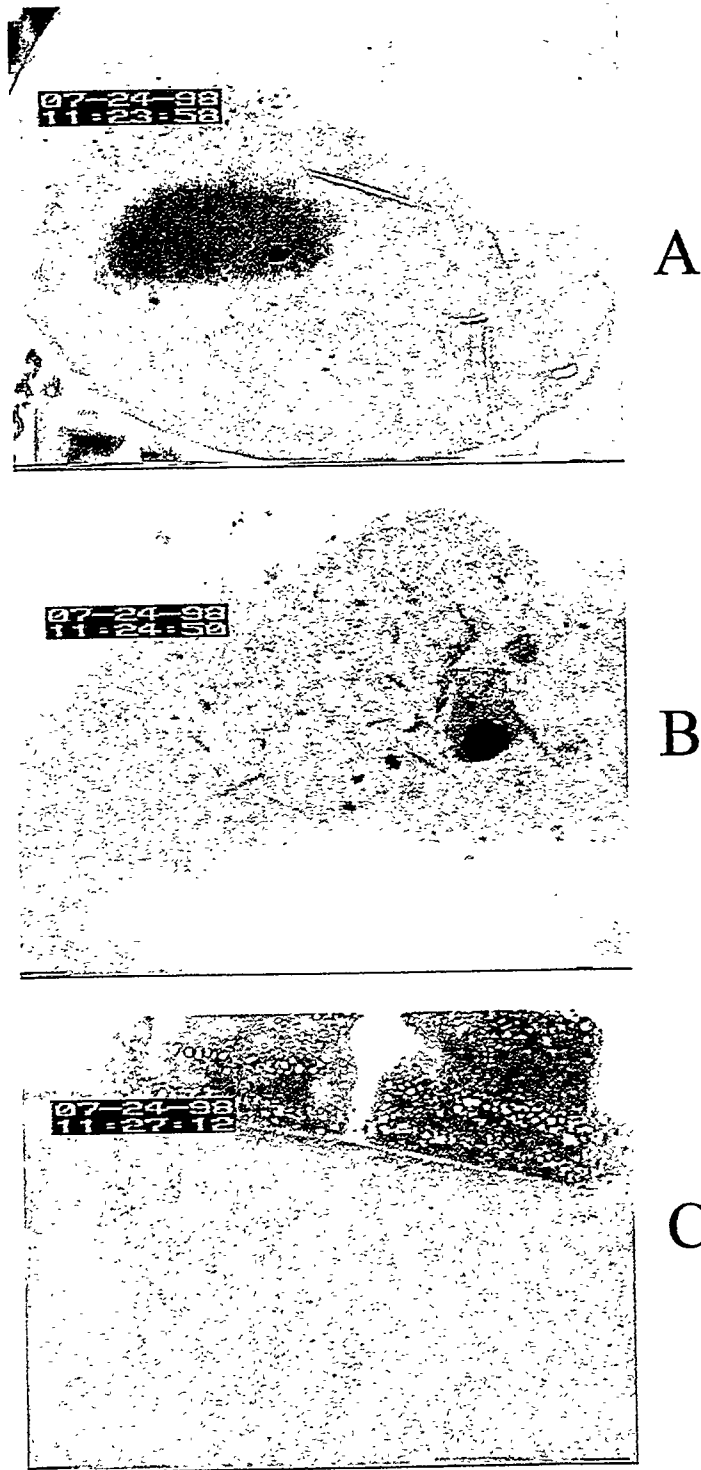
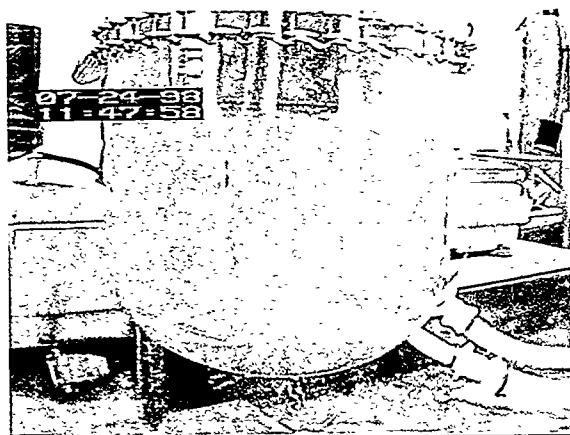
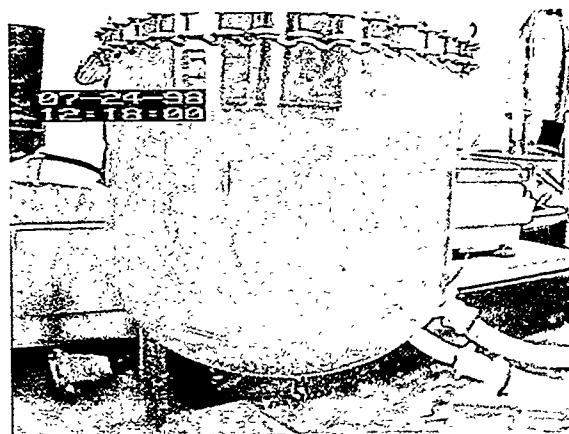


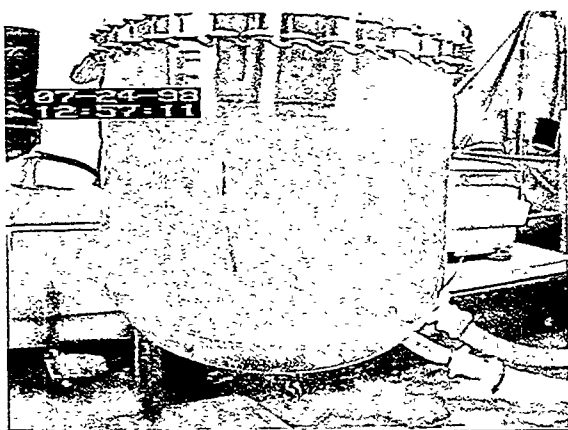
Figure A.3. Dissolver immediately following Test 1.
A) Settled solids in dissolver.
B) Close-up of gel and zirconium needles.
C) Side of vessel showing suspended solids and solids adhered to the wall.



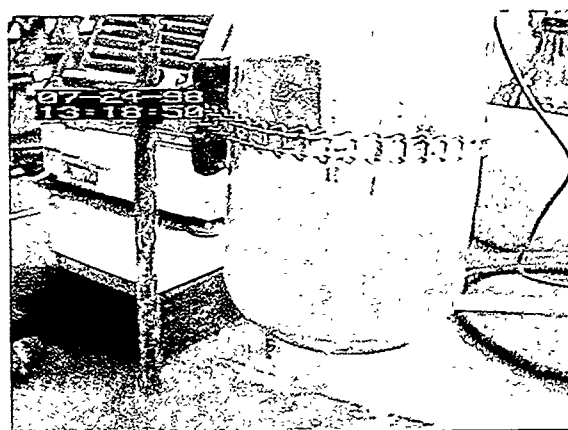
A



B



C



D

Figure A.4. Photographs showing settling of residual solids following Test 1.
A) After 30 minutes of settling and cooling.
B) After 1 hour.
C) After 1 hour and 40 minutes.
D) After 2 hours.
Photographs show most settling occurred within the first 30 minutes. It is not known what fraction of solids remained suspended in solution.

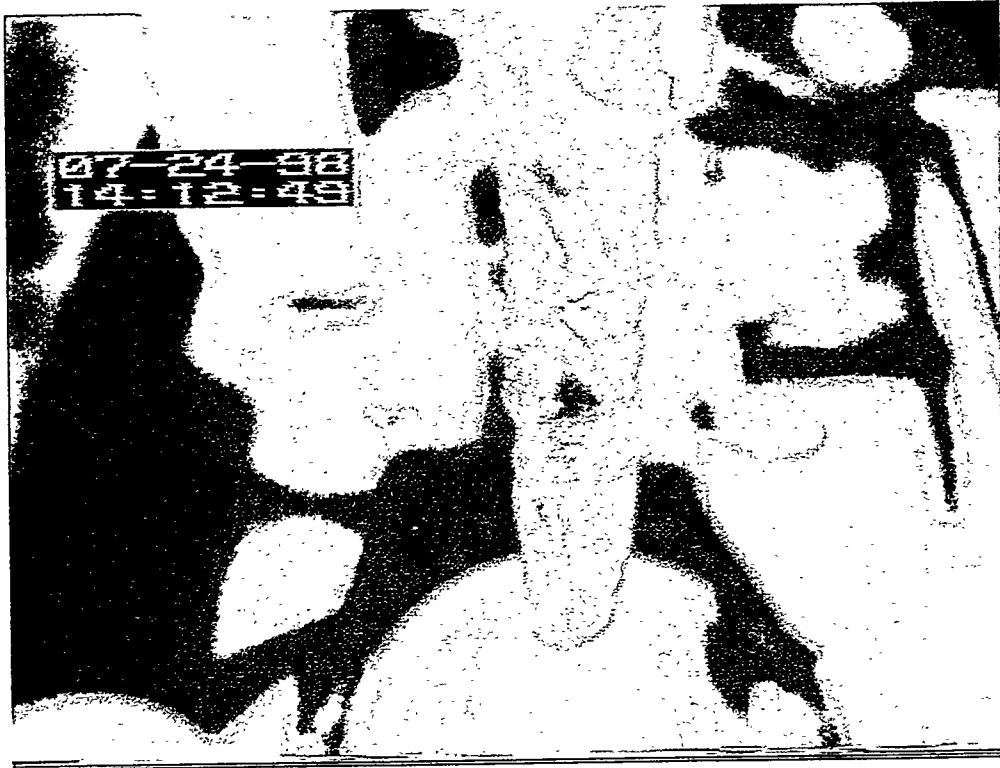


Figure A.5. Gel coating temperature probe following Test 1. Gel rinsed off easily with deionized water.

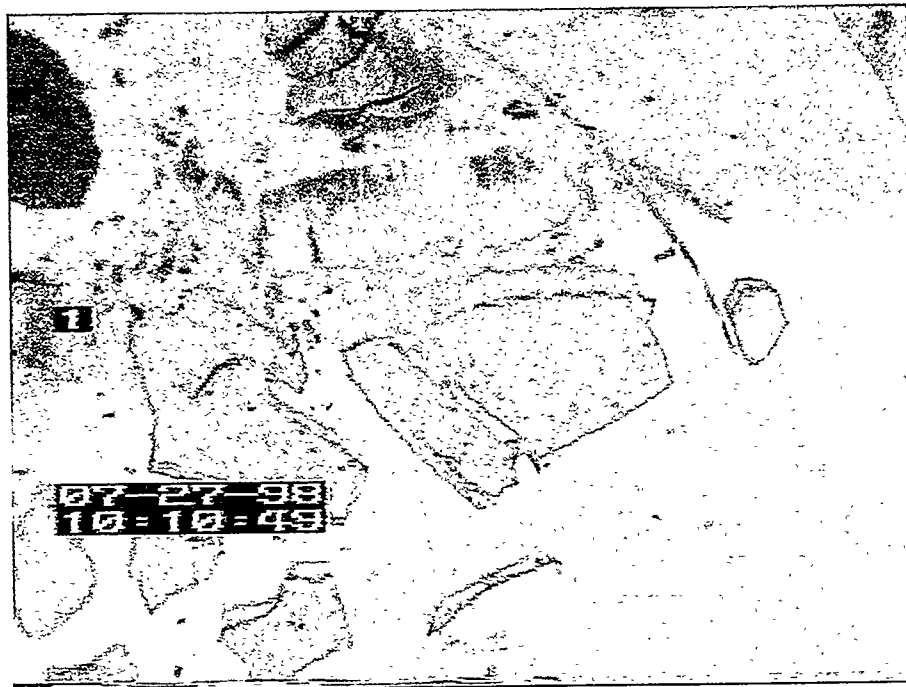
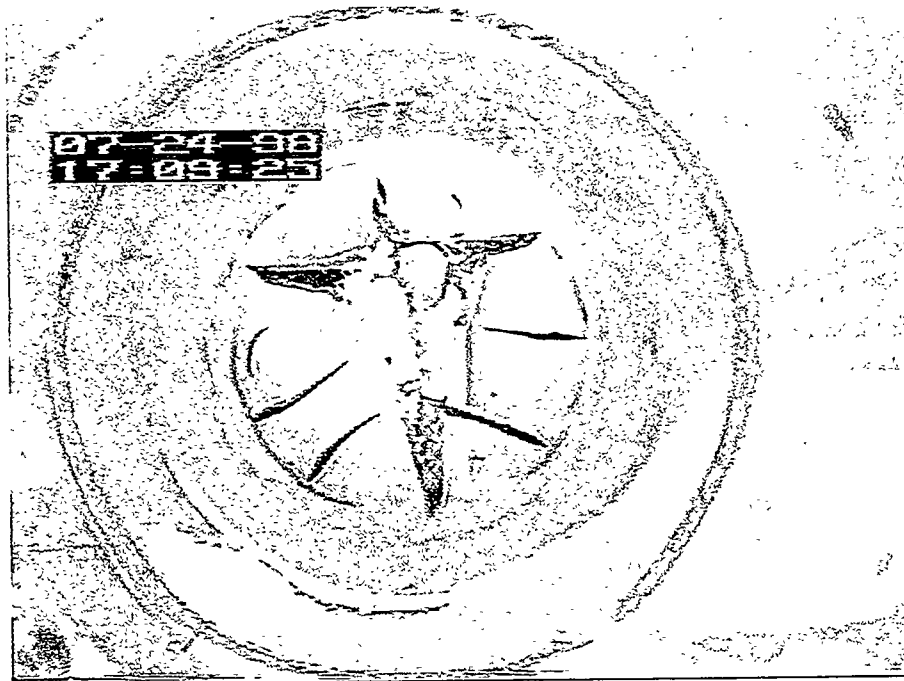


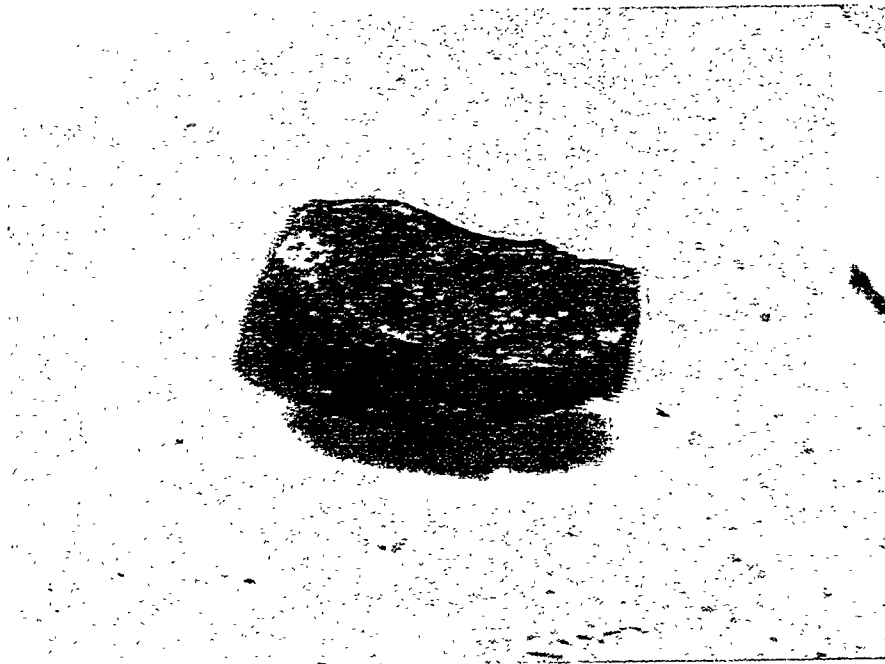
Figure A.6. Filtered residual solids from Test 1.
A) Following vacuum filtration (before drying).
B) Following air drying.

Appendix B

Photographs from Test 2

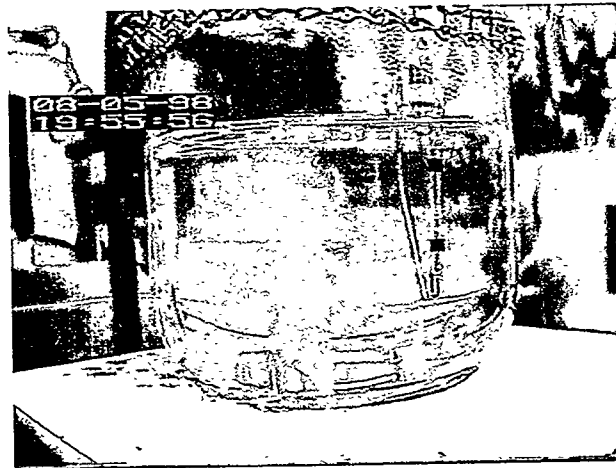


A7-1

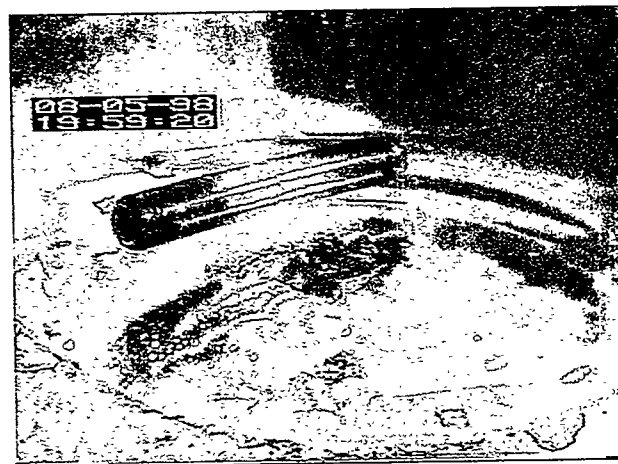


PM3

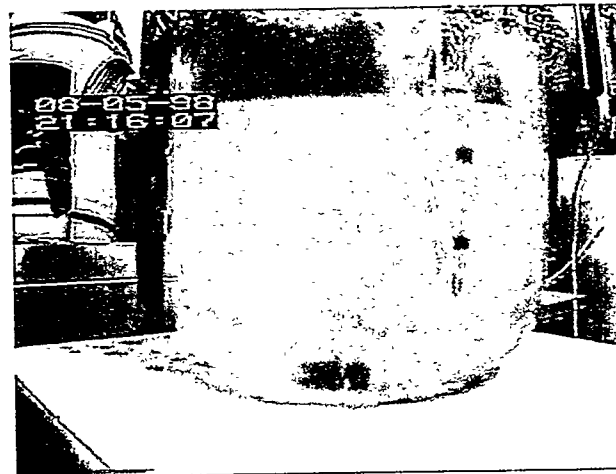
Figure B.1. Spent fuel fragments A7-1 and PM3 added to dissolver during Test 2. Fragment A7-1 (5.84 g) was cut from fragment A7 and shows fresh surfaces, while fragment PM3 (6.25g) was received from 324 Building as shown. These photographs are not to scale, and fragment PM3 is larger than A7-1.



A



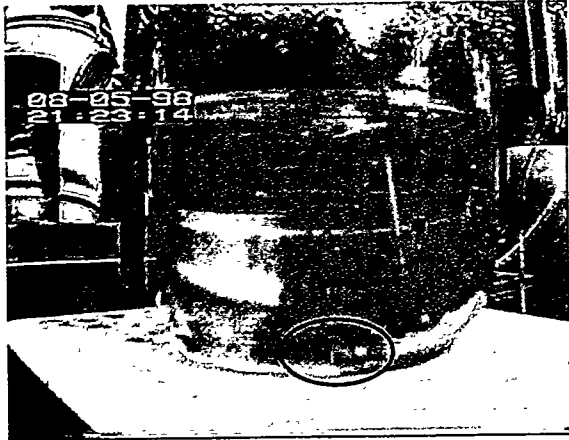
B



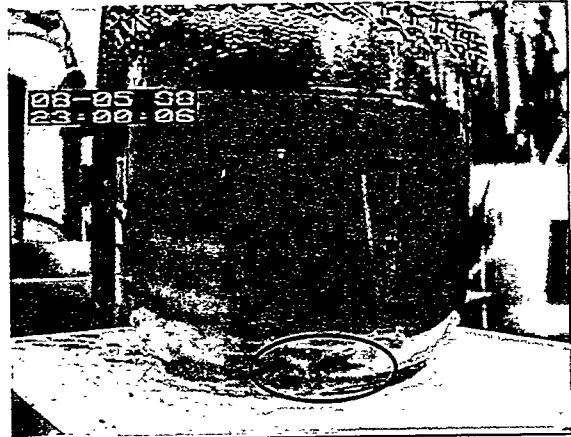
C

Figure B.2. Fuel fragment addition during Test 2 showed that the oxide coatings on the fragments vigorously dissolved, while uranium metal dissolution was slower.

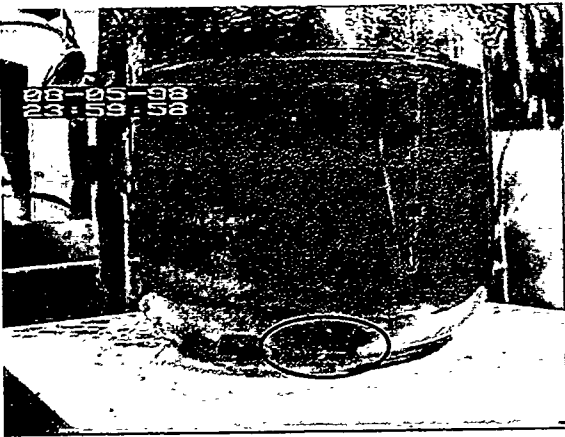
- A) Addition of fragment PM05-1 shows vigorous dissolution of oxide coating (run time = 00:40).
- B) Several pieces slowly dissolving following dissolution of oxide coating (run time = 00:45).
- C) Following addition of K4-1, solution became cloudy for ~1 minute while oxide coating dissolved (run time = 02:00).



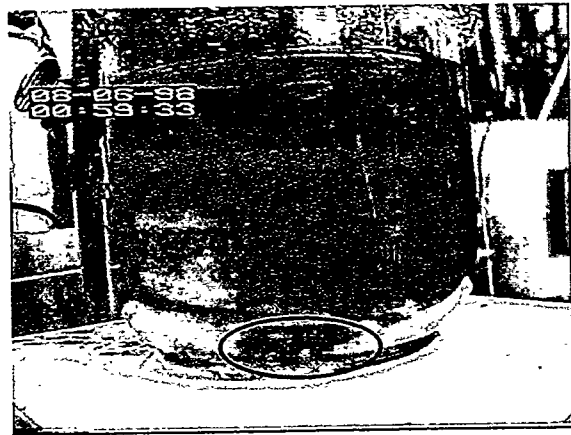
A



B



C



D

Figure B.3. Photographs of fuel dissolution during Test 2.
A) Eight of eleven fragment were added (run time = 02:05).
B) 1 hour after all fragments were added (run time = 03:45).
C) 2 hours after all fragments were added (run time = 04:45).
D) 3 hours after all fragments were added (run time = 05:45).
Location of the fuel has been circled showing shiny uranium metal is present in all photographs.

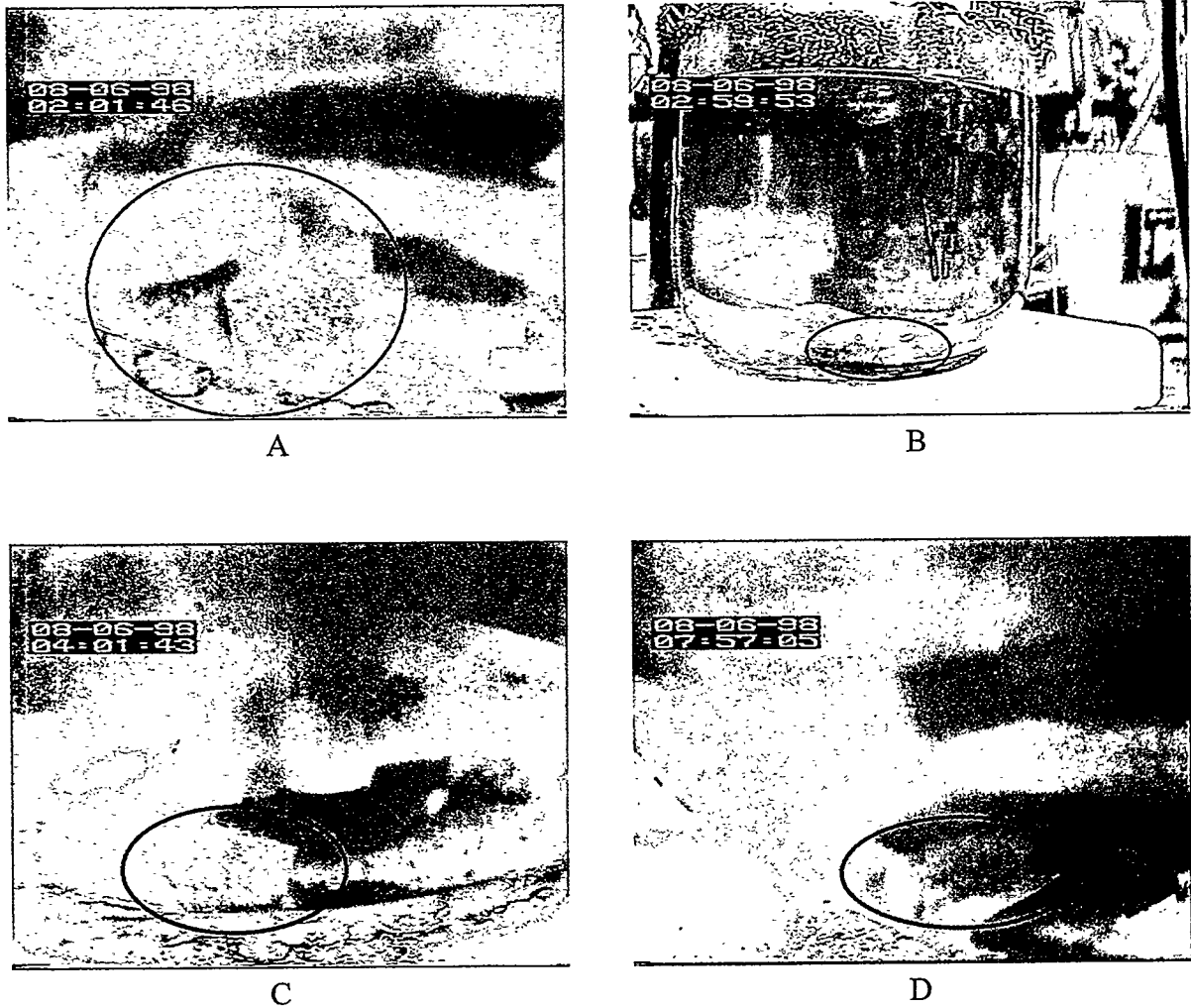
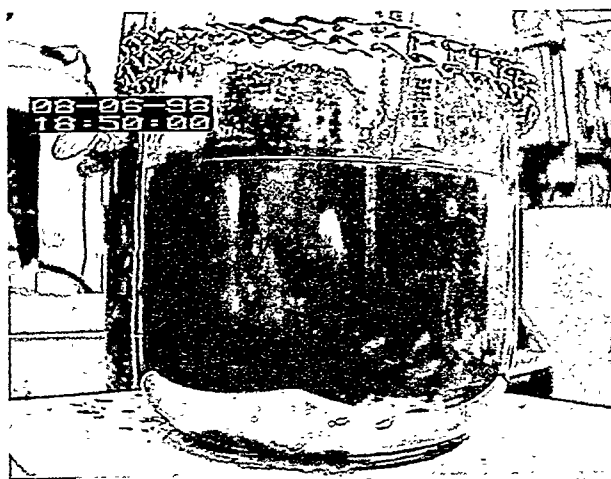
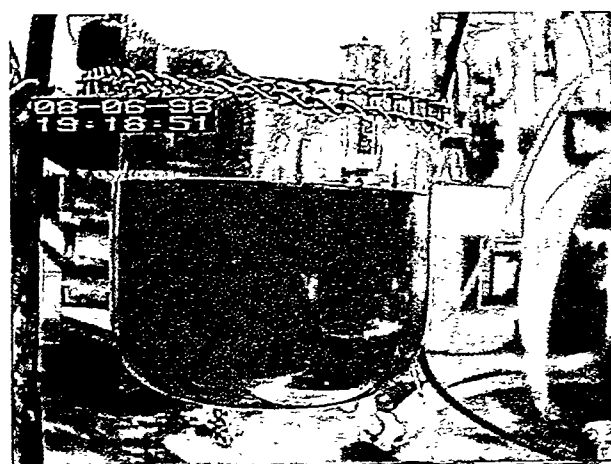


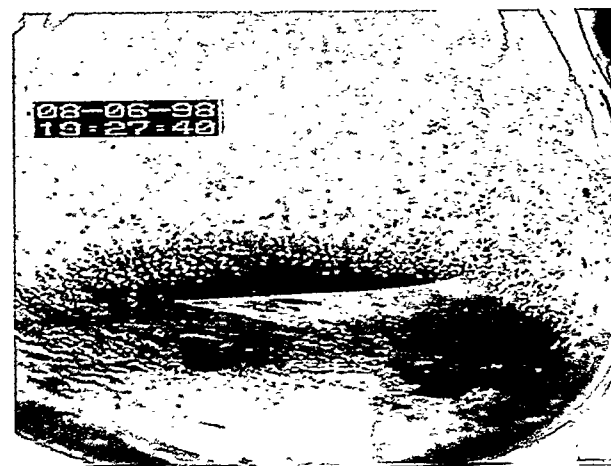
Figure B.4. Photographs (enlarged) of fuel fragment dissolution during Test 2.
 A) 4 hours after all fragment were added (run time 06:45).
 B) 5 hour after all fragments were added (run time = 07:45).
 C) 6 hours after all fragments were added (run time = 08:45).
 D) 10 hours after all fragments were added (run time = 13:45).
 Location of the fuel has been circled showing shiny uranium metal is present in all photographs. Although not shown in the photographs, uranium metal was still observed at run time 16:25 when K East Basin canister sludge was added to the dissolver.



A

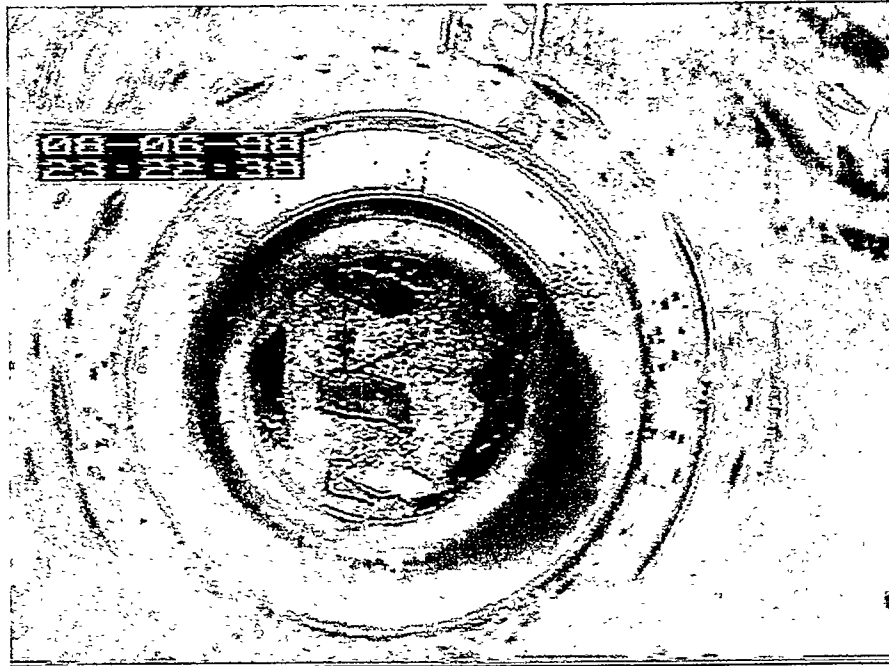


B



C

Figure B.5. Photographs showing settling of residual solids following Test 2.
A) Immediately after turning off heat and agitation.
B) After 30 minutes of cooling and settling.
C) After ~40 minutes.
Photographs show most settling occurred within the first 30 minutes. It is not known what fraction of solids remained suspended in solution.

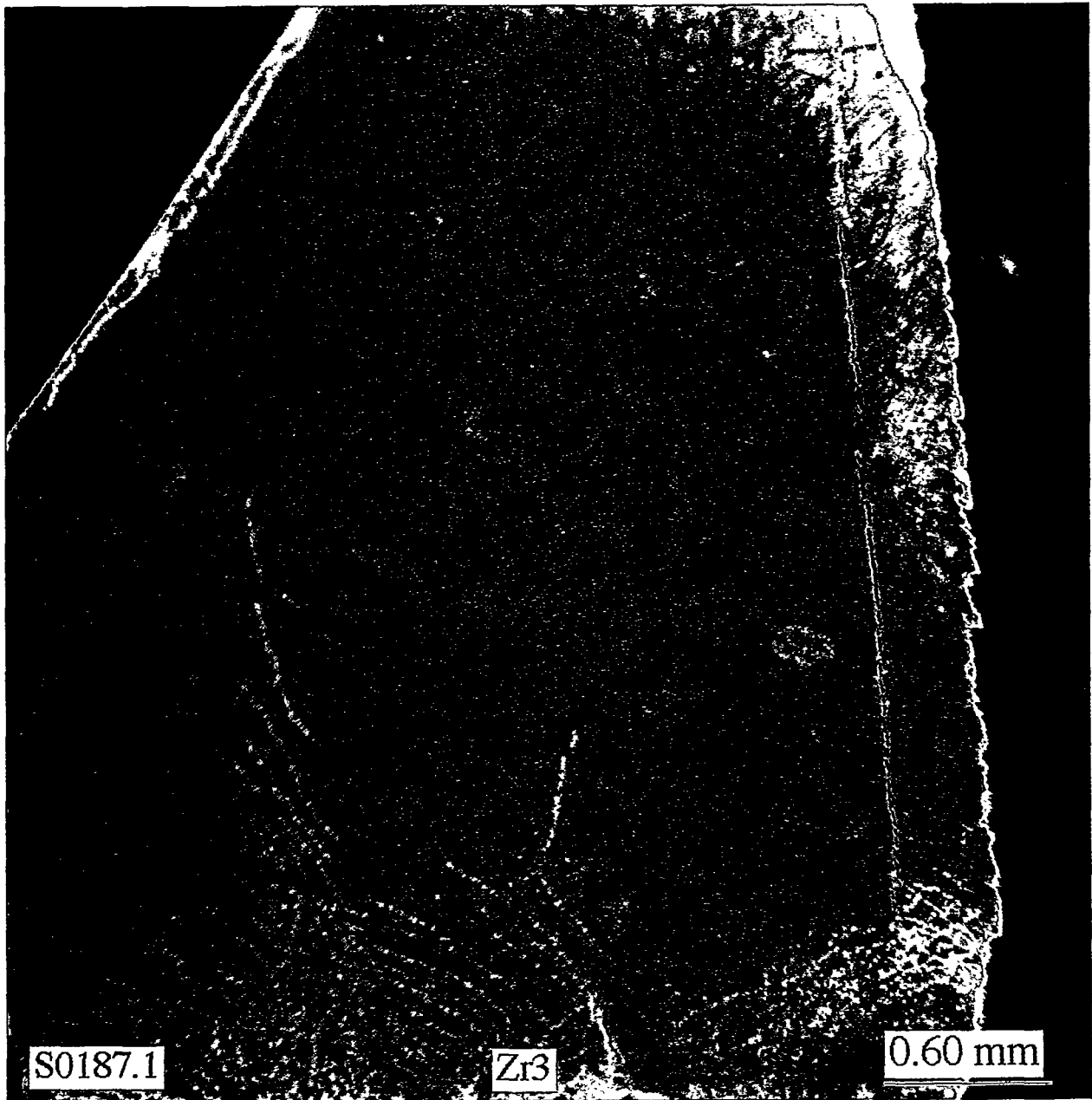


A



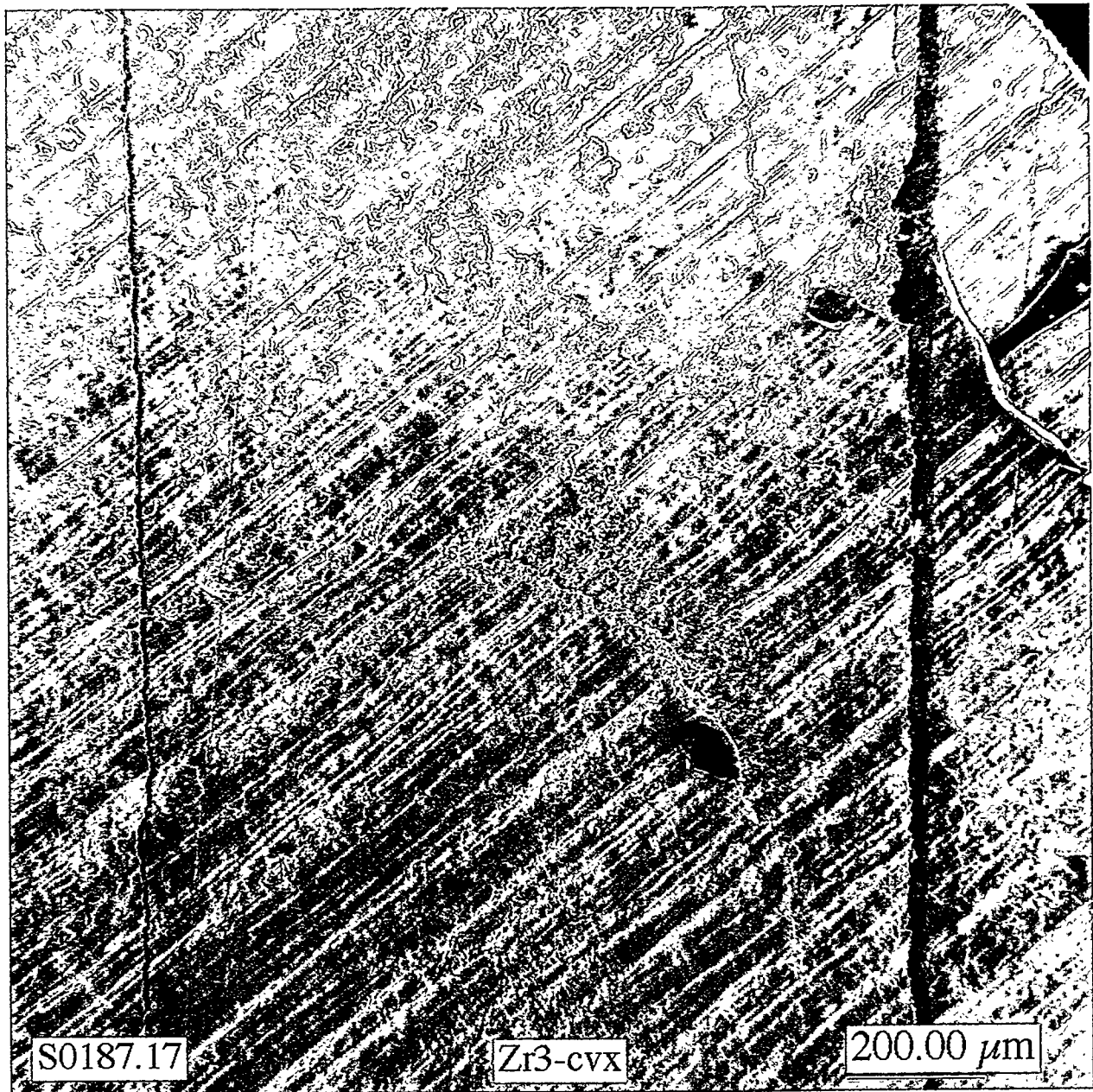
B

Figure B.6. Photographs of vacuum filtered residual solids following Test 2.
A) Wet solids in vacuum filter assembly
B) Close up of filtered solids during air drying.
Both photographs show pieces of Zircaloy cladding in the residual solids.



- NOTES: 1. Zirconium background; oxygen corresponding to ZrO_2 ;
Sn/Zr ratio corresponding to 1.3 wt.% Sn (by energy dispersive X-ray program)
2. Small concentrations of Fe>Mn>Cr generally observed over surface
 3. Some regions with Si
 4. Some regions with Pd?
 5. No uranium detected (indicates coolant side, not fuel side, of cladding)

Figure B.7. Scanning Electron Microscope (SEM) Images of Zircaloy Cladding (concave surface; water side) from Test 2 Residues.

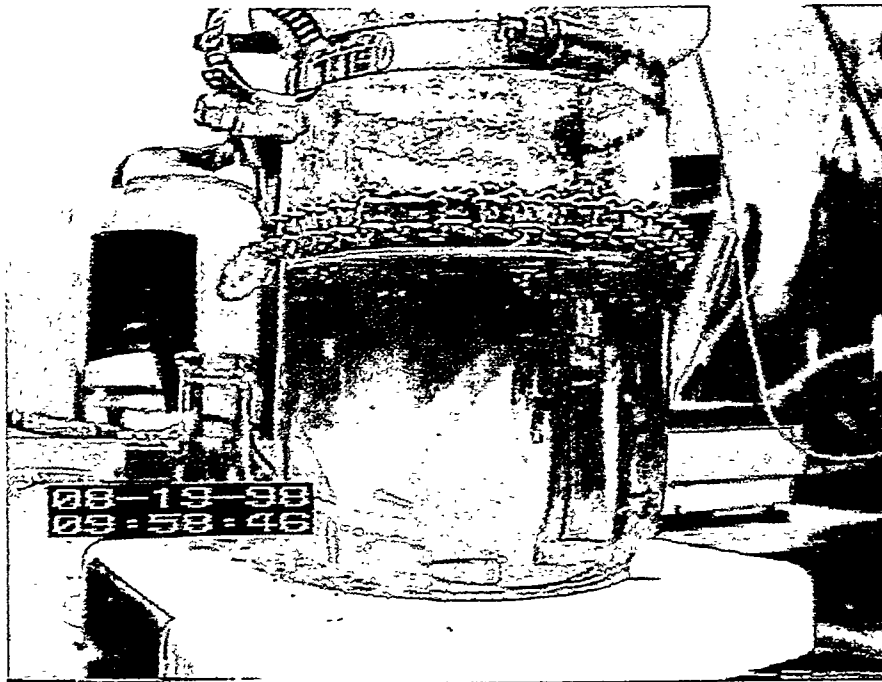


- NOTES: 1. Zirconium background; 1.35 wt.% Sn
2. Uranium in raised scaly areas (indicates fuel metal side)
3. Aluminum and Si also found in raised scaly areas

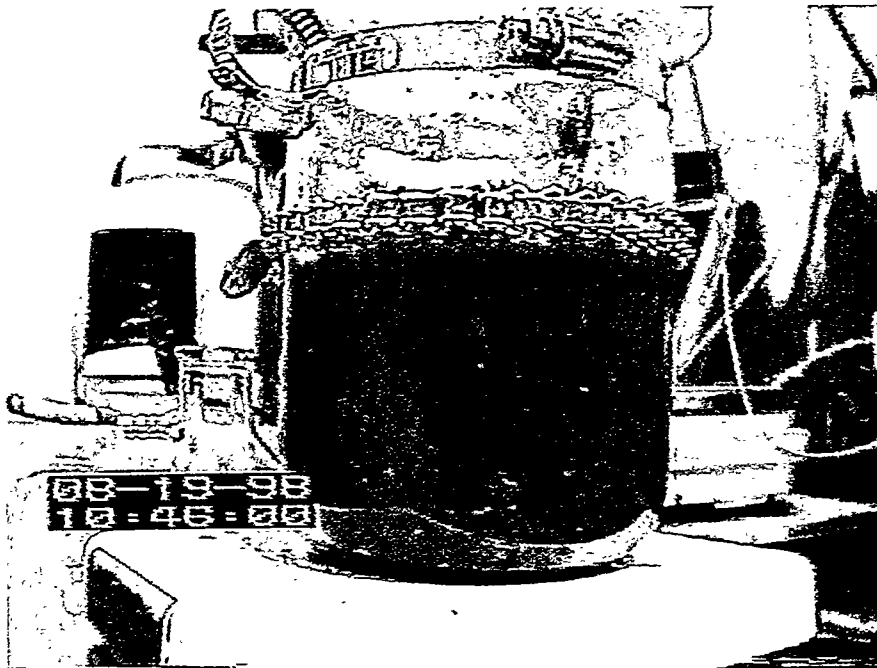
Figure B.8. Scanning Electron Microscope (SEM) Images of Zircaloy Cladding (convex surface; U metal fuel side) from Test 2 Residues.

Appendix C

Photographs from Test 3

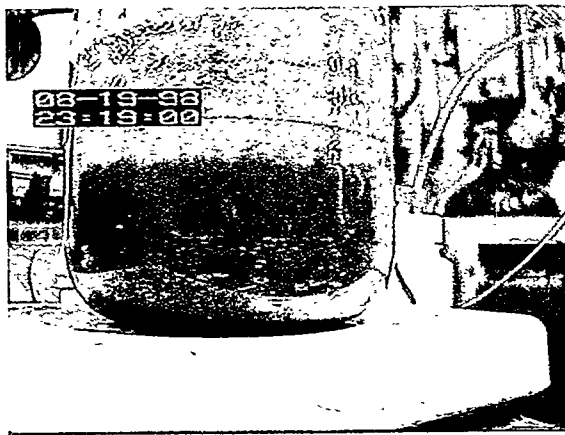


Before

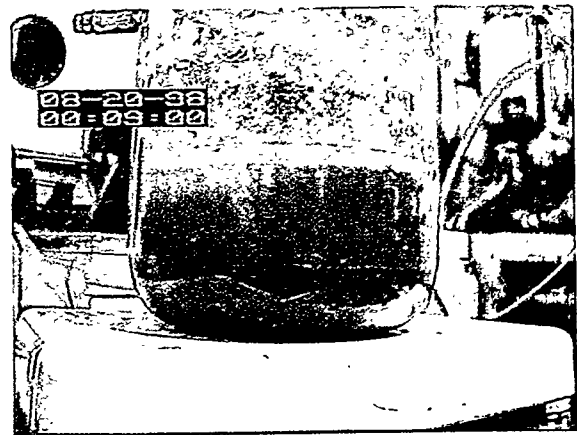


After

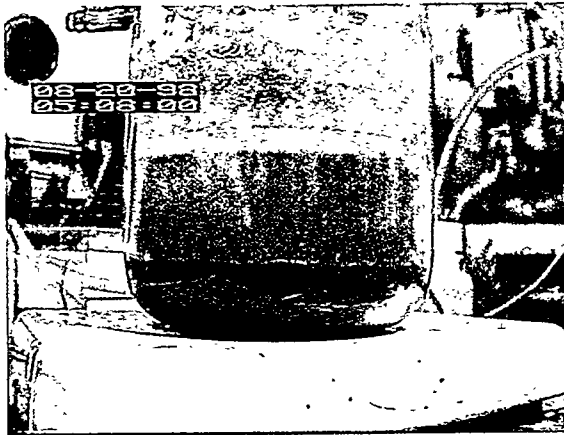
Figure C.1. Photograph of the dissolver during Test 3, before and after addition of first sludge sample. The stainless steel module, which is loaded with ion exchange material, can be seen before the addition of the first sludge sample. After addition of the first sludge sample, the solution turned a muddy brown, obscuring observations during the run.



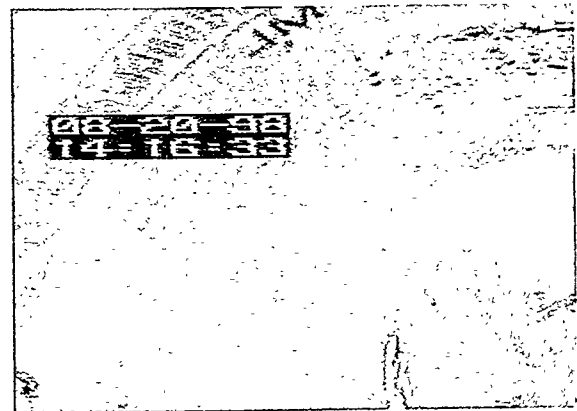
A



B



C



D

Figure C.2. Photographs of settling behavior during first 2% nitric acid rinse of residual solids from Test 3.

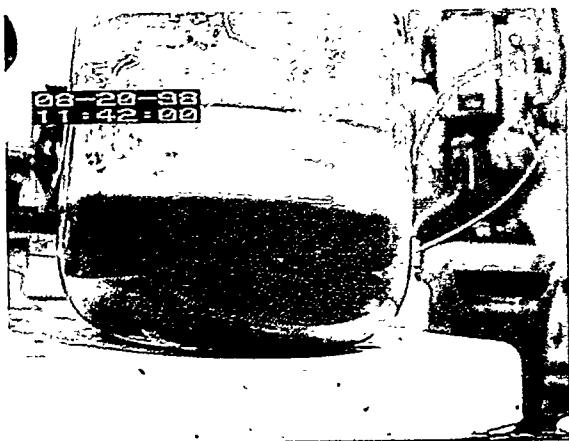
A) 10 minutes after mixer was stopped.

B) 1 hour after mixer was stopped.

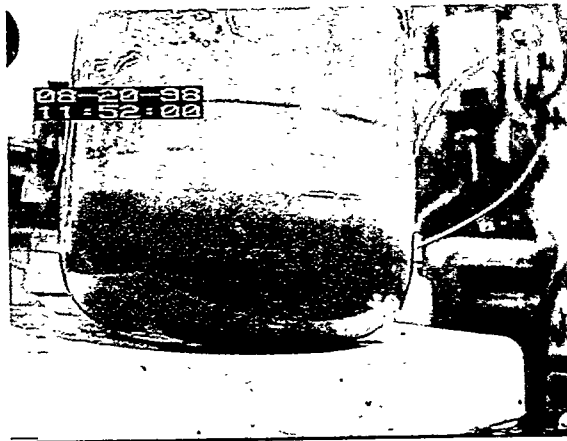
C) 6 hours after mixer was stopped.

Most solids settled within 1 hour after performing the 2% nitric acid rinse.

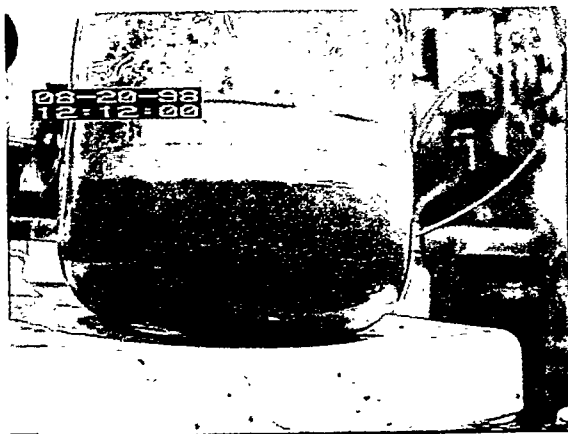
D) Ring of film adhered to dissolver wall after completion of two 2% nitric acid rinses and one water rinse.



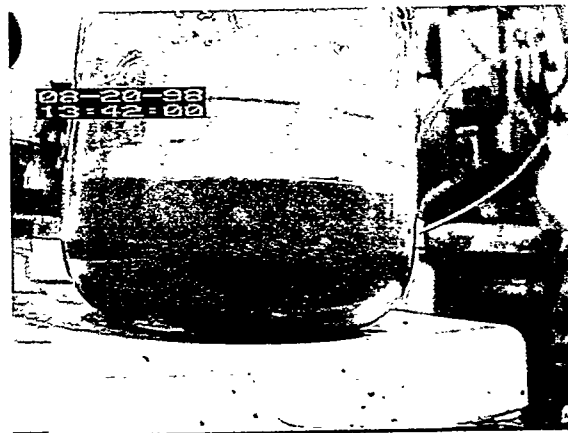
A



B



C



D

Figure C.3. Photographs of settling behavior during water rinse (i.e., final rinse) of residual solids from Test 3.

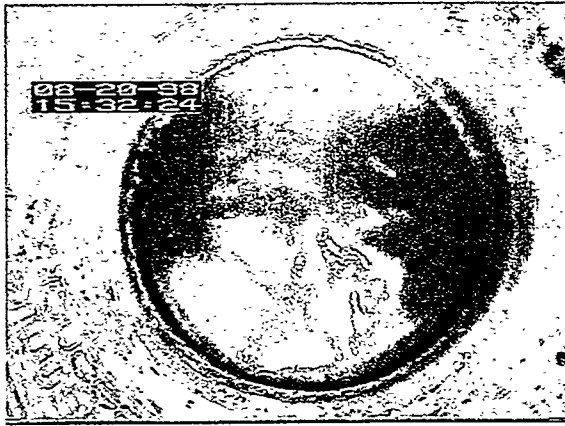
A) Immediately after mixer was stopped.

B) 10 minutes after mixer was stopped.

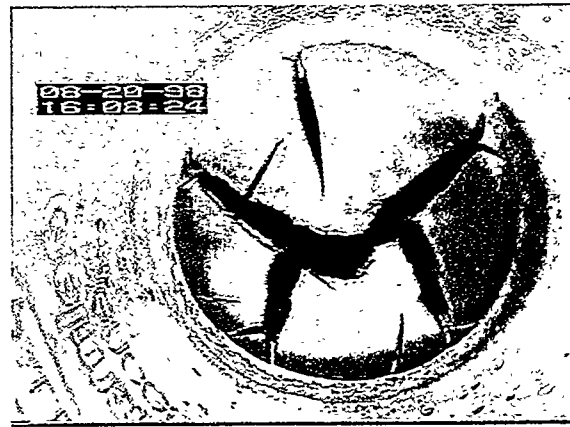
C) 30 minutes after mixer was stopped.

D) 2 hours after mixer was stopped.

While the solution continued to clarify with time, most settling occurred in the first 10 minutes.



A



B



C



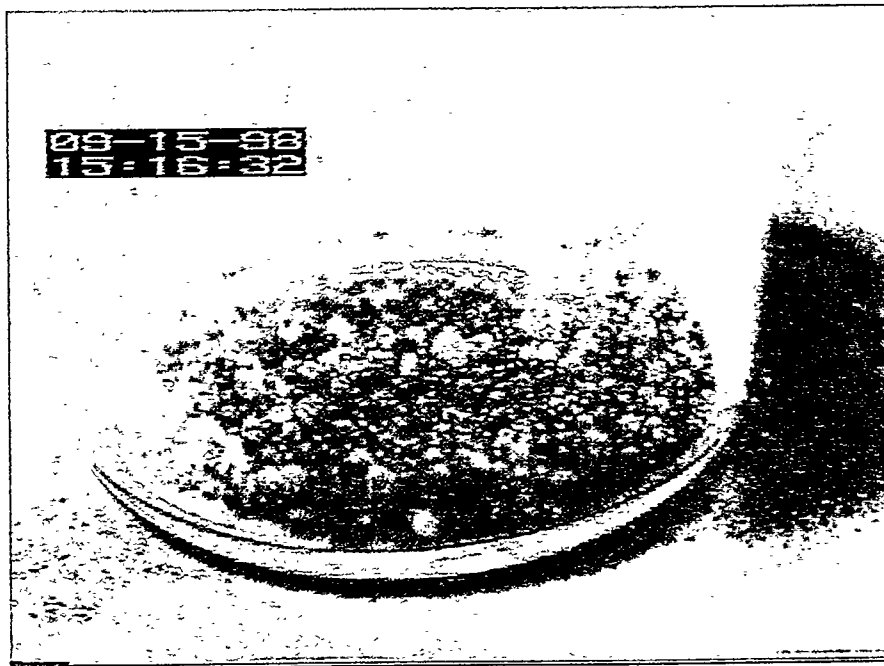
D

Figure C.4. Photographs of filtered residual solids from Test 3.

- A) Filter cake of final solids following water rinse during vacuum filtration. While filter cake exhibited gel-like behavior, the filter did not blind.
- B) Filter cake immediately after completion of vacuum filtration.
- C) Air dried filter cake.
- D) Vacuum filtered residual solids from the slurry collected at 4 hours. An unidentified shiny flake is visible in Photograph D.

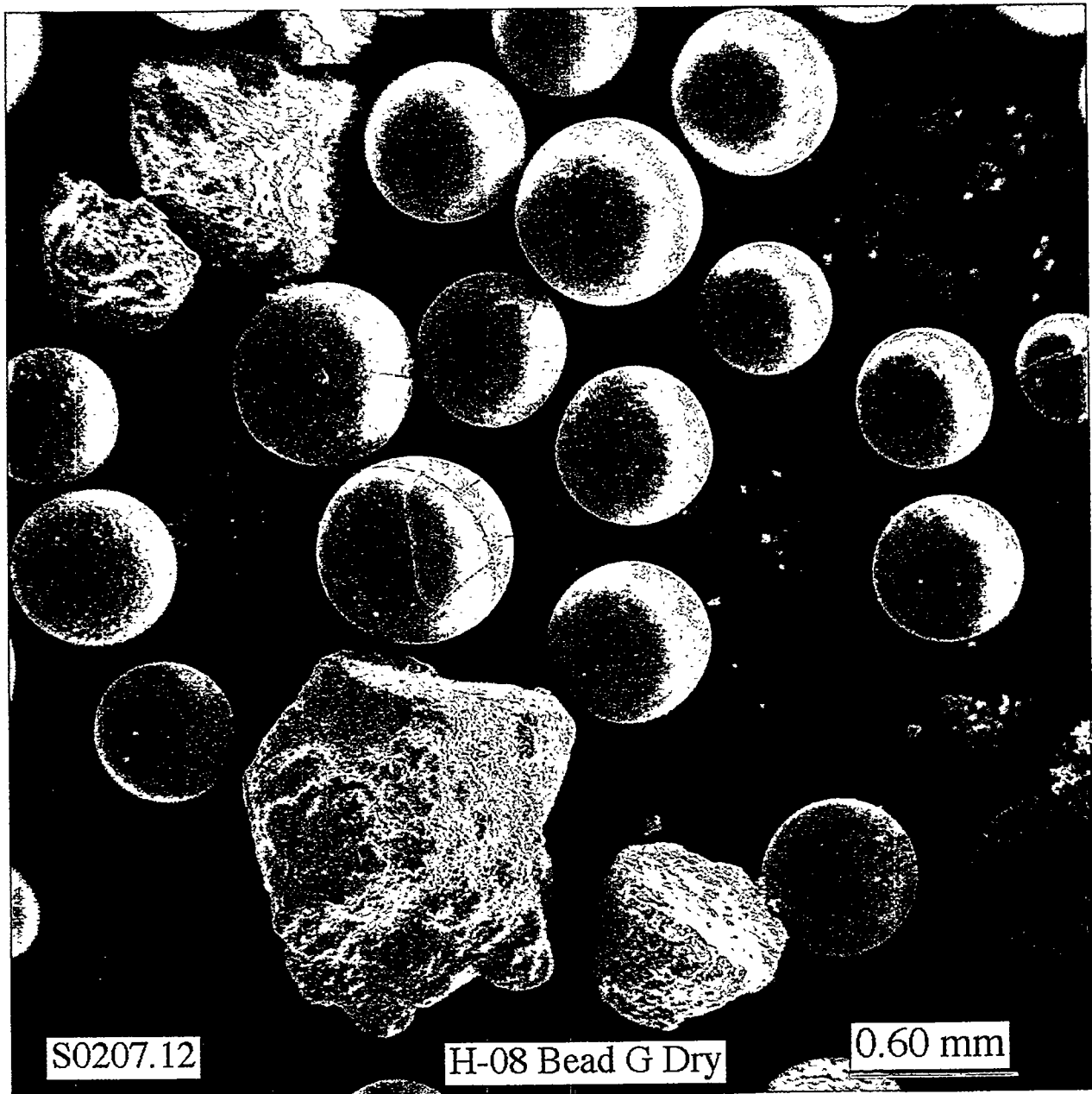


Zeolon



OIER Beads

Figure C.5. Photographs of ion exchange materials taken from the stainless steel module following Test 3 and submitted for characterization. Zeolon and organic ion exchange resin (OIER) bead fractions were separated after completion of Test 3. Some OIER beads were present in the Zeolon fraction, while the OIER bead fraction contained almost no zeolon particles.



- NOTES:
1. Zeolon-900 particles are the irregular white pieces; high porosity observed at higher magnification; Si/Al mole ratio ~6 consistent with mordenite
 2. OIER are the spherical beads; some show cracking; hemispheres observed in other images
 3. anion resin (less sulfur found in resin), e.g., left center edge, has a pitted, orange-peel surface
 4. cation resin (more sulfur found in resin) has a smooth surface
 5. fine particles seen adhering to resin surfaces even for this water-rinsed material
 6. anion resin contains higher concentrations of Si, Cl; also contains S (though not as high as cation resin; likely present as SO_4^{2-})
 7. cation resin contains higher concentrations of Na, K, Mg, Ca, Al, Fe

Figure C.6. Scanning Electron Microscope (SEM) Images of Starting IX Material (H-08 BEAD G) Used in Test 3.

Appendix D

Mass Spectrometry Offgas Data for Test 2

K Basin Dissolution Tests System ResponseTime

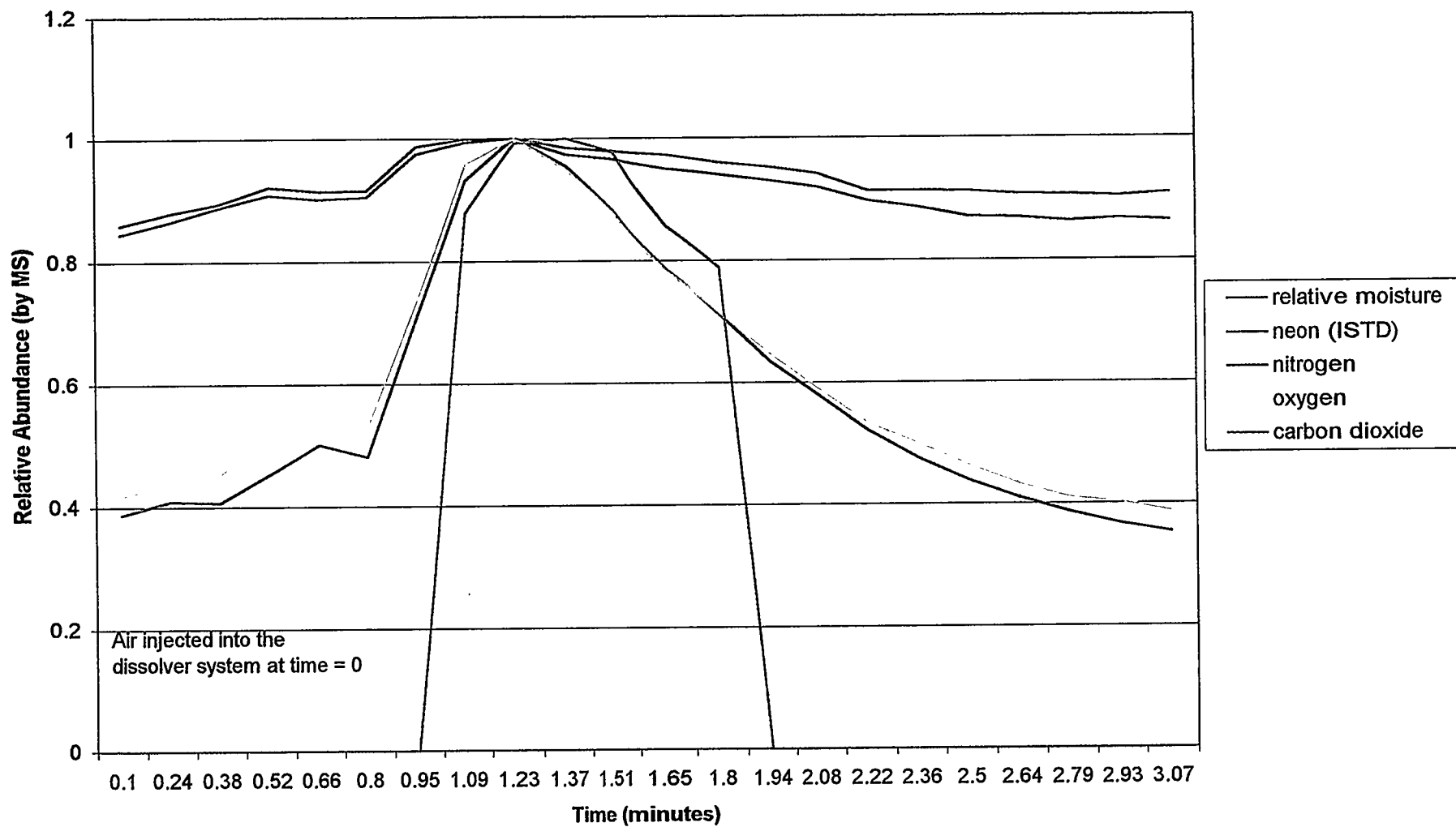


Figure D.1. Offgas system response to injection of 5 mL of air.

K Basin Dissolution Test 2

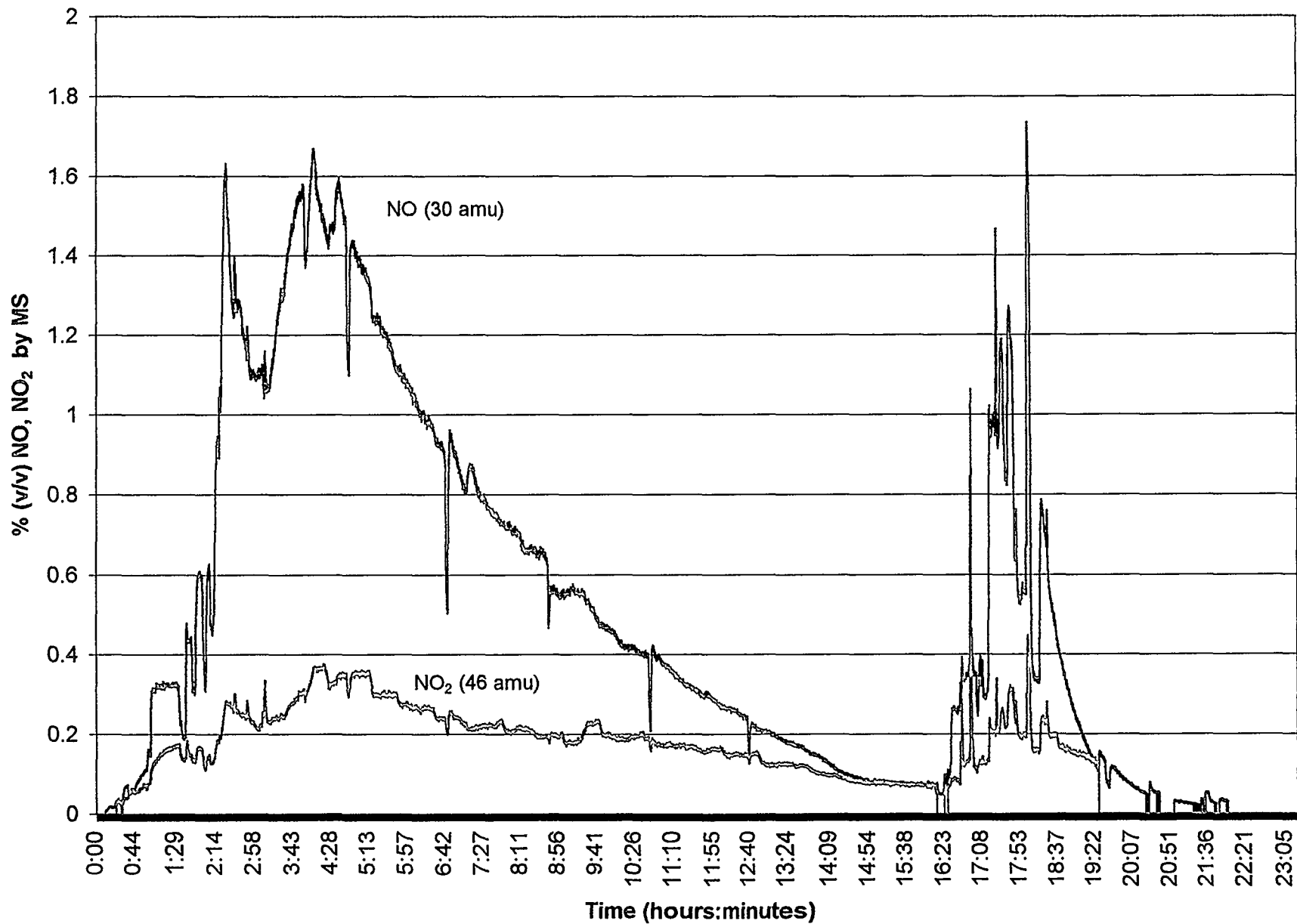


Figure D.2. Concentration of NO (30 amu) and NO₂ (46 amu) for duration of Test 2 (detected by MS).

K Basin Dissolution Test 2

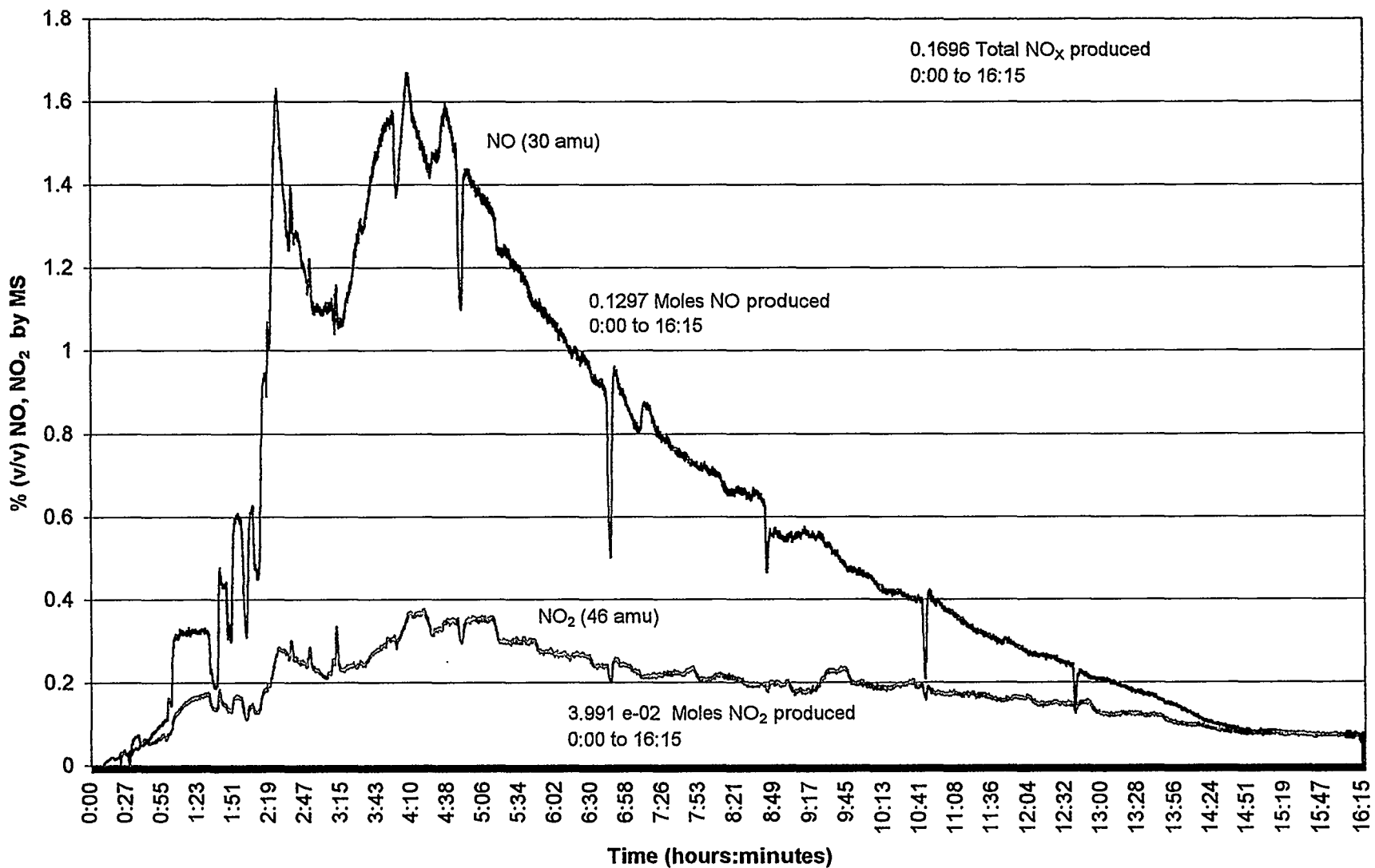


Figure D.3. Concentration of NO (30 amu) and NO₂ (46 amu) during fuel fragment addition in Test 2 (detected by MS).

K Basin Dissolution Test 2

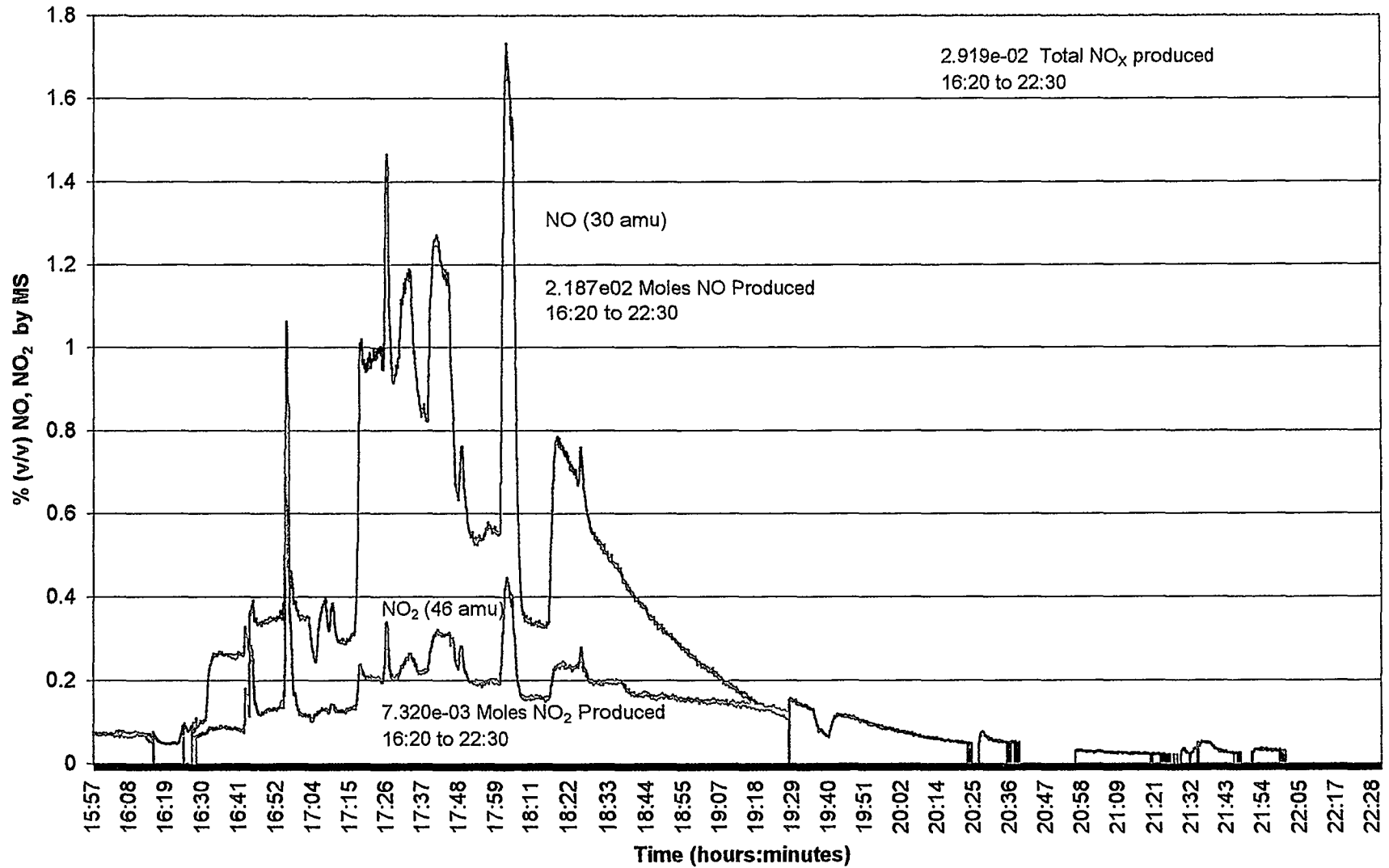


Figure D.4. Concentration of NO (30 amu) and NO₂ (46 amu) during sludge addition in Test 2 (detected by MS).

K Basin Dissolution Test 2

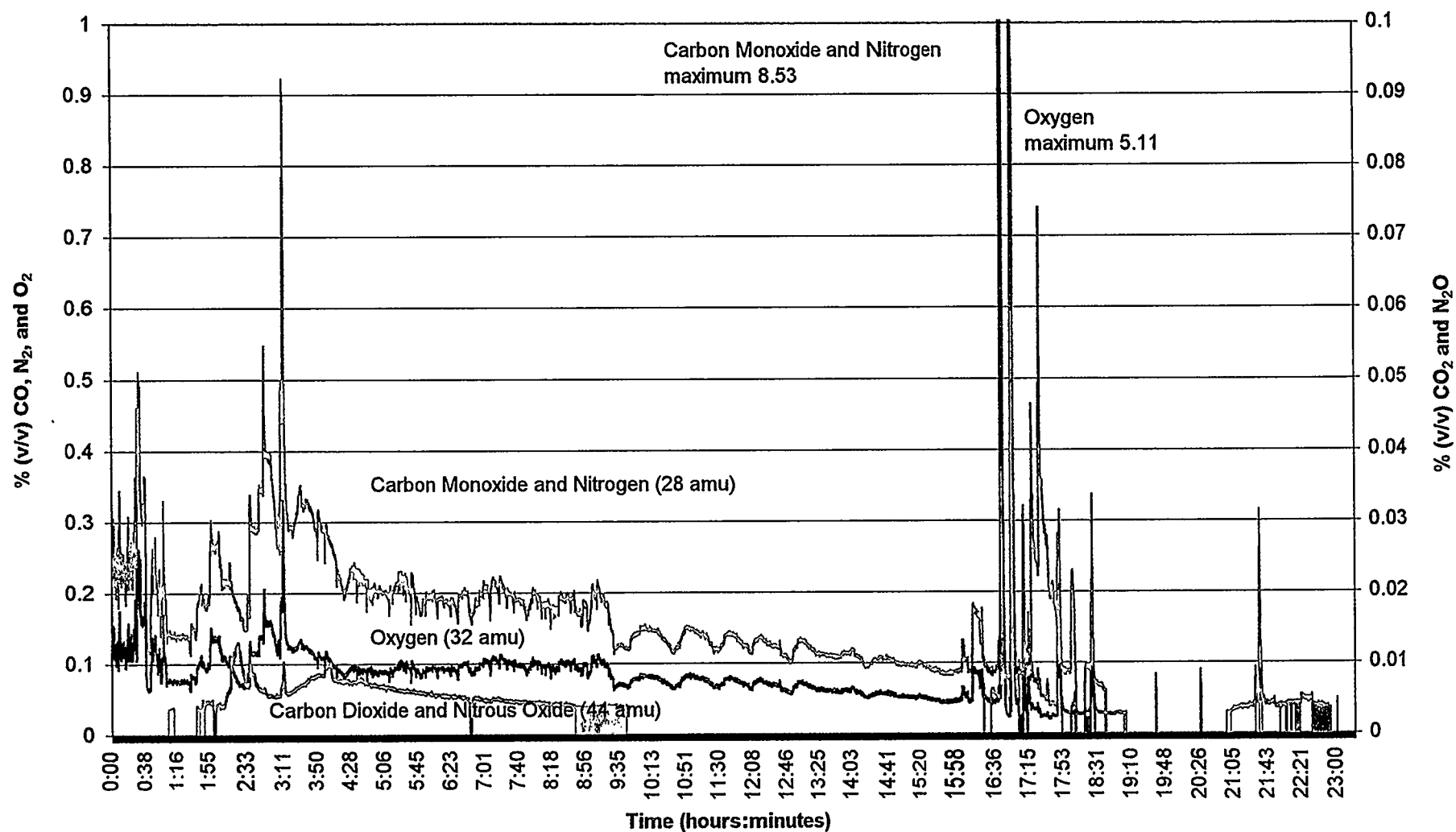


Figure D.5. Concentration of CO and N₂ (28 amu), O₂ (32 amu), and N₂O and CO₂ (44 amu) for duration of Test 2 (detected by MS).

K Basin Dissolution Test 2

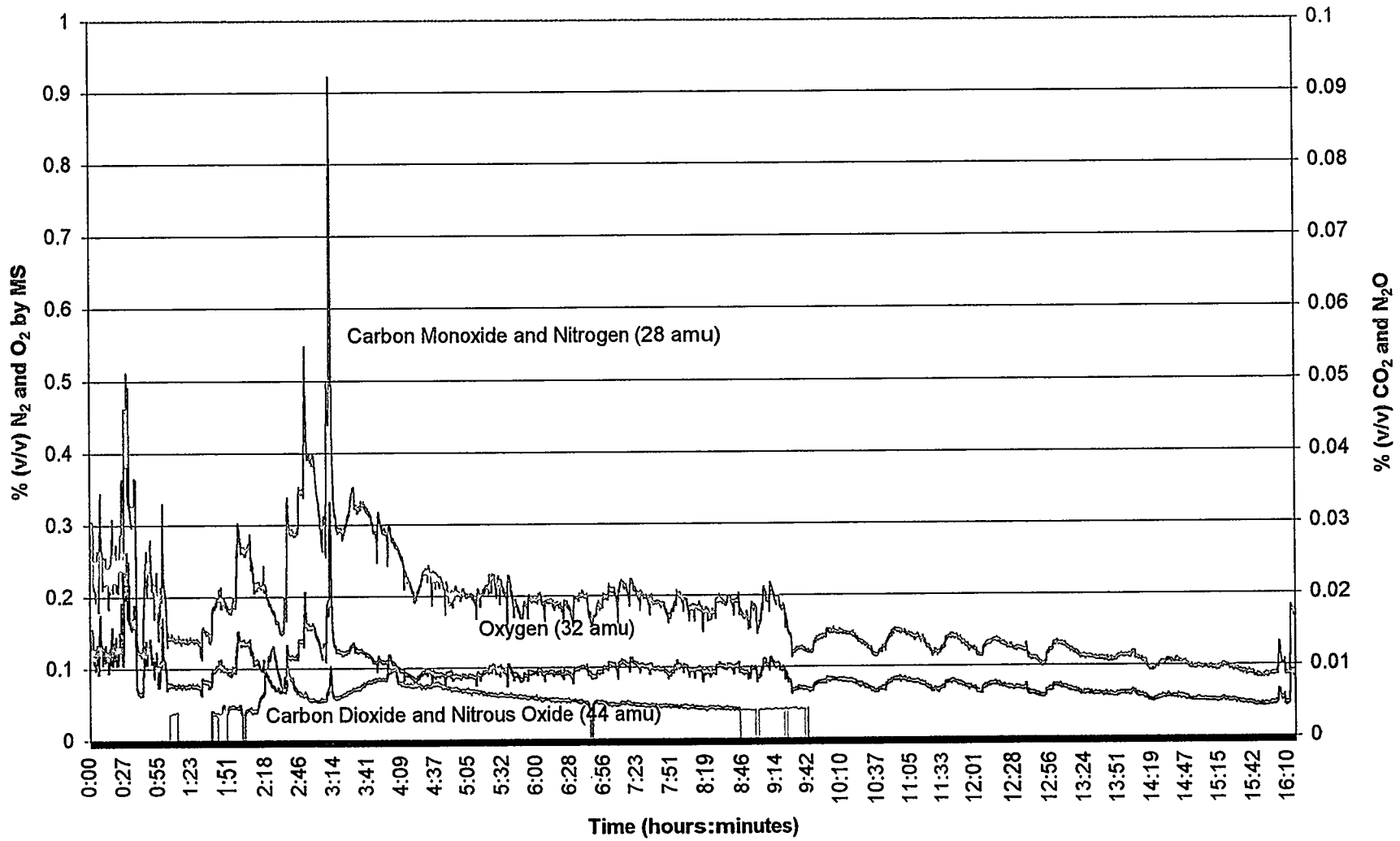


Figure D.6. Concentration of CO and N_2 (28 amu), O_2 (32 amu), and N_2O and CO_2 (44 amu) during fuel fragment addition in Test 2 (detected by MS).

K Basin Dissolution Test 2

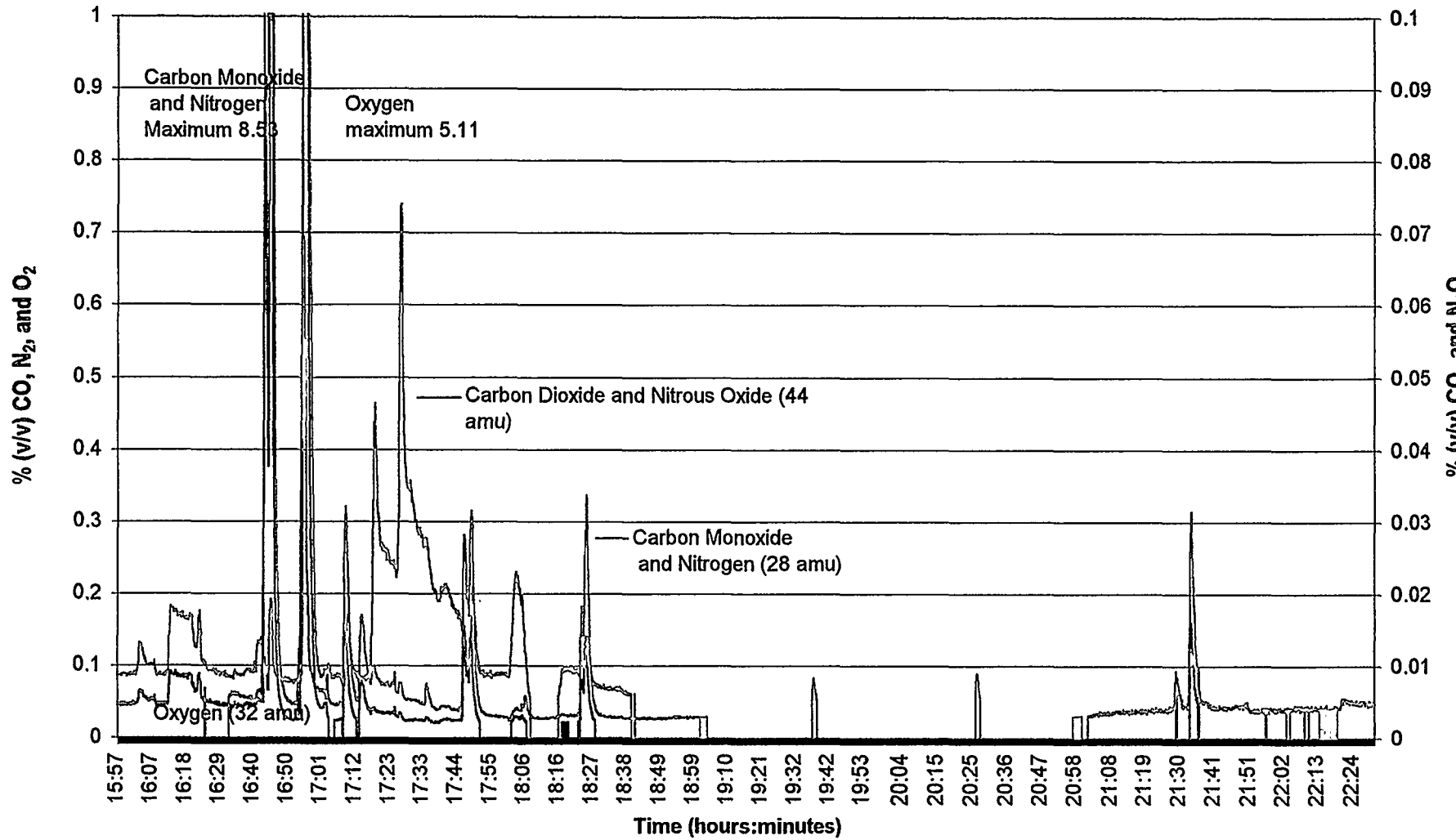


Figure D.7. Concentration of CO and N₂ (28 amu), O₂ (32 amu), and N₂O and CO₂ (44 amu) during sludge addition in Test 2 (detected by MS).

Appendix E

Gas Chromatography Offgas Data for Test 2

K Basin Dissolution Test 2

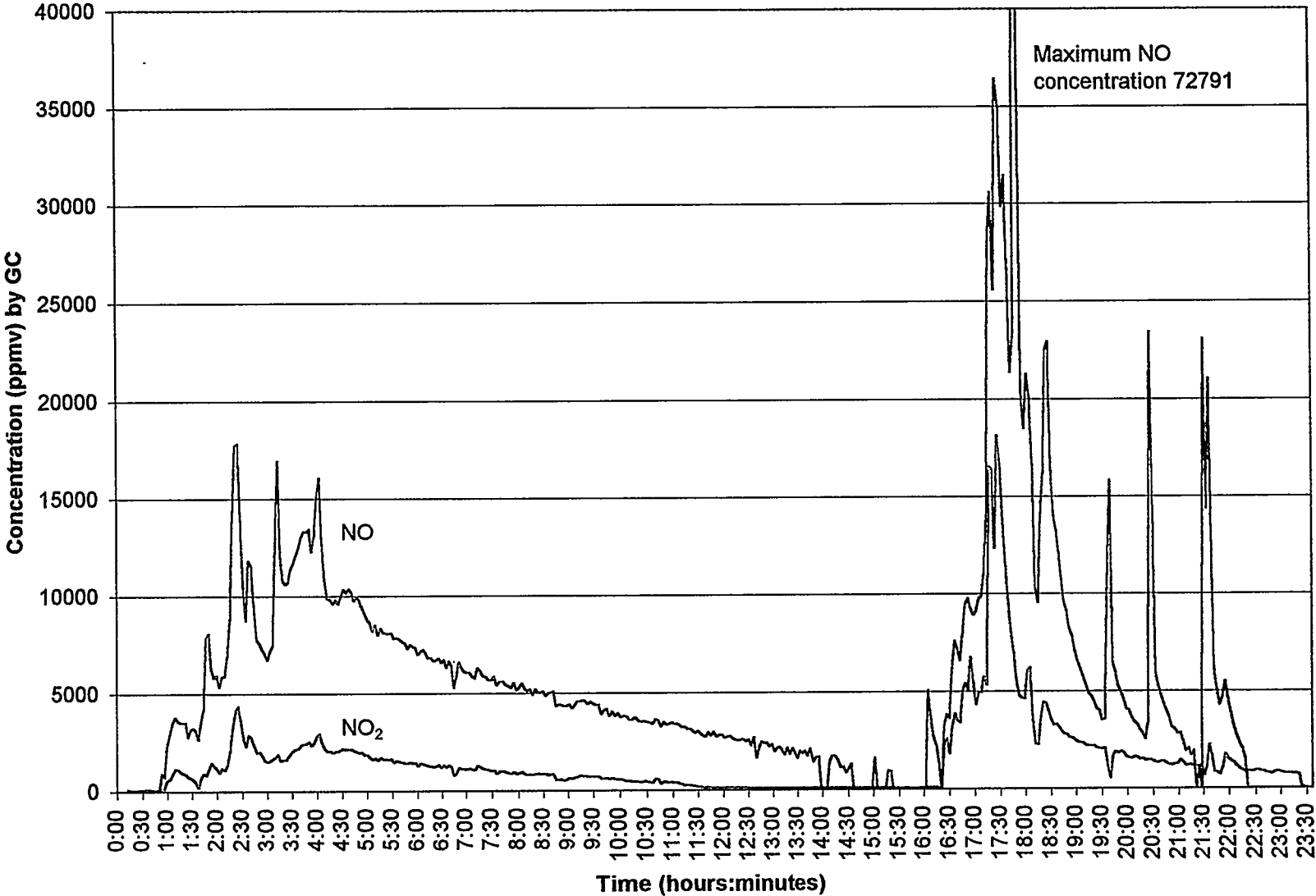


Figure E.1. Concentration of NO and NO₂ for the duration of Test 2 (detected by GC).

K Basin Dissolution Test 2

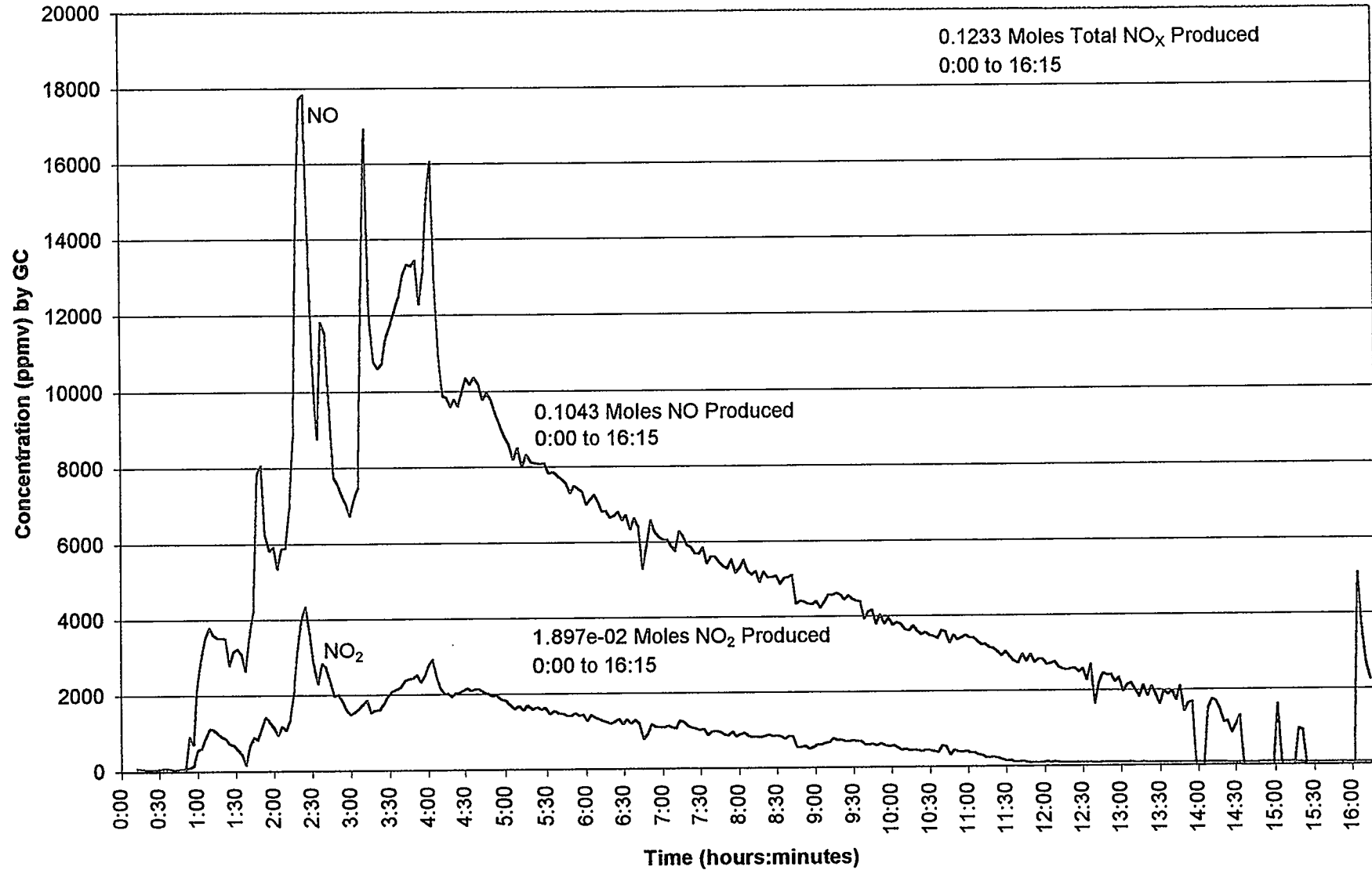


Figure E.2. Concentration of NO and NO₂ during fuel fragment addition in Test 2 (detected by GC).

K Basin Dissolution Test 2

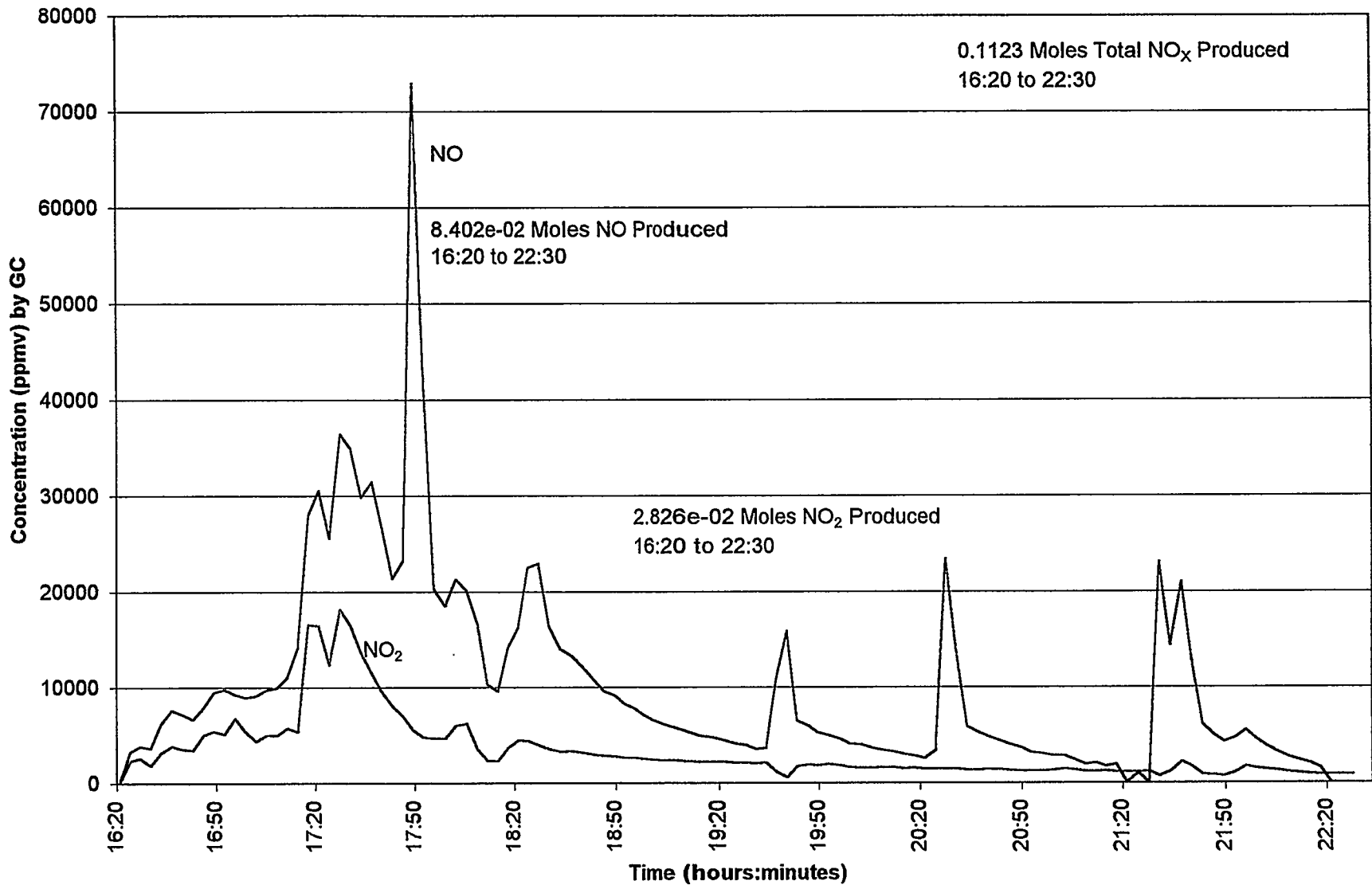


Figure E.3. Concentration of NO and NO₂ during sludge addition in Test 2 (detected by GC).

K Basin Dissolution Test 2

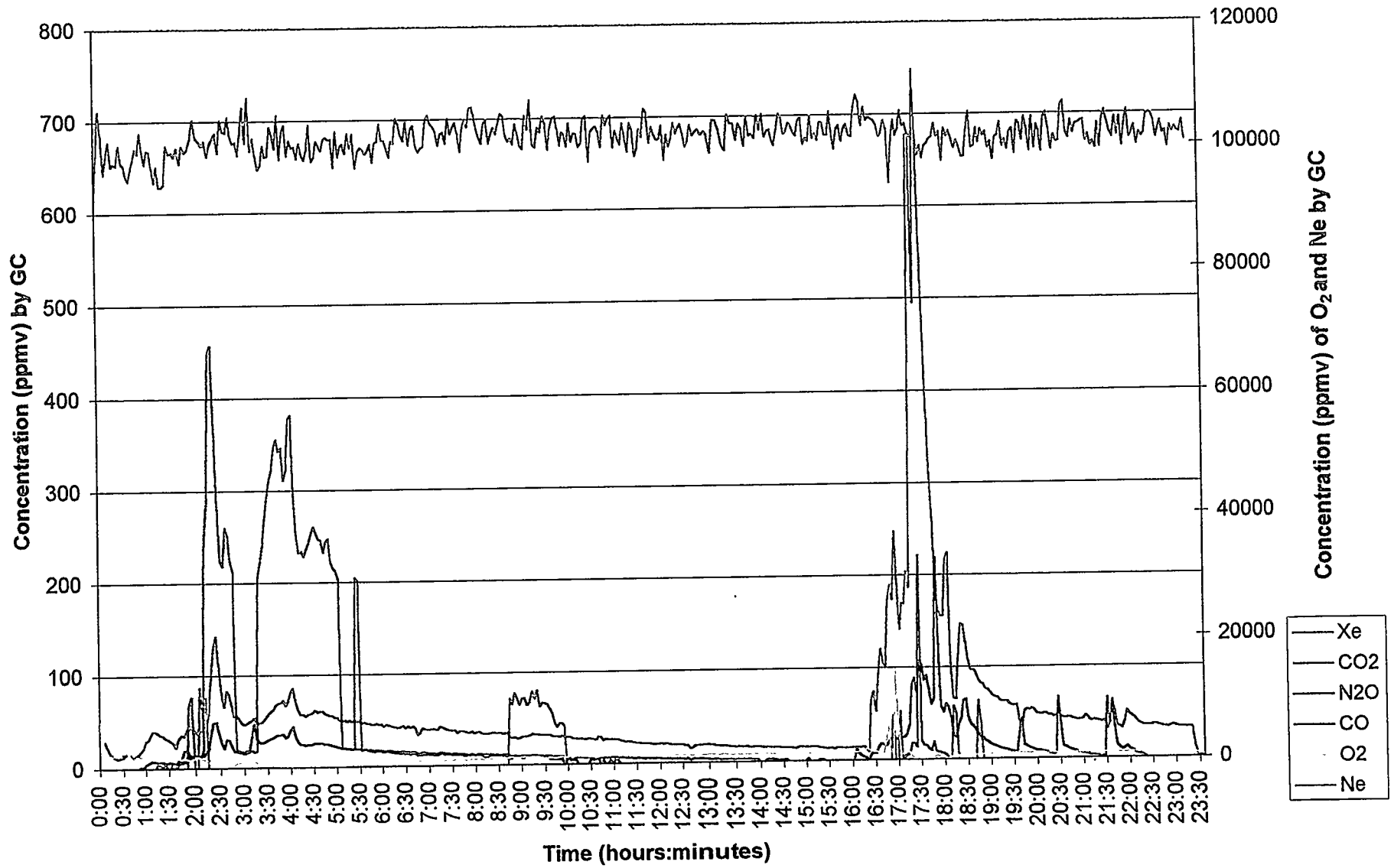


Figure E.4. Concentration of Xe, CO₂, N₂O, CO, O₂, and Ne for the duration of Test 2 (detected by GC).

K Basin Dissolution Test 2

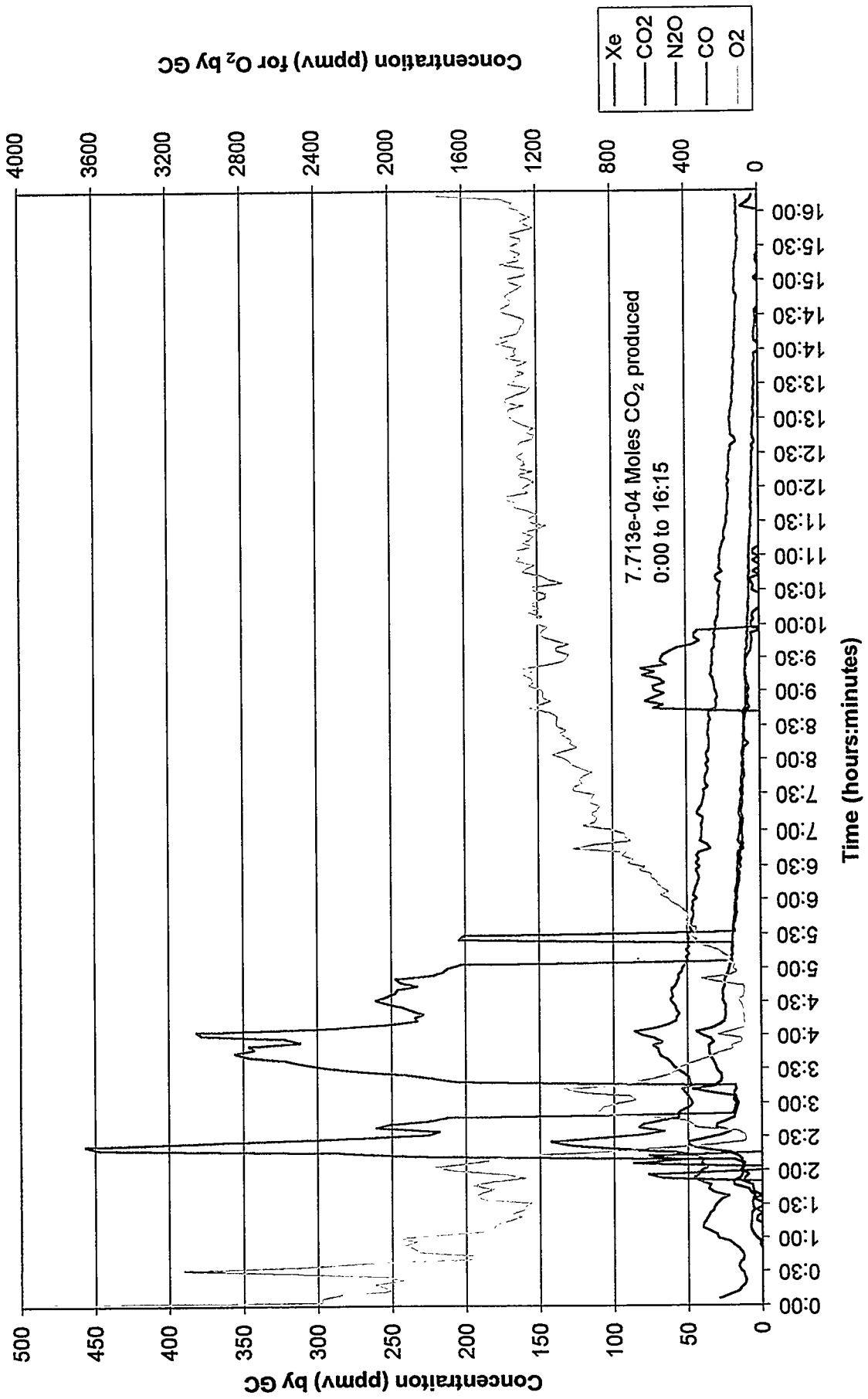


Figure E.5. Concentration of Xe, CO₂, N₂O, CO, and O₂ during fuel fragment addition in Test 2 (detected by GC).

K Basin Dissolution Test 2

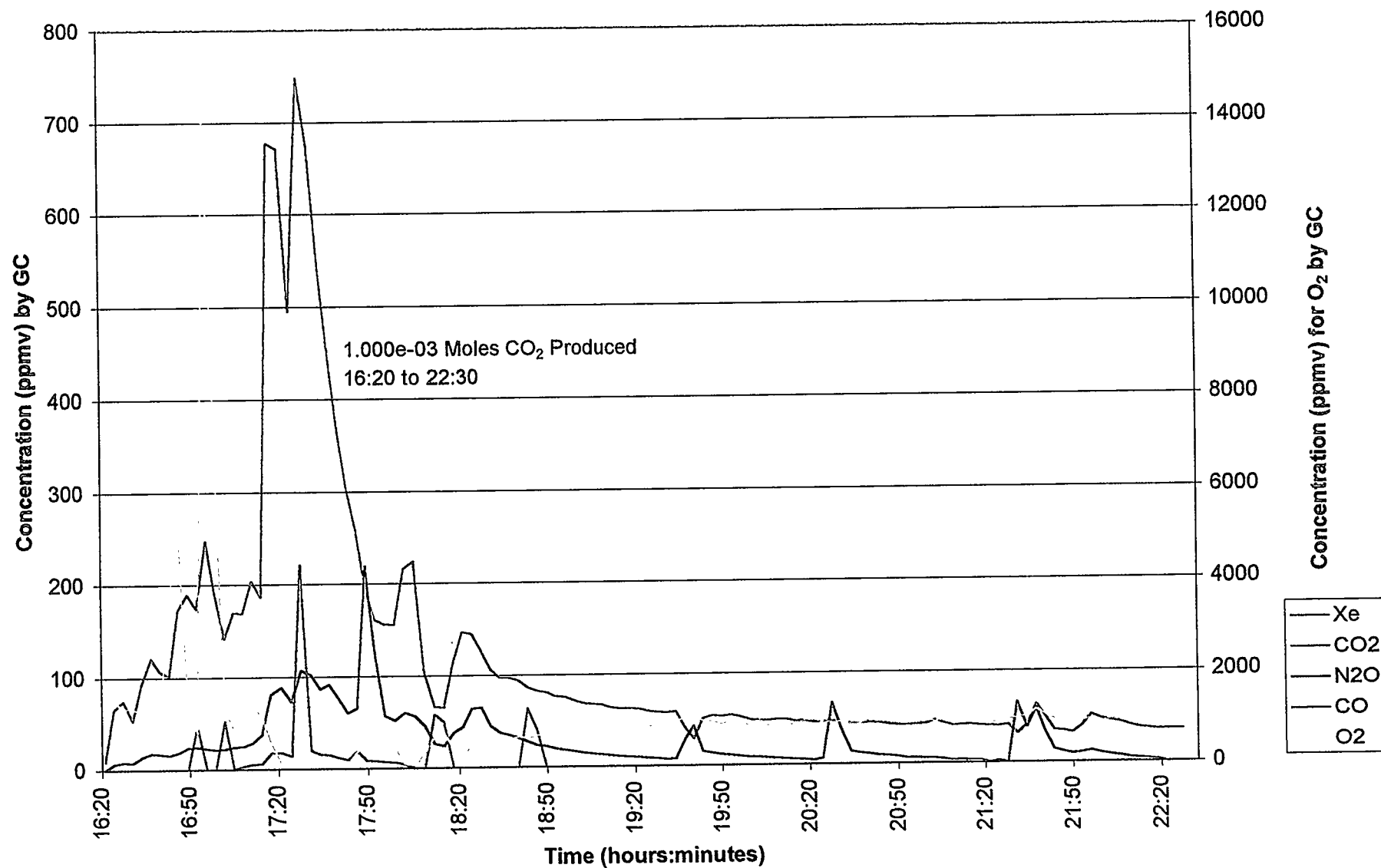


Figure E.6. Concentration of Xe, CO₂, N₂O, CO, and O₂ during sludge addition in Test 2 (detected by GC).

Appendix F

Mass Spectrometry and Gas Chromatography Offgas Data for Test 3

K Basin Dissolution Test 3

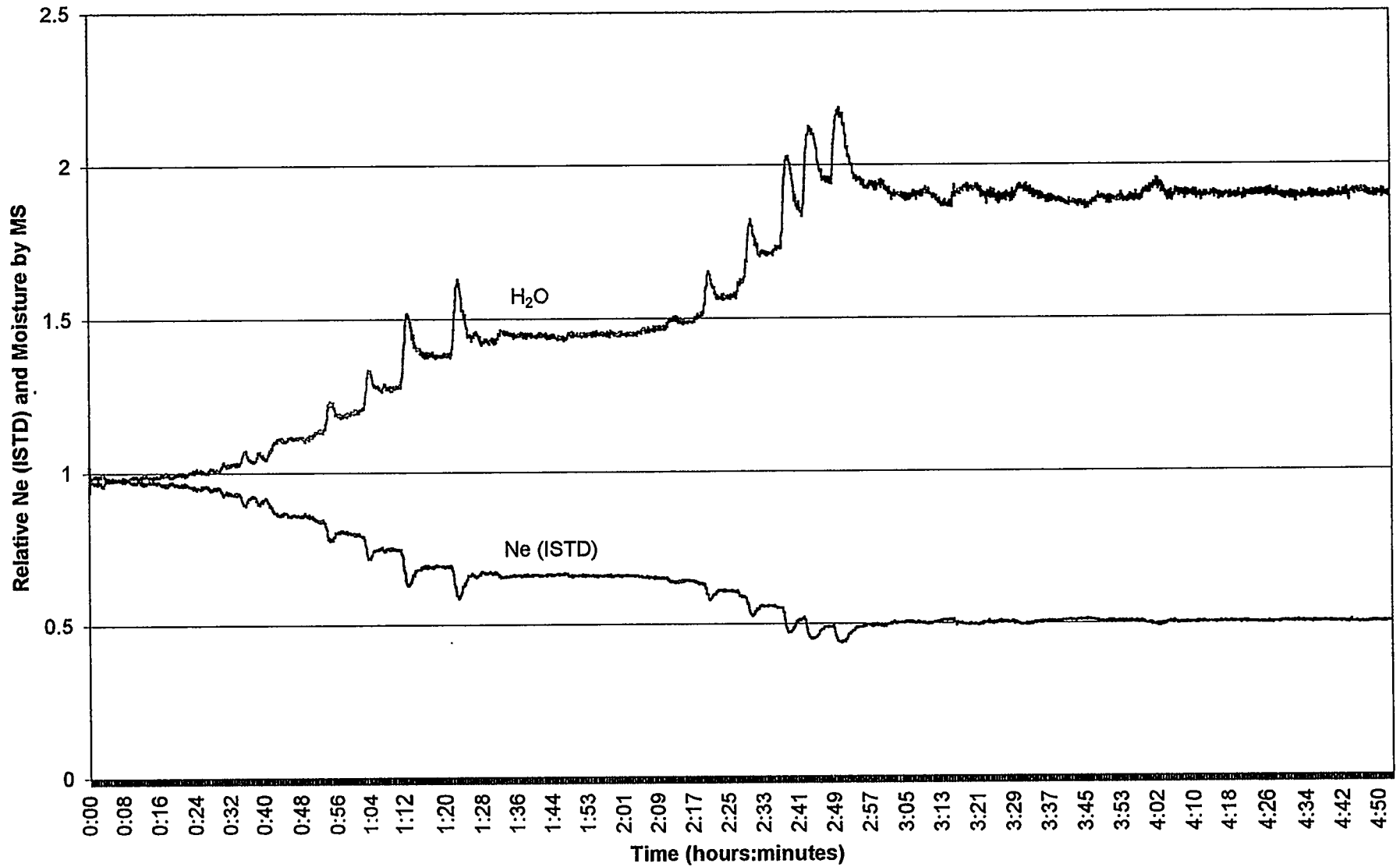


Figure F.1. Relative response of neon and moisture for the first half of Test 3 (detected by MS).

K Basin Dissolution Test 3

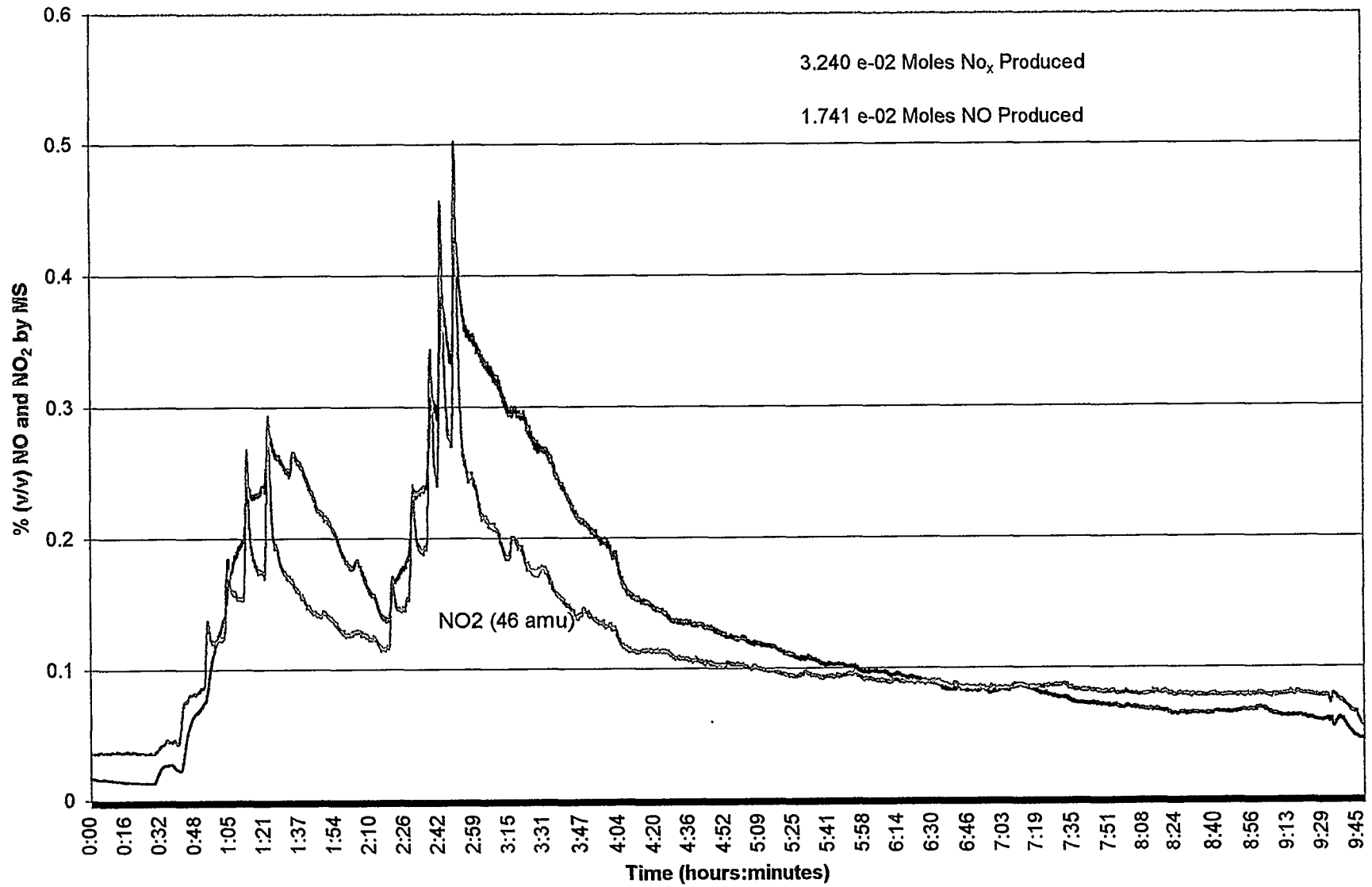


Figure F.2. Concentration of NO (30 amu) and NO₂ (46 amu) for the duration of Test 3 (detected by MS).

K Basin Dissolution Test 3

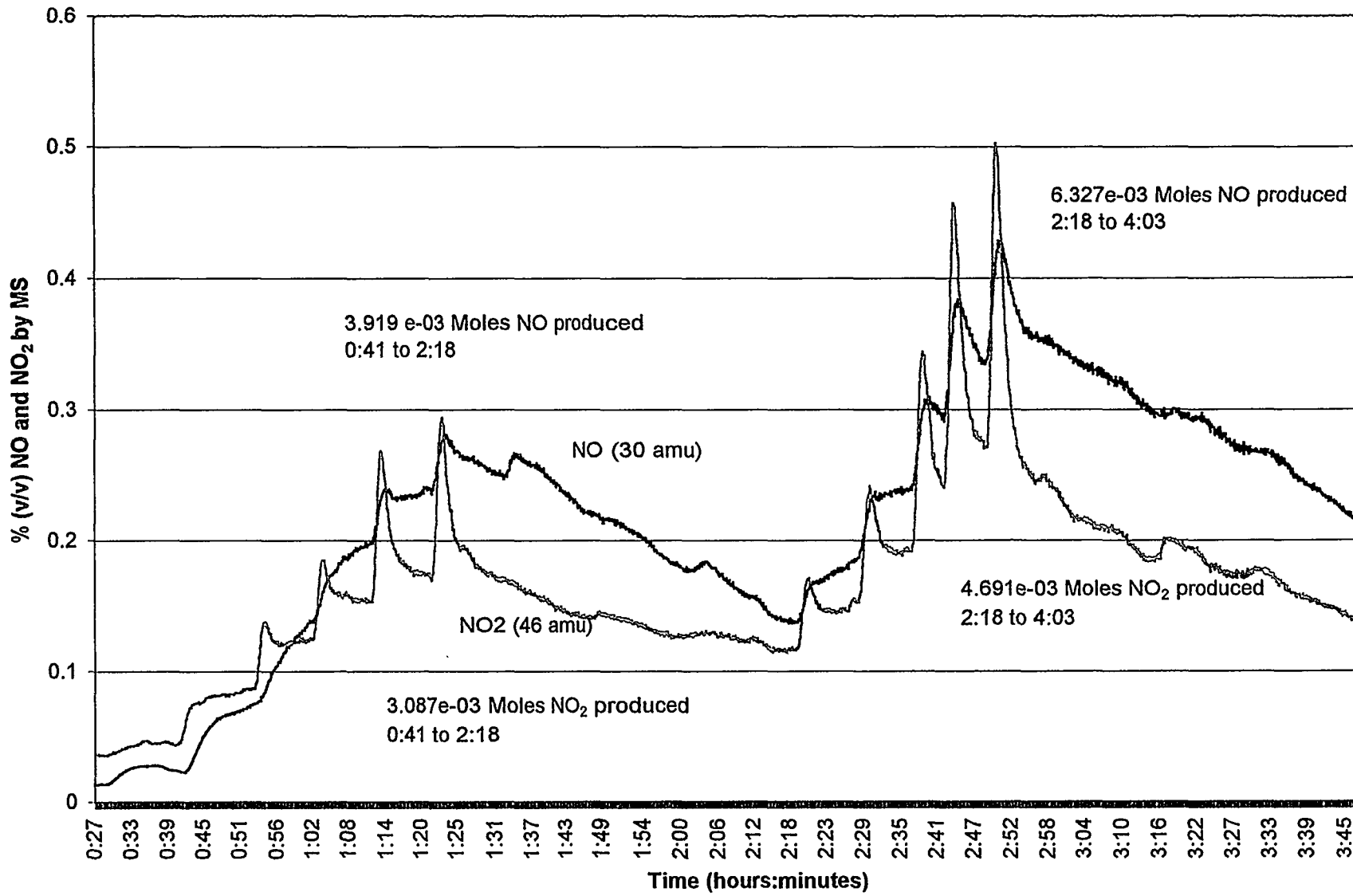


Figure F.3. Concentration of NO (30 amu) and NO₂ (46 amu) during sludge addition in Test 3 (detected by MS).

K Basin Dissolution Test 3

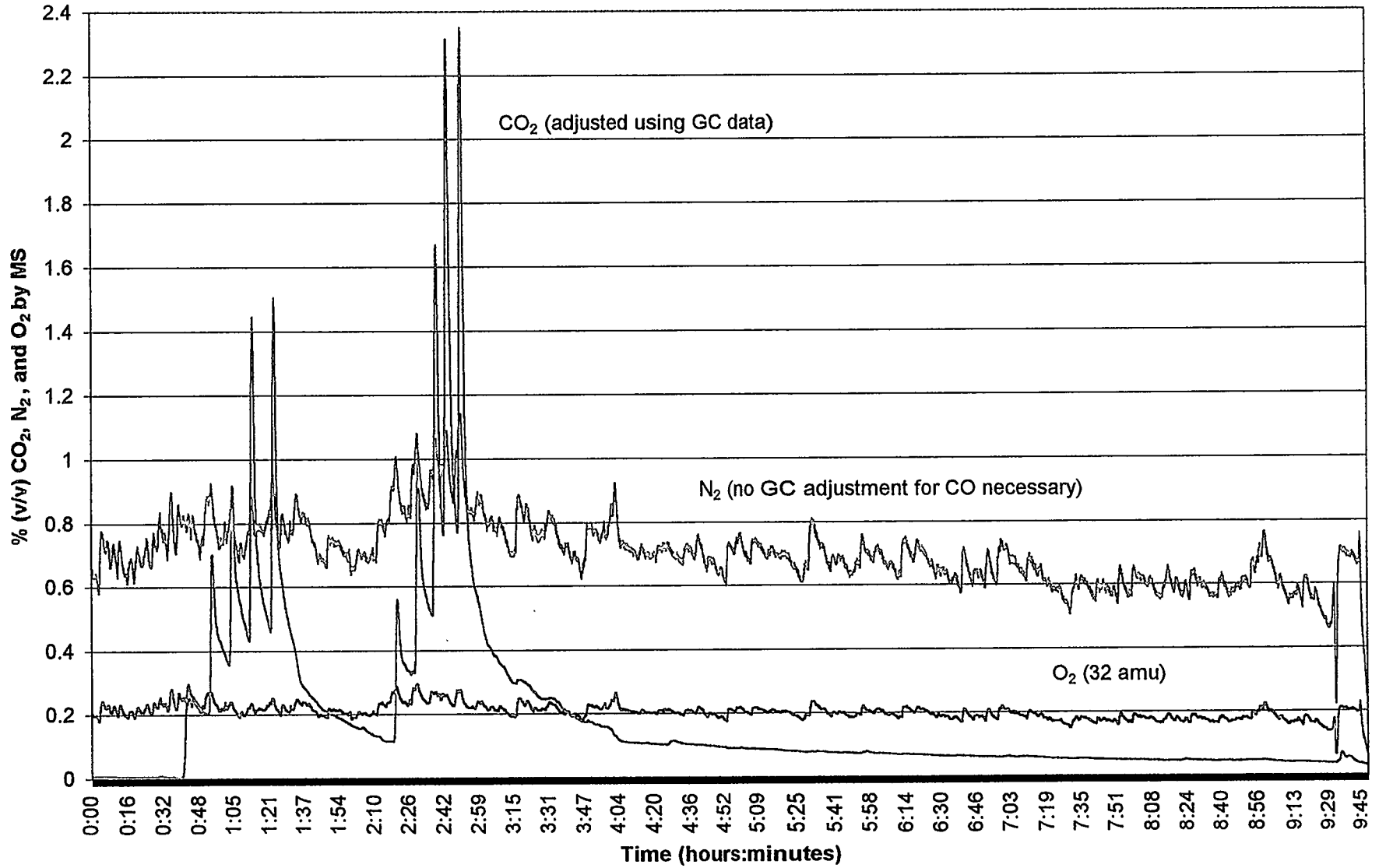


Figure F.4. Concentration of CO₂, N₂, and O₂ for the duration of Test 3 (detected by MS).

K Basin Dissolution Test 3

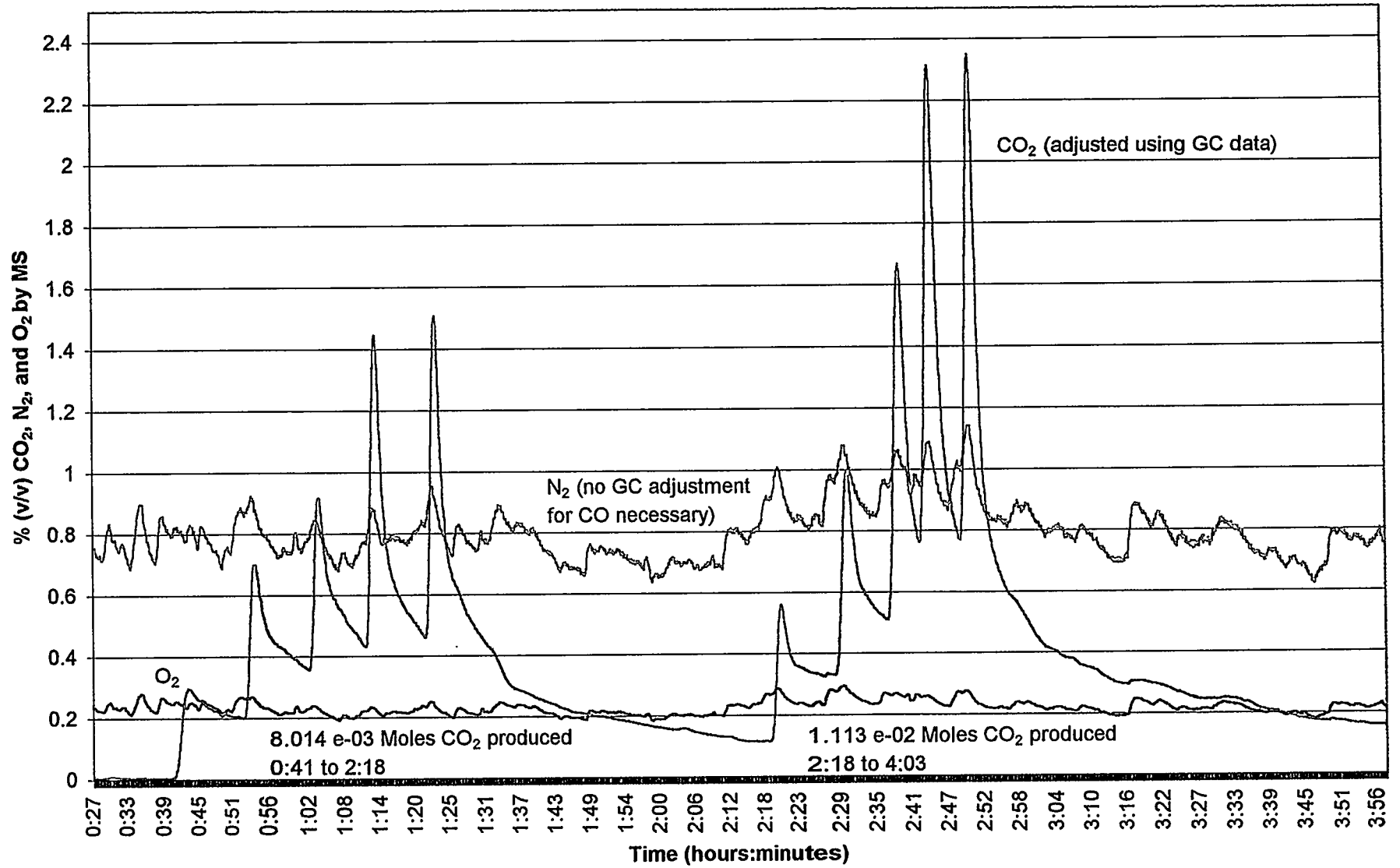


Figure F.5. Concentration of CO₂, N₂, and O₂ during sludge addition in Test 3 (detected by MS).

K Basin Dissolution Test 3

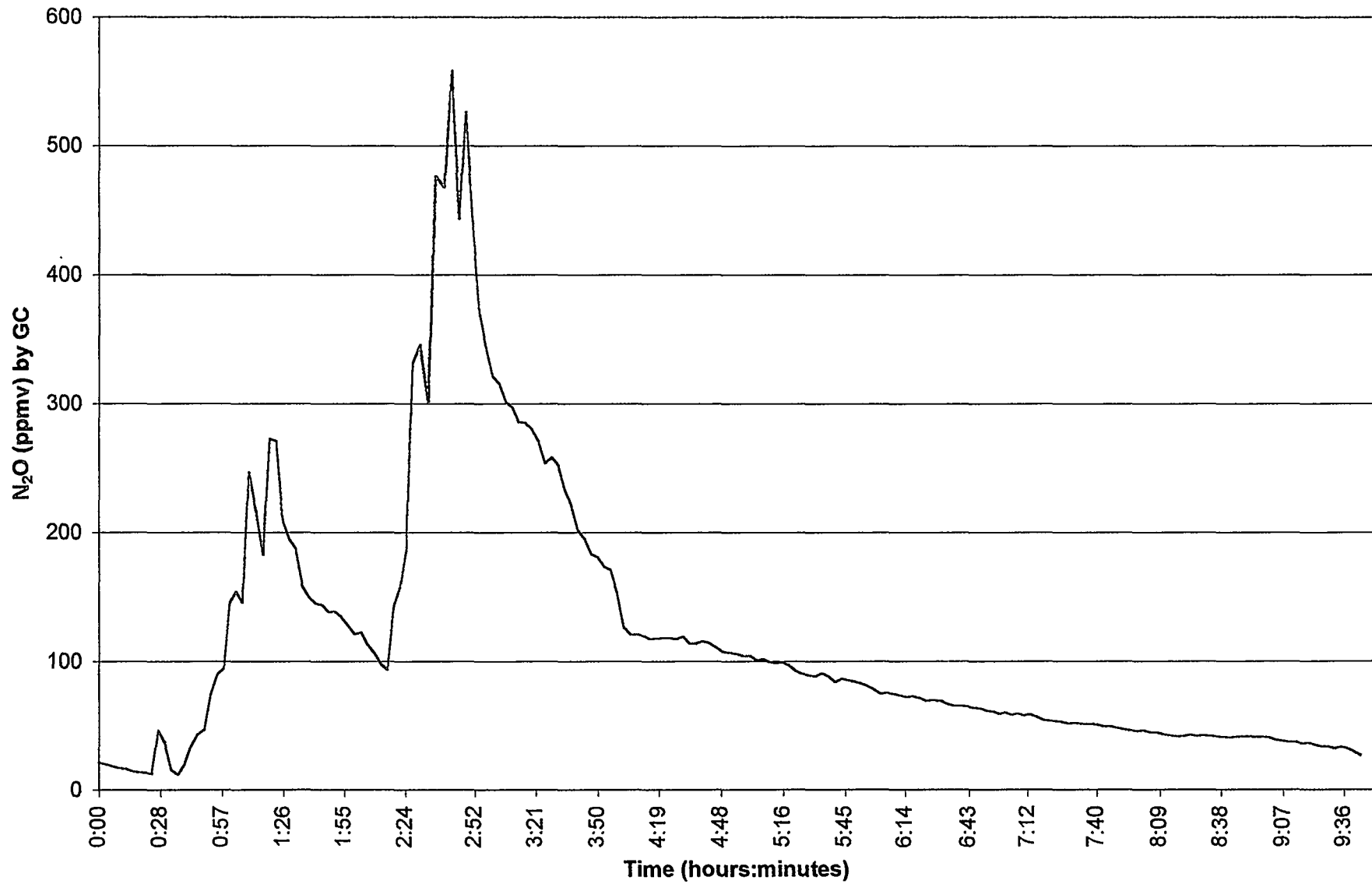


Figure F.6. Concentration of N₂O for duration of Test 3 (detected by GC).

K Basin Dissolution Test 3

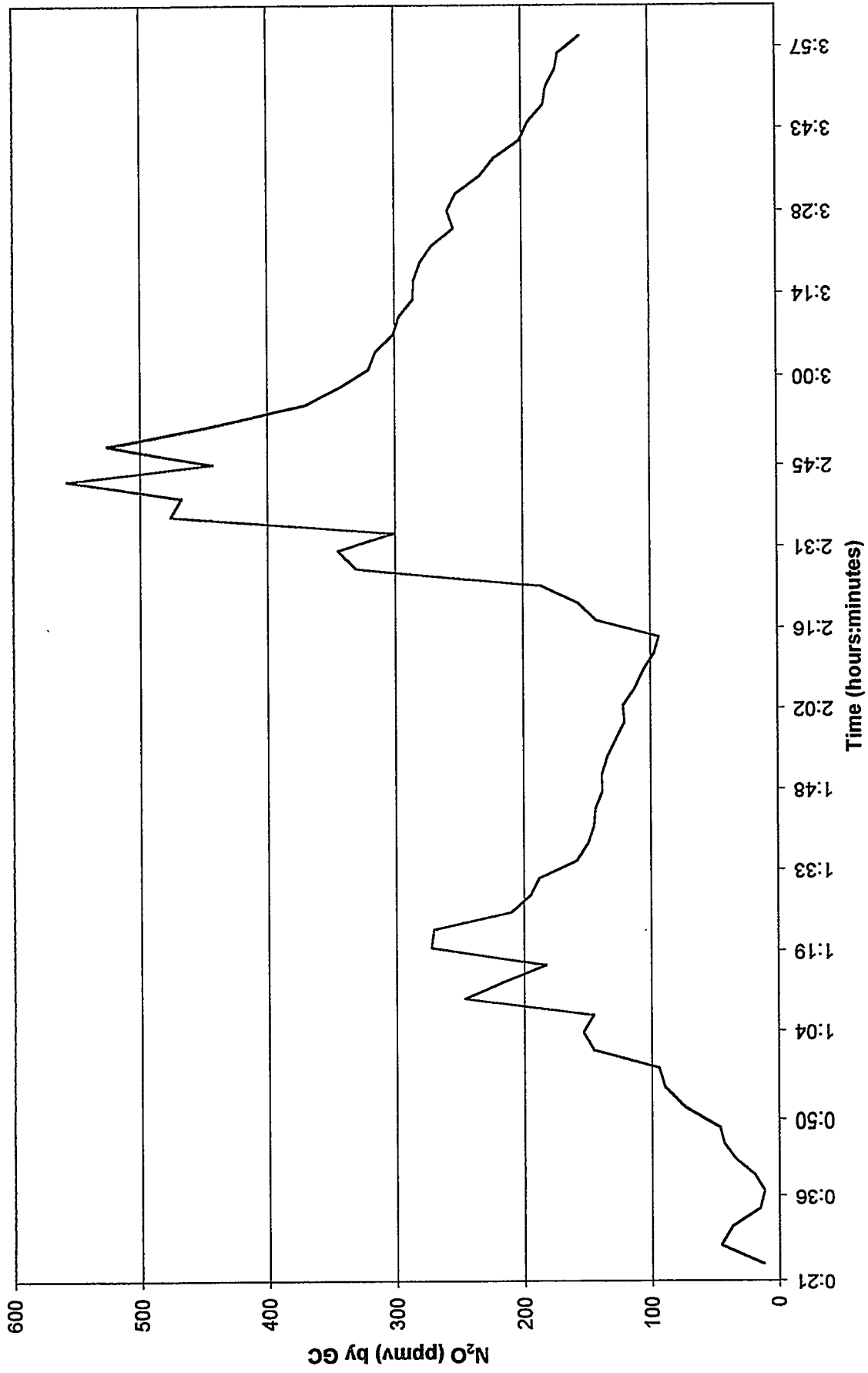


Figure F.7. Concentration of N₂O during sludge addition in Test 3 (detected by GC).

K Basin Dissolution Test 3

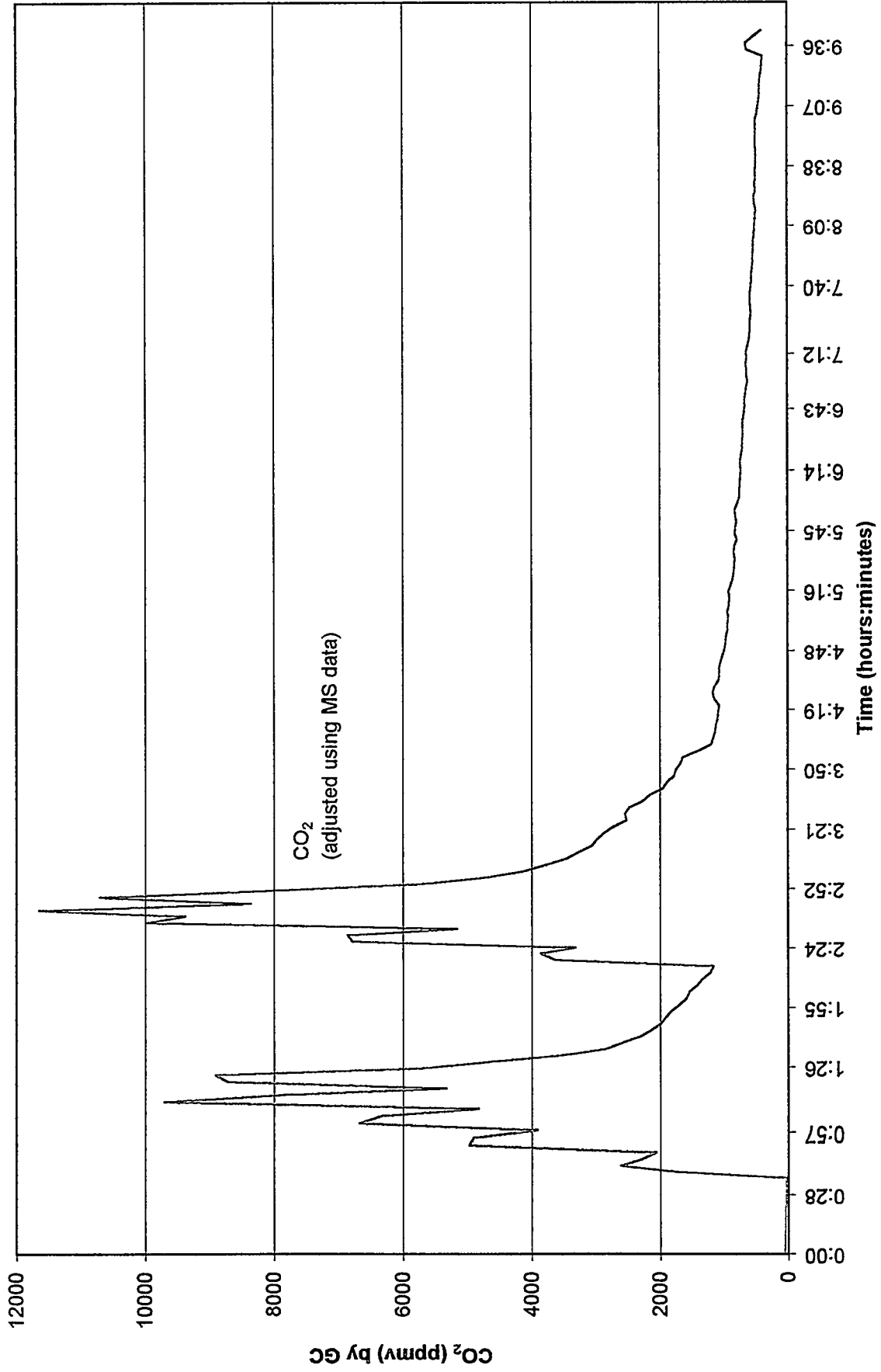


Figure F.8. Concentration of CO₂ for the duration of Test 3 (detected by GC).

K Basin Dissolution Test 3

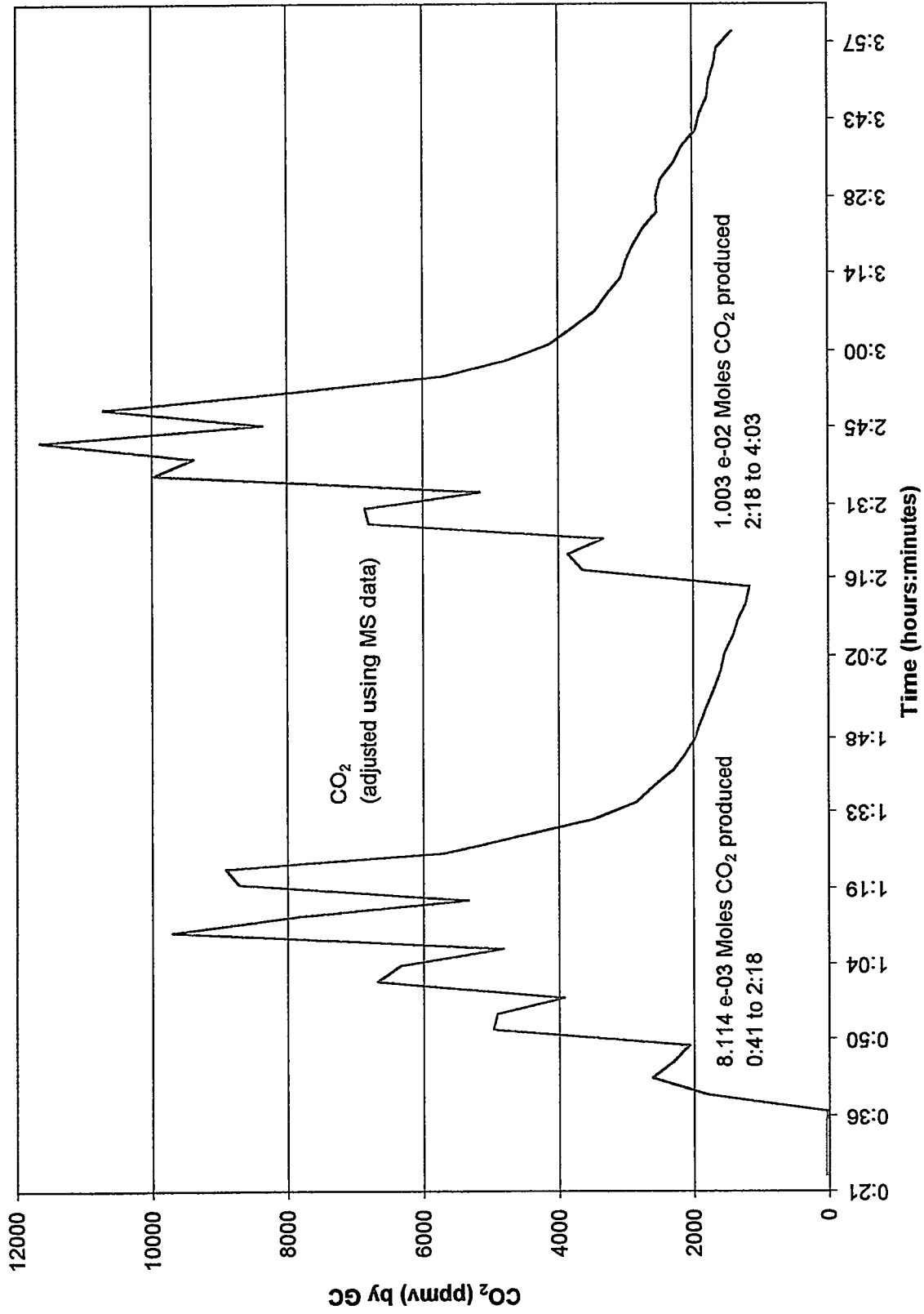


Figure F.9. Concentration of CO₂ during sludge addition in Test 3 (detected by GC).

Appendix G

Electrical Conductivity Measurements of Nitric Acid Solutions

Electrical Conductivity Measurements of Nitric Acid Solutions

Solution electrical conductivities were measured to monitor the progress of the dissolution reactions in the validation testing. Electrical conductivity is a sensitive measure of reaction progress because the primary conducting electrolyte in nitric acid solution is the hydrogen ion, H^+ . It is shown in this section that the sludge dissolution reactions strongly decrease the H^+ activity. For simple systems, electrical conductivity also can be used to monitor solution concentrations. For example, online conductivity measurements, in combination with online density measurements, can be used to determine jointly the uranium and nitric acid concentrations in the relatively pure nitric acid solutions of uranium produced in reprocessing plants (Schmieder and Kuhn 1972). The results of literature and laboratory studies of electrical conductivity of nitric acid solutions of iron, aluminum, and uranium as a function of temperature are described.

Aqueous solutions of nitric acid have the highest known electrical conductivity of any aqueous solution. The conductivity initially increases steeply with increasing nitric acid concentration, reaching a maximum at about 6 M HNO_3 , before decreasing at higher acid concentrations (Figure G.1). The decrease is caused by the inhibition, caused by the common ion effect, that the added HNO_3 has on dissociation of HNO_3 to form the H^+ and NO_3^- ions. The relative amount of water available to solvate the separate H^+ and NO_3^- ions also decreases with increasing HNO_3 concentration (at 6 M HNO_3 , for example, only about 3 molecules of water are available to solvate each H^+ and NO_3^- ion).

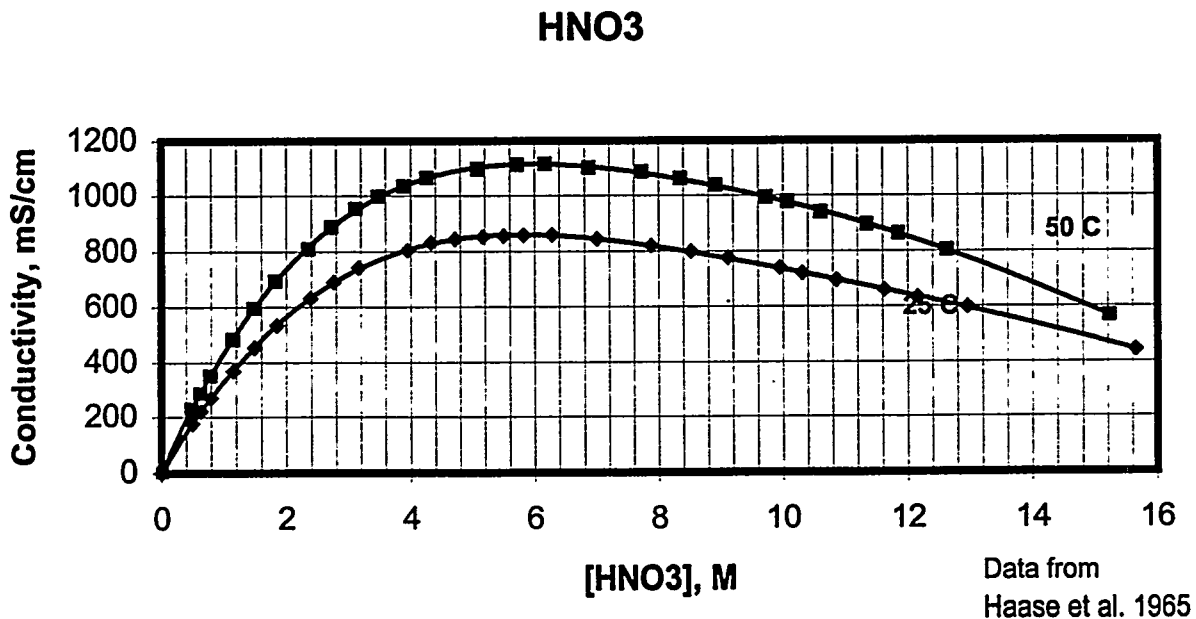


Figure G.1. Conductivity of HNO_3 Solution as Functions of Concentration and Temperature

The electrical conductivity increases with temperature (Figure G.1). Even at 50°C , however, the conductivity maximum still occurs at about 6 M HNO_3 and the maximum conductivity at 95°C occurs at about 7 M HNO_3 . Because sludge dissolution will occur in hot nitric acid, the effect of temperature on the conductivity of 6 M HNO_3 was measured. These data (Figure G.2) show the conductivity increases smoothly, but with slightly decreasing slope, as temperature increases.

6 M HNO₃

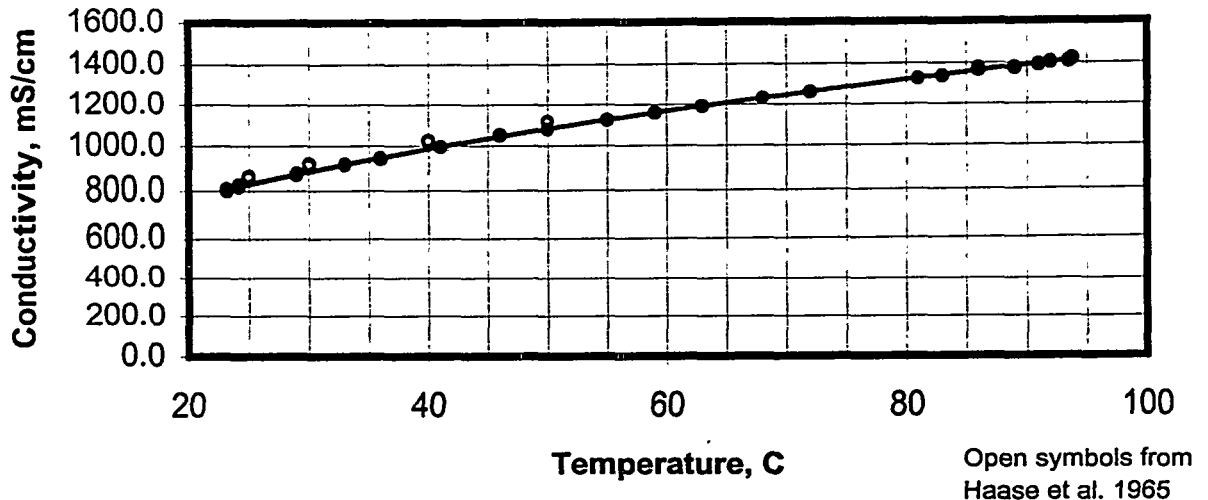


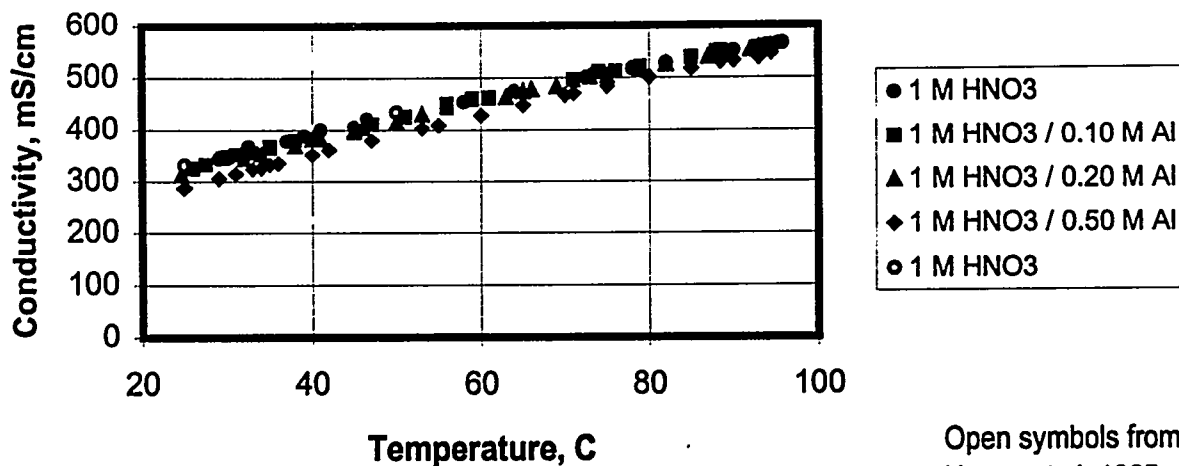
Figure G.2. Conductivity of 6 M HNO₃ Solution as Function of Temperature

As shown in Figure G.1, conductivity decreases almost linearly to near zero below about 2 M HNO₃. Conductivity measurements thus offer a promising process monitoring technique in the case of K Basin sludge dissolution to guarantee that solutions are kept acidic and prevent plutonium polymerization. For conductivity to be a more useful process monitoring tool, it is necessary to know the effects of temperature and added solutes [such as Fe(III) nitrate, Al(III) nitrate, and U(VI) nitrate from sludge dissolution] on conductivity.

To achieve this goal, the effects of Al(III) and Fe(III) nitrates on HNO₃ solution conductivity were measured at 1 and 4 M HNO₃ as functions of temperature and metal salt concentration. These data were compared with data on conductivity of U(VI) nitrate in HNO₃ found in the technical literature (Slepyan and Karpacheva 1960; Spencer 1991).

It was found that in 1 M HNO₃, Al(III) and Fe(III) both affect HNO₃ solution conductivity to the same extent on a molar basis [that is, for a given metal concentration, Al(III) and Fe(III) nitrate have equal influence on conductivity; compare Figures G.3 and G.4]. Uranium (VI) nitrate has a somewhat greater effect on conductivity (Figure G.5). However, in all cases, the additions of metal nitrate salts to 1 M HNO₃ decrease total solution conductivity. The decrease is relatively minor up to about 0.5 M salt. Even with 1 M Fe(NO₃)₃ at the anticipated 95°C processing temperature, the decrease is less than about 10%; for 1 M UO₂(NO₃)₃, the decrease at 95°C is about 25%.

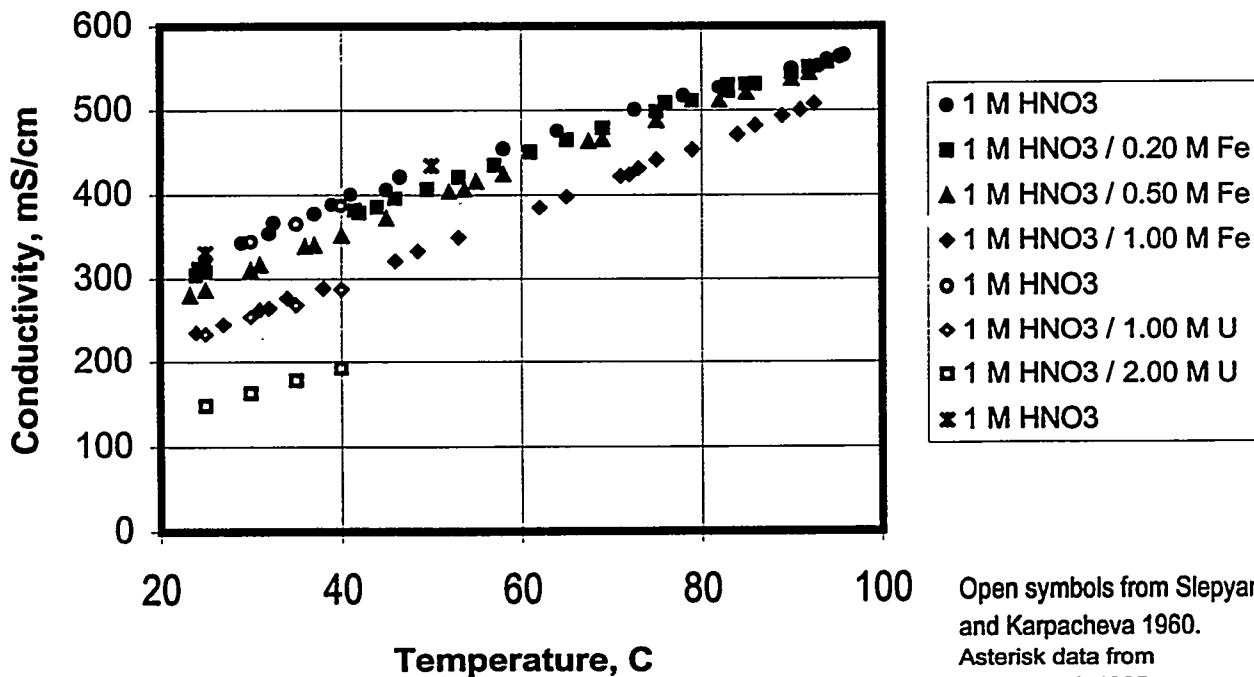
1 M HNO₃ with Al(NO₃)₃



Open symbols from Haase et al. 1965

Figure G.3. Conductivity of Al(NO₃)₃/1 M HNO₃ Solution as Function of Concentration and Temperature

1 M HNO₃ with Fe(NO₃)₃ and UO₂(NO₃)₂



Open symbols from Slepyan and Karpacheva 1960.
Asterisk data from Haase et al. 1965.

Figure G.4. Conductivity of Fe(NO₃)₃ in 1 M HNO₃ Solution as Function of Concentration and Temperature

The conductivity decrease observed as electrolyte concentration increases might not be expected upon initial consideration. The conductivity decreases because the added nitrate provided by the metal salt inhibits HNO_3 dissociation. The decreased dissociation means less of the highly conductive H^+ ion is released to solution and, thus, conductivity becomes lower.

The effects of Al(III) and Fe(III) nitrate on conductivity in 4 M HNO_3 are more pronounced. These data, presented in Figures G.6 and G.7, show that conductivity decreases by about 25% from that observed in pure 4 M HNO_3 by addition of 0.5 M metal and about 40% by addition of 1 M Fe(III) nitrate. The effects are similar for uranium at least up to 3 M HNO_3 and 40°C (Slepyan and Karpacheva 1960) and at higher acid concentrations and temperatures (Figure G.8; Spencer 1991). The more pronounced influence of added metal nitrate salt on decreasing nitric acid solution conductivity at 4 M HNO_3 versus that observed at 1 M HNO_3 is because the nitric acid at 4 M is already approaching its maximum conductivity. Thus, the addition of nitrate salt, with its nitrate common ion influence on HNO_3 dissociation and consumption of solvating water, has a more pronounced and immediate effect.

1 M HNO_3 with $\text{UO}_2(\text{NO}_3)_2$

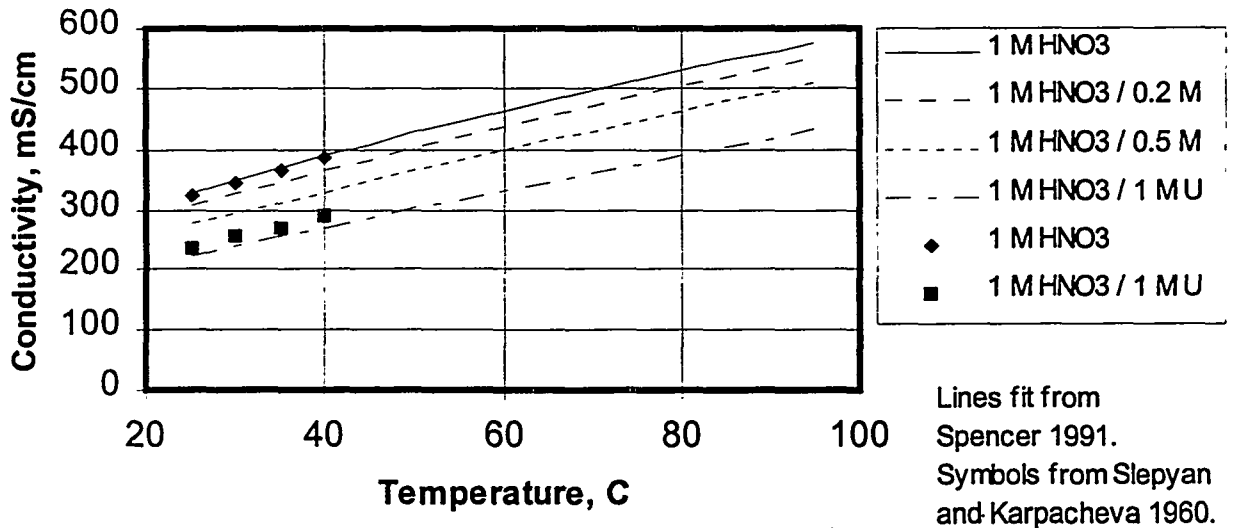


Figure G.5. Conductivity of $\text{UO}_2(\text{NO}_3)_2$ in 1 M HNO_3 Solution as Function of Concentration and Temperature

4 M HNO₃ with Al(NO₃)₃

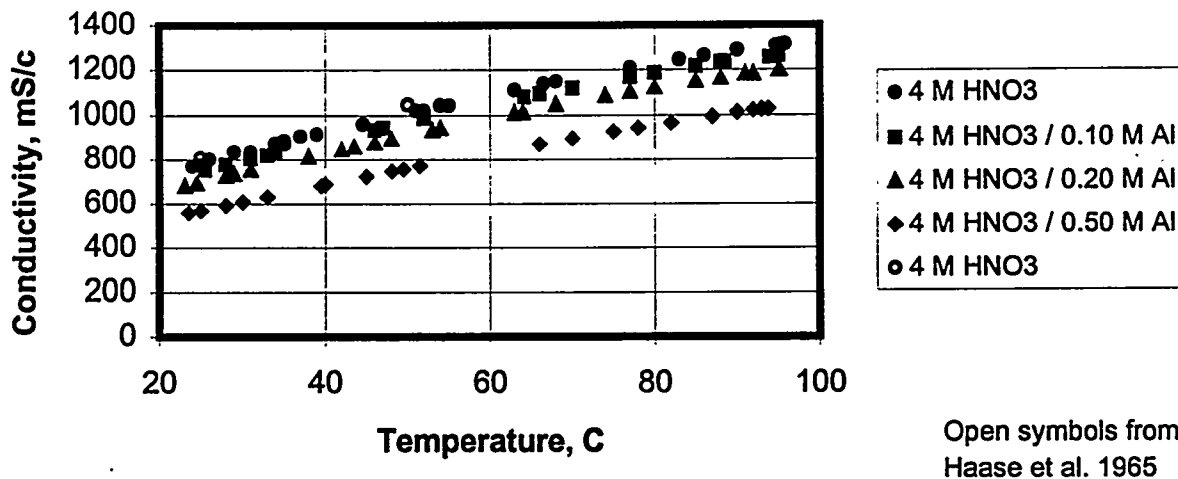


Figure G.6. Conductivity of Al(NO₃)₃/4 M HNO₃ Solution as Function of Concentration and Temperature

4 M HNO₃ with Fe(NO₃)₃

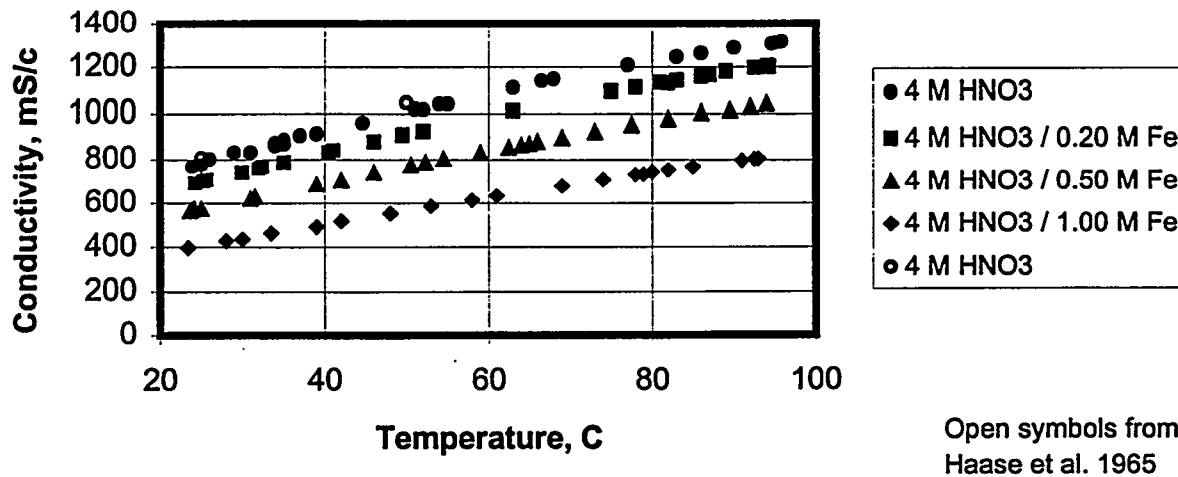


Figure G.7. Conductivity of Fe(NO₃)₃ / 4 M HNO₃ Solution as Function of Concentration and Temperature

4 M HNO₃ with UO₂(NO₃)₂

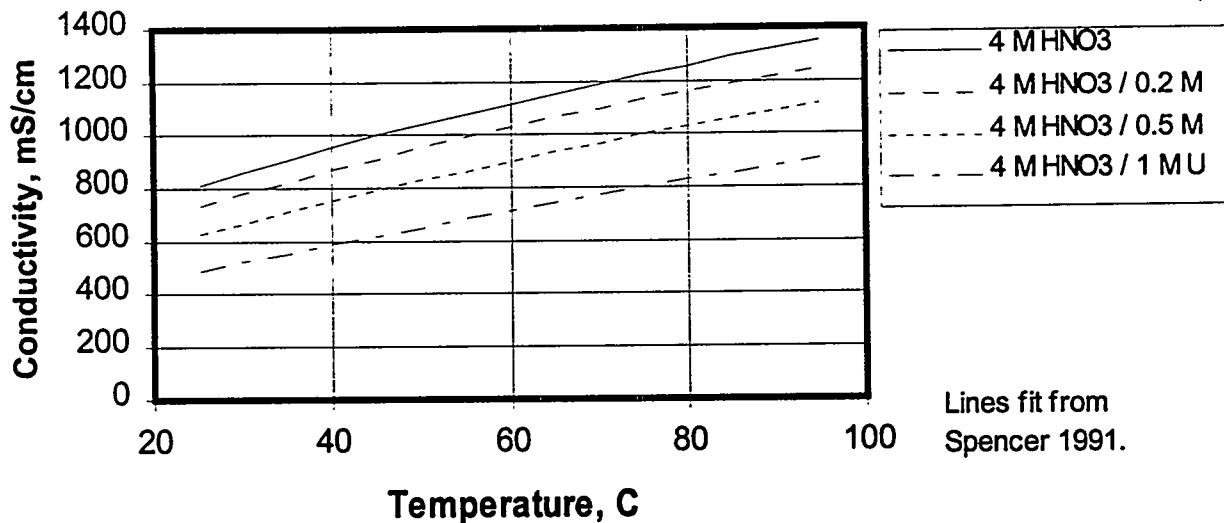
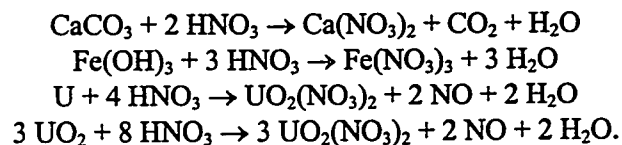


Figure G.8. Conductivity of UO₂(NO₃)₂ / 4 M HNO₃ Solution as Function of Concentration and Temperature

According to the reference flowsheet, the dissolution of K Basin sludge is to begin with 6 M HNO₃ (i.e., at the conductivity peak of nitric acid). The dissolution reactions will consume H⁺ (HNO₃) and put metal salts into solution. Some illustrative reactions are given:



As shown in the previous discussion, both acid consumption and metal salt dissolution decrease nitric acid solution conductivity. The solution conductivity thus is a very sensitive indicator of the progress of the dissolution reactions. In addition, because the effect of dissolved salts becomes lower at lower HNO₃ concentration, the conductivity measurement becomes a better (less ambiguous) indicator of remaining HNO₃ concentration. Both these properties commend electrical conductivity for process monitoring.

References

- Haase, R., P. F. Sauermann, and K. H. Dücker. 1965. "Conductivities of Concentrated Electrolyte Solutions. II. Nitric Acid." *Zeitschrift für Physikalische Chemie (Frankfurt)* 46:129-139 (in German).
- Schmieder, H., and E. Kuhn. 1972. "Automatic Control and Measurement of Reprocessing of Nuclear Fuel through Spectrophotometry and Conductivity Measurement." *Chemie Ingenieur Technik* 44:104-111 (in German).
- Slepyan, T. A., and S. M. Karpacheva. 196., "Physicochemical Properties of Nitric Acid Solutions of Uranyl Nitrate and Determination of their Composition by Density, Electrical Conductivity and Index of Refraction." *Soviet Radiochemistry* 2(3):108-115.
- Spencer, B. B. 1991. "Simultaneous Determination of Nitric Acid and Uranium Concentrations in Aqueous Solutions from Measurements of Electrical Conductivity, Density, and Temperature." CONF-910901-1, *Fourth International Conference on Facility Operations – Safeguards Interface*, September 29-October 4, 1991.